Protective or Problematic? Investigating the role of the innate immune receptor NLRX1 as a tumor suppressor or promoter in breast and pancreatic cancer.

Margaret Ann Nagai-Singer

Dissertation submitted to the faculty of the Virginia Polytechnic Institute and State University in partial fulfillment of the requirements for the degree of

Doctor of Philosophy
In
Biomedical and Veterinary Sciences

Irving C. Allen, MBA, PhD, Chair
Sheryl Coutermarsh-Ott, DVM, PhD, DACVP
Xin M. Luo, PhD
Eva M. Schmelz, PhD
Kenneth J. Oestreich, PhD

October 19, 2022
Blacksburg, Virginia

Keywords: NOD-like receptors, pattern recognition receptors, cancer, immunology, innate immunity

Protective or Problematic? Investigating the role of the innate immune receptor NLRX1 as a tumor suppressor or promoter in breast and pancreatic cancer.

Margaret Ann Nagai-Singer

ABSTRACT

The innate immune system houses cellular signaling proteins called pattern recognition receptors (PRRs) that are responsible for recognizing highly-conserved molecular patterns associated with pathogens or damage to elicit an immune response. However, NLRX1 is a unique PRR in the NOD-like receptor (NLR) family that instead functions to attenuate pro-inflammatory pathways that are activated by other PRRs, such as NF-κB and type-1 interferon signaling which both have implications in cancer. NLRX1 can regulate additional cancer-associated pathways, such as MAPK and AKT, and cancer-associated functions like metabolism and reactive oxygen species (ROS) production. Interestingly, depending on the type and subtype of cancer, NLRX1 can either be tumor promoting or tumor suppressing. Here, we investigate the role of NLRX1 in two deadly cancers: triple-negative breast cancer (TNBC) and pancreatic cancer. In a murine mammary tumor model that highly mimics TNBC, we discovered that NLRX1 is protective against disease burden *in vivo* when NLRX1 is expressed in healthy host cells. NLRX1 exerts its protection through limiting the recruitment of eosinophils to the tumor, suppressing epithelial-mesenchymal transition (EMT), and attenuating the formation of the metastatic niche. Conversely, when NLRX1 is instead expressed by the mammary tumor cells, NLRX1 promotes cancer-associated characteristics *in vitro* and disease burden *in vivo* by promoting EMT. This indicates that the role of NLRX1 in TNBC is highly dependent on cellular context. Conversely, in murine pancreatic cancer cells, we found that NLRX1 expression by the tumor cells is protective against cancer-associated characteristics *in vitro*, and that this is likely driven by NF-κB, MAPK, AKT, and inflammasome signaling with a potential to also limit immune evasion. Together, this research indicates that the role of NLRX1 can be highly variable based on the cell and tumor type and identifies the underlying mechanisms through which NLRX1 functions in these two cancer models. This is critical information for drug development initiatives so therapies can be developed that target NLRX1 in the appropriate cell type and in the appropriate disease.

Protective or Problematic? Investigating the role of the innate immune receptor NLRX1 as a tumor suppressor or promoter in breast and pancreatic cancer.

Margaret Ann Nagai-Singer

GENERAL AUDIENCE ABSTRACT

Inflammation, which is characterized by redness, heat, pain, swelling, and sometimes loss of function, is a critical way in which our bodies fight infections and repair tissue damage. However, chronic inflammation occurs when our bodies are unable to turn inflammation off and can result in cancerous mutations. Therefore, the successful resolution of inflammation is critical to maintaining inflammatory balance and has previously been dubbed the "Goldilocks Conundrum". The immune system houses a class of cellular signaling proteins called pattern recognition receptors (PRRs), which often function to turn inflammation on. However, a unique PRR in the NOD-like receptor (NLR) family called "NLRX1" functions to turn inflammation off and therefore plays an important role in preventing damaging chronic inflammation. NLRX1 has historically been studied in the context of infectious diseases, but because NLRX1 is involved in inflammation and because inflammation is a critical factor of cancer, its role as a tumor suppressor or tumor promoter has recently become an area of interest. NLRX1 has also been found to regulate biological pathways beyond inflammation that are also important for cancer initiation and progression. Interestingly, depending on the type and subtype of cancer, NLRX1 can either be tumor promoting or tumor suppressing.

Here, we investigate the role of NLRX1 in two deadly cancers: triple-negative breast cancer (TNBC) and pancreatic cancer. In a mouse mammary tumor model that highly mimics TNBC, we discovered that NLRX1 is protective against disease burden when NLRX1 is expressed in healthy, non-tumor cells. NLRX1 exerts its protection through impacting the immune cells recruited to the tumor, limiting the ability of the tumor cells to leave the original tumor and spread throughout the body in the process known as metastasis, and suppressing the formation of a favorable tumor metastasis environment in the lung. Conversely, when NLRX1 is instead expressed by the mammary tumor cells, NLRX1 promotes disease burden by helping tumor cells leave the original tumor and spread throughout the body. This indicates that the role of NLRX1 in TNBC is highly dependent on cellular context, including if the cell is healthy or cancerous. Conversely, in mouse pancreatic cancer cells, we found that NLRX1 expression by the tumor cells is protective against cancer-associated characteristics. Together, this research indicates that the role of NLRX1 can be highly variable based on the cell and tumor type. This is critical information for drug development initiatives so therapies can be developed that turn NLRX1 on or off in the appropriate cell type and in the appropriate disease.

To my Nana, Donna Joyce, who would have little idea what these data mean but would have been this dissertation's biggest fan anyways. Losing you was the most difficult moment of my graduate school career and I miss you every day.

In her memory, I would like to share a few words of wisdom and life lessons she imparted to me:

1) Magnify your blessings

2) Never leave the house without a book

3) Speak your mind, love deeply, and stand up for others

ACKNOWLEDGEMENTS

Firstly, I would like to thank Dr. Coy Allen for giving me the amazing opportunity to join his lab, which we endearingly call the "Inflammology Lab" despite his disapproval because it "isn't a real word". Thank you for your training and guidance over the last few years, and for your support for my extracurricular endeavors and career goals. (And thank you to your wonderful family for their kindness as well.) It has been an honor to work in your lab and contribute to the numerous and important projects you lead. I would also like to thank my committee members, Dr. Sheryl Coutermarsh-Ott, Dr. Xin Luo, Dr. Eva Schmelz, and Dr. Ken Oestreich, for their support and intellectual contributions to this research that made me a better scientist.

To the current and previous Allen Lab members, including Dr. Veronica Scaia, Dr. Rebecca Brock, Dr. Alissa Hendricks-Wenger, Holly Morrison, Jus Tupik, Imran Khan, Hannah Ivester, Dr. Brie Trusiano, Endia Fletcher, as well as my mentees Mackenzie Woolls and Katerina Leedy who were absolutely instrumental to this research, I couldn't have done this without you all. Thank you for being the best friends, co-workers, and fellow piggy doulas a person could ask for. I've learned so much from each of you and we've made each other better people and better scientists.

I also owe a huge thank you Bettina Heid, who makes everything we do in the Allen lab possible, and to the staff who run the ICTAS Doctoral Scholars program, Dr. Mary Kasarda, Shelley Johnson, and Mike Ervine. Additionally, I'd like to thank the Animal Resource and Care Division (ARCD) and Teaching and Research Animal Care Support Service (TRACSS) for their hard work and dedication to our research animals.

And of course, I am forever grateful for my family. Thank you to my sisters, Katie, Victoria, and Elizabeth, who make my heart whole, and Mom and Jim, for literally everything. Dad – please go get vaccinated. To my grandparents, aunts, uncles, cousins, and in-laws, thank you for all of your love and support. To my husband and life partner, Will Singer, we did it!! Words can't adequately describe how grateful I am to share my life with you, especially through our hectic life as graduate students. And thank you to our dog Peanut for being patient during the long work hours we've put in the last few years and loving us unconditionally. You deserve an honorary degree and all the treats in the world.

Lastly, I'd like to acknowledge that collectively, we've all recently experienced so much grief and trauma but have been doing the most in spite of it all. Between a deadly pandemic, violent wars, natural disasters exacerbated by climate change, a national racial reckoning and its violent backlash, an insurrection, and guns now having more rights than people with a uterus, the historical and social context surrounding my PhD experience has been exhausting. If no one has told you lately, you're doing a good job, despite the chaos.

ATTRIBUTIONS

Chapter Two: MNS was responsible for writing the manuscript and incorporating edits from ICA and HAM. HAM designed the figures in BioRender and provided edits to the manuscript.

Chapter Three: MNS was responsible for writing the manuscript, data collection and analysis, making all figures, and incorporating edits from ICA and other authors. All other authors were responsible for providing edits to the manuscript and helping with data collection.

Chapter Four: MNS was responsible for writing the manuscript, data collection and analysis, making figures, and incorporating edits from ICA and other authors. All other authors helped with data collection and providing edits to the manuscript.

Chapter Five: MNS was responsible for writing the manuscript, data collection and analysis, making figures, and incorporating edits from ICA and other authors. All other authors helped with data collection and providing edits to the manuscript.

TABLE OF CONTENTS

CHAPTER ONE

Introduction

Margaret A. Nagai-Singer

The relationship between the immune system and cancer has been of interest for many years, with Rudolph Virchow hypothesizing the link between tumors and inflammation as early as 1863 and the development of "Coley's Toxins" in 1891.[1,2] Since then, our understanding of the role of the immune system in cancer has become significantly more refined, but aspects of the relationship, especially in innate immunity, remain relatively undefined.[3] As part of our first line of immunological defense, pattern recognition receptors (PRRs) are sensors housed in the innate immune system that recognize highly-conserved pathogen-associated molecular patters (PAMPs) and damage-associated molecular patterns (DAMPs). The recognition of PAMPs or DAMPs by PRRs typically triggers the formation of various multiprotein complexes that initiate an immune response to counter the threat to the host. The concept of PRRs was originally hypothesized by Janeway in 1989, which prompted the exploration of PRRs and innate immunity more broadly.[4,5] Since their initial conceptualization, 5 classes of PRRs have been identified. These include Toll-like receptors (TLRs), Rig-I-like receptors (RLRs), C-type lectin receptors (CLRs), AIM2-like receptors (ALRs), and NOD-like receptors (NLRs).[5] PRRs have been implicated in many types of disease, and due to the several cancer-associated pathways that can be regulated by PRRs, there is increasing interest in exploring PRRs in the context of cancer.[3,5] This collection of research investigates an NLR family member with unique and elusive characteristics, NLRX1.

NLRs are comprised of a tripartite domain structure that includes a C-terminal leucine rich repeat (LRR) for autoinhibition, a central NACHT domain for nucleotide binding, and an N-terminal domain that interacts with other proteins.[6,7] The N-terminal domain defines the nomenclature of the NLR; for example, NLRs with an N-terminal "caspase activation recruitment domain" (CARD) are NLRCs, and NLRs with an N-terminal pryin domain (PYD) are NLRPs.[7] NLRX1 is named for its relatively undefined and uncharacterized N-terminal domain, which later was found to contain a mitochondria-

targeting sequence that allows NLRX1 to target the matrix of the mitochondria.[8] However, its subcellular localization and subsequent functions are subject to debate.[9–12] The specific functions of NLRX1 are reviewed in detail in Chapter Two and throughout the remaining Chapters, but in general, NLRX1 deviates from many of the more well-characterized inflammasome-forming NLRs. Instead of forming an inflammasome, NLRX1 functions to attenuate NF-κB signaling and type 1 interferon production to limit overzealous inflammation.[12–16] Both of these functions were originally described in host-pathogen interactions, but also indicate NLRX1 can limit tumorigenic chronic inflammation or increase susceptibility to viral-induced cancers.[17–21] NLRX1 can also regulate MAPK, AKT, STAT3, and IL-6 pathways, metabolism, mitochondrial-lysosomal crosstalk, autophagy/mitophagy, and reactive oxygen species (ROS) production, all of which can impact tumorigenesis and disease progression/severity.[17–19,22–24]

Consequently, NLRX1 has been studied in a handful of cancers. However, its role as a tumor suppressor or tumor promoter appears to be heavily dependent on the type and subtype of cancer (**Fig. 1**).[17–19,22–26] The research presented here seeks to understand the role of NLRX1 in two deadly malignancies, triple-negative breast cancer (TNBC) and pancreatic cancer, to further define this enigmatic NLR. The current literature discussing NLRX1 in cancer in general and in the importance of both of these malignancies is discussed in greater detail in the subsequent chapters. Consistent with the variable role of NLRX1 in the literature, we find that NLRX1 expression by the tumor cells has diametric effects between murine mammary tumor cells versus pancreatic tumor cells, and also diametric effects between healthy host cells and murine mammary tumor cells. We also highlight mechanisms and pathways responsible for these observations.

In **Chapter Two**, we review the function of NLRX1 in significantly more detail and discuss some of the conflicting literature regarding NLRX1 function and location. In **Chapter Three**, we describe a computer-based method to quantify lung metastasis in the 4T1 murine mammary tumor model. In **Chapter Four**, we examine the role of NLRX1 in the murine 4T1 mammary tumor model which is highly representative of TNBC through *in vitro* and *in vivo* loss-and gain-of-function studies.[27] In **Chapter Five**, we examine the

role of NLRX1 in the murine Pan02 pancreatic cancer model through *in vitro* loss- and gain-of-function studies. In **Chapter Six**, I discuss conclusions from this collection of research and future directions for further studies.

REFERENCES

1. Singh, N.; Baby, D.; Rajguru, J. P.; Patil, P. B.; Thakkannavar, S. S.; Pujari, V. B. Inflammation and Cancer. *Ann Afr Med* **2019**, *18* (3), 121–126. https://doi.org/10.4103/aam.aam_56_18.
2. McCarthy, E. F. The Toxins of William B. Coley and the Treatment of Bone and Soft-Tissue Sarcomas. *Iowa Orthop J* **2006**, *26*, 154–158.
3. Man, S. M.; Jenkins, B. J. Context-Dependent Functions of Pattern Recognition Receptors in Cancer. *Nat Rev Cancer* **2022**, *22* (7), 397–413. https://doi.org/10.1038/s41568-022-00462-5.
4. Janeway, C. A. Approaching the Asymptote? Evolution and Revolution in Immunology. *Cold Spring Harb Symp Quant Biol* **1989**, *54 Pt 1*, 1–13. https://doi.org/10.1101/sqb.1989.054.01.003.
5. Li, D.; Wu, M. Pattern Recognition Receptors in Health and Diseases. *Sig Transduct Target Ther* **2021**, *6* (1), 1–24. https://doi.org/10.1038/s41392-021-00687-0.
6. Maruta, N.; Burdett, H.; Lim, B. Y. J.; Hu, X.; Desa, S.; Manik, M. K.; Kobe, B. Structural Basis of NLR Activation and Innate Immune Signalling in Plants. *Immunogenetics* **2022**, *74* (1), 5–26. https://doi.org/10.1007/s00251-021-01242-5.
7. Fritz, J. H.; Ferrero, R. L.; Philpott, D. J.; Girardin, S. E. Nod-like Proteins in Immunity, Inflammation and Disease. *Nat Immunol* **2006**, *7* (12), 1250–1257. https://doi.org/10.1038/ni1412.
8. Arnoult, D.; Soares, F.; Tattoli, I.; Castanier, C.; Philpott, D. J.; Girardin, S. E. An N-Terminal Addressing Sequence Targets NLRX1 to the Mitochondrial Matrix. *Journal of Cell Science* **2009**, *122* (17), 3161–3168. https://doi.org/10.1242/jcs.051193.
9. Nagai-Singer, M. A.; Morrison, H. A.; Allen, I. C. NLRX1 Is a Multifaceted and Enigmatic Regulator of Immune System Function. *Front Immunol* **2019**, *10*, 2419. https://doi.org/10.3389/fimmu.2019.02419.
10. Soares, F.; Tattoli, I.; Wortzman, M. E.; Arnoult, D.; Philpott, D. J.; Girardin, S. E. NLRX1 Does Not Inhibit MAVS-Dependent Antiviral Signalling. *Innate Immun* **2013**, *19* (4), 438–448. https://doi.org/10.1177/1753425912467383.
11. Qin, Y.; Xue, B.; Liu, C.; Wang, X.; Tian, R.; Xie, Q.; Guo, M.; Li, G.; Yang, D.; Zhu, H. NLRX1 Mediates MAVS Degradation To Attenuate the Hepatitis C Virus-Induced Innate Immune Response through PCBP2. *J Virol* **2017**, *91* (23), e01264-17. https://doi.org/10.1128/JVI.01264-17.
12. Moore, C. B.; Bergstralh, D. T.; Duncan, J. A.; Lei, Y.; Morrison, T. E.; Zimmermann, A. G.; Accavitti-Loper, M. A.; Madden, V. J.; Sun, L.; Ye, Z.; Lich, J. D.; Heise, M. T.; Chen, Z.; Ting, J. P.-Y. NLRX1 Is a Regulator of Mitochondrial Antiviral Immunity. *Nature* **2008**, *451* (7178), 573–577. https://doi.org/10.1038/nature06501.
13. Allen, I. C.; Moore, C. B.; Schneider, M.; Lei, Y.; Davis, B. K.; Scull, M. A.; Gris, D.; Roney, K. E.; Zimmermann, A. G.; Bowzard, J. B.; Ranjan, P.; Monroe, K. M.; Pickles, R. J.; Sambhara, S.; Ting, J. P. Y. NLRX1 Protein Attenuates Inflammatory Responses to Infection by Interfering with the RIG-I-

MAVS and TRAF6-NF-KB Signaling Pathways. *Immunity* **2011**, *34* (6), 854–865. https://doi.org/10.1016/j.immuni.2011.03.026.
14. Xia, X.; Cui, J.; Wang, H. Y.; Zhu, L.; Matsueda, S.; Wang, Q.; Yang, X.; Hong, J.; Songyang, Z.; Chen, Z. J.; Wang, R.-F. NLRX1 Negatively Regulates TLR-Induced NF-KB Signaling by Targeting TRAF6 and IKK. *Immunity* **2011**, *34* (6), 843–853. https://doi.org/10.1016/j.immuni.2011.02.022.
15. Lei, Y.; Wen, H.; Ting, J. P. Y. The NLR Protein, NLRX1, and Its Partner, TUFM, Reduce Type I Interferon, and Enhance Autophagy. *Autophagy* **2013**, *9* (3), 432–433. https://doi.org/10.4161/auto.23026.
16. Lei, Y.; Wen, H.; Yu, Y.; Taxman, D. J.; Zhang, L.; Widman, D. G.; Swanson, K. V.; Wen, K.-W.; Damania, B.; Moore, C. B.; Giguère, P. M.; Siderovski, D. P.; Hiscott, J.; Razani, B.; Semenkovich, C. F.; Chen, X.; Ting, J. P.-Y. The Mitochondrial Proteins NLRX1 and TUFM Form a Complex That Regulates Type I Interferon and Autophagy. *Immunity* **2012**, *36* (6), 933–946. https://doi.org/10.1016/j.immuni.2012.03.025.
17. Tattoli, I.; Killackey, S. A.; Foerster, E. G.; Molinaro, R.; Maisonneuve, C.; Rahman, M. A.; Winer, S.; Winer, D. A.; Streutker, C. J.; Philpott, D. J.; Girardin, S. E. NLRX1 Acts as an Epithelial-Intrinsic Tumor Suppressor through the Modulation of TNF-Mediated Proliferation. *Cell Reports* **2016**, *14* (11), 2576–2586. https://doi.org/10.1016/j.celrep.2016.02.065.
18. Coutermarsh-Ott, S.; Simmons, A.; Capria, V.; LeRoith, T.; Wilson, J. E.; Heid, B.; Philipson, C. W.; Qin, Q.; Hontecillas-Magarzo, R.; Bassaganya-Riera, J.; Ting, J. P.-Y.; Dervisis, N.; Allen, I. C. NLRX1 Suppresses Tumorigenesis and Attenuates Histiocytic Sarcoma through the Negative Regulation of NF-ΛB Signaling. *Oncotarget* **2016**, *7* (22), 33096–33110. https://doi.org/10.18632/oncotarget.8861.
19. Koblansky, A. A.; Truax, A. D.; Liu, R.; Montgomery, S. A.; Ding, S.; Wilson, J. E.; Brickey, W. J.; Mühlbauer, M.; McFadden, R.-M. T.; Hu, P.; Li, Z.; Jobin, C.; Lund, P. K.; Ting, J. P.-Y. The Innate Immune Receptor NLRX1 Functions as a Tumor Suppressor by Reducing Colon Tumorigenesis and Key Tumor-Promoting Signals. *Cell Rep* **2016**, *14* (11), 2562–2575. https://doi.org/10.1016/j.celrep.2016.02.064.
20. Fan, Z.; Pan, J.; Wang, H.; Zhang, Y. NOD-like Receptor X1, Tumor Necrosis Factor Receptor-Associated Factor 6 and NF-KB Are Associated with Clinicopathological Characteristics in Gastric Cancer. *Exp Ther Med* **2021**, *21* (3), 208. https://doi.org/10.3892/etm.2021.9640.
21. Castaño-Rodríguez, N.; Kaakoush, N. O.; Goh, K.-L.; Fock, K. M.; Mitchell, H. M. The NOD-like Receptor Signalling Pathway in Helicobacter Pylori Infection and Related Gastric Cancer: A Case-Control Study and Gene Expression Analyses. *PLoS One* **2014**, *9* (6), e98899. https://doi.org/10.1371/journal.pone.0098899.
22. Hu, B.; Ding, G.-Y.; Fu, P.-Y.; Zhu, X.-D.; Ji, Y.; Shi, G.-M.; Shen, Y.-H.; Cai, J.-B.; Yang, Z.; Zhou, J.; Fan, J.; Sun, H.-C.; Kuang, M.; Huang, C. NOD-like Receptor X1 Functions as a Tumor Suppressor by Inhibiting Epithelial-Mesenchymal Transition and Inducing Aging in Hepatocellular Carcinoma

Cells. *J Hematol Oncol* **2018**, *11*, 28. https://doi.org/10.1186/s13045-018-0573-9.

23. Singh, K.; Roy, M.; Prajapati, P.; Lipatova, A.; Sripada, L.; Gohel, D.; Singh, A.; Mane, M.; Godbole, M. M.; Chumakov, P. M.; Singh, R. NLRX1 Regulates TNF-α-Induced Mitochondria-Lysosomal Crosstalk to Maintain the Invasive and Metastatic Potential of Breast Cancer Cells. *Biochimica et Biophysica Acta (BBA) - Molecular Basis of Disease* **2019**, *1865* (6), 1460–1476. https://doi.org/10.1016/j.bbadis.2019.02.018.
24. Singh, K.; Poteryakhina, A.; Zheltukhin, A.; Bhatelia, K.; Prajapati, P.; Sripada, L.; Tomar, D.; Singh, R.; Singh, A. K.; Chumakov, P. M.; Singh, R. NLRX1 Acts as Tumor Suppressor by Regulating TNF-α Induced Apoptosis and Metabolism in Cancer Cells. *Biochimica et Biophysica Acta (BBA) - Molecular Cell Research* **2015**, *1853* (5), 1073–1086. https://doi.org/10.1016/j.bbamcr.2015.01.016.
25. Soares, F.; Tattoli, I.; Rahman, M. A.; Robertson, S. J.; Belcheva, A.; Liu, D.; Streutker, C.; Winer, S.; Winer, D. A.; Martin, A.; Philpott, D. J.; Arnoult, D.; Girardin, S. E. The Mitochondrial Protein NLRX1 Controls the Balance between Extrinsic and Intrinsic Apoptosis. *J Biol Chem* **2014**, *289* (28), 19317–19330. https://doi.org/10.1074/jbc.M114.550111.
26. Luo, X.; Donnelly, C. R.; Gong, W.; Heath, B. R.; Hao, Y.; Donnelly, L. A.; Moghbeli, T.; Tan, Y. S.; Lin, X.; Bellile, E.; Kansy, B. A.; Carey, T. E.; Brenner, J. C.; Cheng, L.; Polverini, P. J.; Morgan, M. A.; Wen, H.; Prince, M. E.; Ferris, R. L.; Xie, Y.; Young, S.; Wolf, G. T.; Chen, Q.; Lei, Y. L. HPV16 Drives Cancer Immune Escape via NLRX1-Mediated Degradation of STING. *J Clin Invest* **2020**, *130* (4), 1635–1652. https://doi.org/10.1172/JCI129497.
27. Schrörs, B.; Boegel, S.; Albrecht, C.; Bukur, T.; Bukur, V.; Holtsträter, C.; Ritzel, C.; Manninen, K.; Tadmor, A. D.; Vormehr, M.; Sahin, U.; Löwer, M. Multi-Omics Characterization of the 4T1 Murine Mammary Gland Tumor Model. *Frontiers in Oncology* **2020**, *10*.

FIGURE LEGENDS

Figure 1: The conflicting roles of NLRX1 in different cancer models. Summary figure showing the protective and problematic functions of NLRX1 in various cancer models. For each type of cancer, the specific models and the underlying mechanism for the protective or problematic function is summarized.

FIGURES

Figure 1:

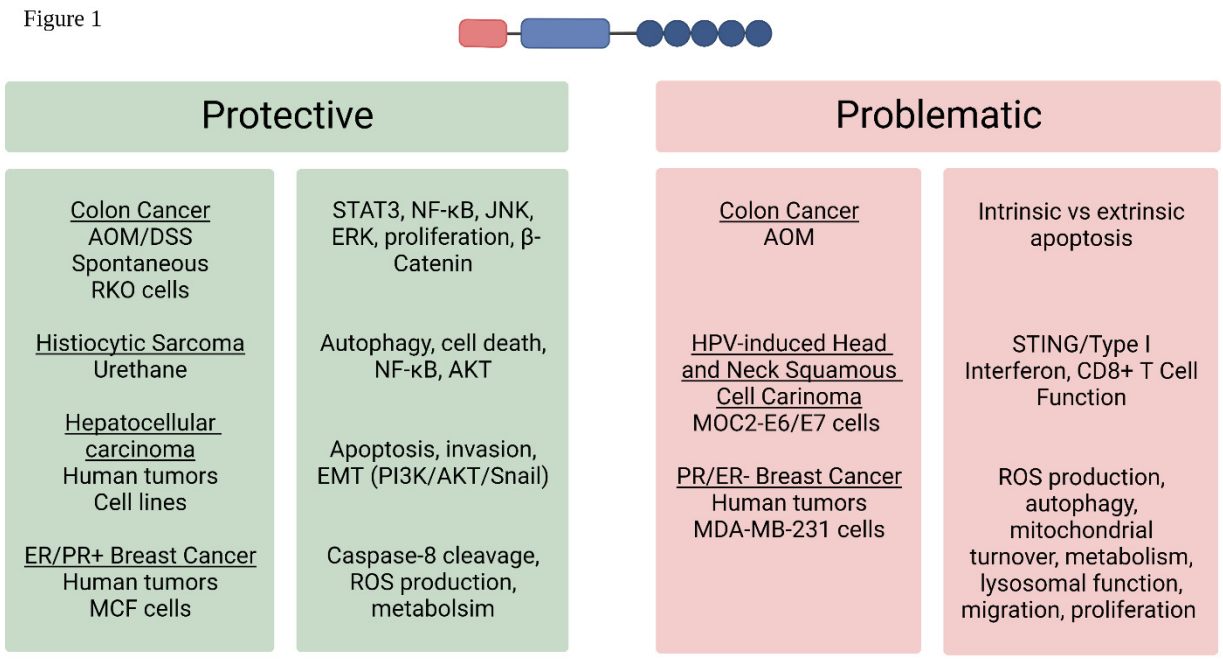

CHAPTER TWO

NLRX1 Is a Multifaceted and Enigmatic Regulator of Immune System Function

Margaret A. Nagai-Singer[1], Holly A. Morrison[1], and Irving C. Allen[1,2]

[1]Department of Biomedical Sciences and Pathobiology, Virginia-Maryland College of Veterinary Medicine, Virginia Tech, Blacksburg, VA, United States
[2]Department of Basic Science Education, Virginia Tech Carilion School of Medicine, Roanoke, VA, United States

Reprinted from Frontiers in Immunology. *Full citation:* Nagai-Singer MA, Morrison HA, Allen IC. NLRX1 Is a Multifaceted and Enigmatic Regulator of Immune System Function. Front Immunol. 2019 Oct 11;10:2419. doi: 10.3389/fimmu.2019.02419. PMID: 31681307; PMCID: PMC6797603.

ABSTRACT

Over the last decade, significant progress has been achieved in defining mechanisms underlying NLR regulation of immune system function. However, several NLR family members continue to defy our best attempts at characterization and routinely exhibit confounding data. This is particularly true for NLR family members that regulate signaling associated with the activation of other pattern recognition receptors. NLRX1 is a member of this NLR sub-group and acts as an enigmatic regulator of immune system function. NLRX1 has been shown to negatively regulate type-I interferon, attenuate pro-inflammatory NF-κB signaling, promote reactive oxygen species production, and modulate autophagy, cell death, and proliferation. However, the mechanism/s associated with NLRX1 modulation of these pathways is not fully understood and there are inconsistencies within the field. Likewise, it is highly likely that the full repertoire of biological functions impacted by NLRX1 are yet to be defined. Recent mouse studies have shown that NLRX1 significantly impacts a multitude of diseases, including cancer, virus infection, osteoarthritis, traumatic brain injury, and inflammatory bowel disease. Thus, it is essential that the underlying mechanism associated with NLRX1 function in each of these diseases be robustly defined. Here, we summarize the current progress in understanding mechanisms associated with NLRX1 function. We also offer insight into both unique and overlapping mechanisms regulated by NLRX1 that likely contribute to disease pathobiology. Ultimately, we believe that an improved understanding of NLRX1 will result in better defined mechanisms associated with immune system attenuation and the resolution of inflammation in a myriad of diseases.

NLRX1: THE ENIGMATIC NLR

Since the initial description of the NLR family of pattern recognition receptors over 20 years ago, significant progress has been made in understanding their biology. However, NLRX1 remains an enigma. NLRX1 (NOD5/NOD9/CLR11.3) has several atypical features that contribute to its complexity and uniqueness within the NLR family. For example, members of the NLR family are defined by their tripartite domain structure, which includes a variable combination of a limited repertoire of protein domains (typically pyrin or CARD domains) on the N-terminus, a conserved nucleotide binding domain in the

central region, and a variable number of leucine rich repeats (LLR) on the C-terminus (1). NLRX1 lacks a fully characterized N-terminus, hence the "X" nomenclature used to define the gene/protein. To date, the only defined domain of the N-terminus of NLRX1 is a mitochondria-targeting sequence (MTS) (2–5). The C-terminus of NLRX1 is also unique, consisting of 7 LRRs followed by an uncharacterized three-helix bundle (6). This three-helix bundle likely has a range of diverse functions, potentially including participation in molecular recognition and scaffolding. NLRX1 is considered to be ubiquitously expressed in mammalian cells, with evidence supporting cell type specific differences in function (2, 7, 8). Like the other NLR family members, NLRX1 appears to function as a scaffolding protein following activation and facilitates the formation of multiprotein complexes. However, the full range of pathogen-associated- and damage-associated molecular patterns sensed by NLRX1 is far from clear and the interacting proteins are only minimally characterized. The current dogma in the NLR field places NLRX1 in a unique sub-family of regulatory NLRs that are non-inflammasome forming and function, in part, through the regulation of inflammation signaling associated with the activation of other pattern recognition receptors (9). Other NLRs in this sub-family include NOD1, NOD2, NLRC3, and NLRP12 (9). NOD1 and NOD2 are positive regulatory NLRs, as they augment inflammatory signaling networks. NLRX1, NLRC3, and NLRP12 function as negative regulatory NLRs, thought to attenuate overzealous immune system activation and likely participate in inflammation resolution (9). Specifically, NLRX1 has been shown to negatively regulate NF-κB and type-I interferon (IFN-I) signaling, modulate the production of reactive oxygen species (ROS), participate in autophagy and cell death, and impact JNK and MAPK pathways (**Figure 1**). This review will explore the proposed mechanisms by which NLRX1 affects these processes and attempt to provide insight into this mysterious NLR family member.

NLRX1 ATTENUATES PATTERN RECOGNITION RECEPTOR SIGNALING IN THE CYTOSOL

The majority of well-characterized NLRs function as cytosolic sensors, where upon activation, they act as a scaffold to form multiprotein complexes and promote inflammation. NLRX1 has also been found in the cytoplasm (10, 11). However, as

mentioned above and similar to NLRC3 and NLRP12, cytosolic NLRX1 functions as a negative regulator of inflammation (12). While all three of these negative regulatory NLRs likely have other functions in the cytosol, all appear to attenuate inflammation through targeting components of the NF-κB signaling pathway (12). In the case of NLRX1, activation results in an interaction with TRAF6 (7, 10). At baseline, NF-κB are bound to the inhibitor IκB and NLRX1 appears to be complexed with TRAF6 in the cytosol (10). Following activation, IκB Kinase (IKK) phosphorylates IκB, resulting in its degradation and freeing the NF-κB for nuclear transit and transcription initiation (10). However, in the presence of lipopolysaccharide likely associated with TLR4 activation, NLRX1 and TRAF6 undergo K63-linked polyubiquitination resulting in complex disassociation (10). Once detached, the LRR domain of NLRX1 binds to the kinase domain of the activated IKK complex, resulting in the attenuation of the NF-κB pathway (10). The targeting of TRAFs is not unique to NLRX1. Both NLRC3 and NLRP12 have been shown to interact with TRAF6 and TRAF3, resulting in the respective attenuation of either canonical or non-canonical NF-κB signaling pathways (7, 13). The multiprotein complex that forms between these specific NLRs and the respective TRAF family members has been dubbed the "TRAFasome" (12, 13). However, significant mechanistic details pertaining to the signals leading up to TRAFasome formation, the temporal regulation of the pathways, additional biological functions regulated by the multiprotein complex, and other proteins directly or indirectly involved in complex formation are not fully understood. It should be noted that NLRX1 attenuation of NF-κB signaling has been predominately defined in the context of host-pathogen interactions. However, several studies have also characterized this mechanism underlying NLRX1's role as a tumor suppressor in various types of cancer (**Table 1**) (8, 28).

In addition to negatively regulating NF-κB signaling, an intriguing hypothesis has also been proposed that suggests NLRX1 actually shuttles from the cytosol to the mitochondria to regulate inflammation and mitochondrial functions (12). Under this postulated scenario, once released from TRAF6 as described above, NLRX1 transits alone or in complex with a currently unidentified chaperone/s to the mitochondria. Consistent with this hypothesis, several other NLRs shuttle between cellular compartments. For

example, NLRC5 and CIITA/NLRA can translocate from the cytosol to the nucleus to regulate inflammation signaling during virus infection (12, 48–51). Similarly, NOD1 and NOD2 have also been shown to shuttle between the cytosol and the plasma membrane (12, 52). As NLRX1 lacks many of the traditional translocation sequences, the mechanism underlying how NLRX1 may move between cellular compartments is still unclear. However, its ability to form multiprotein complexes opens the possibility of interactions with potential chaperones. For example, several NLRs have been shown to interact with Heat Shock Proteins, which are critical molecular chaperones for driving translocation between cellular compartments (53–57). Consistent with this hypothesis, HSP90 has been shown to interact with NLRP12 and controls its negative regulation of non-canonical NF-κB signaling (53). NLRX1 has been localized in the cytoplasm on different layers of the mitochondria, and even in mitochondrial granules (2, 4, 5, 7, 11, 24, 58). Each of these locations have significant biological implications that potentially impact NLRX1 function.

NLRX1 REGULATES IMMUNE SYSTEM FUNCTION THROUGH MITOCHONDRIA LOCALIZATION

In addition to negatively regulating NF-κB signaling, NLRX1 has also been shown to directly modulate pattern recognition receptor signaling associated with Rig-I-like Helicase Receptors (RLRs) (2). Specifically, NLRX1 inhibits the interaction between two RLRs, RIG-I and MDA5, and the Mitochondrial Anti-Viral Signaling (MAVS) protein following virus exposure to attenuate IFN-I signaling (2, 7, 10, 59, 60). MAVS is an adaptor protein located on the outer mitochondrial membrane. It is used by RIG-I to restrict virus infection by activating NF-κB and IFN regulatory factor 3 and 7 (IRF3 and IRF7) to produce IL-6 and IFN-I (2, 10, 24). Additionally, it is necessary for MAVS-dependent NLRP3 inflammasome formation (14). Mechanistically, NLRX1 was originally shown to form a multiprotein complex with MAVS on the outer membrane of the mitochondria and compete with RIG-I/MDA5 binding to MAVS (2, 12). This original model suggests the C-terminal LRR of NLRX1 is responsible for preventing MAVS from producing IFNs (2). This mechanism has been somewhat refined in more recent studies. It is now postulated that in the presence of viral RNA, the nucleotide-binding domain of NLRX1 interacts with MAVS and poly(rC) binding protein 2, causing K48-linked polyubiquitination of MAVS

(24). This degradation inhibits MAVS, leading to a suppressed immune response due to decreased IFN production and inflammation. Regardless of which domain is responsible for interacting with MAVS, decreased IFN levels put the host at a higher risk for infections like HIV, HCV, influenza, and Kaposi's sarcoma-associated herpesvirus reactivation (7, 24, 30, 34). However, attenuation of inflammation is also critical to maintain immune system homeostasis during the process of resolution once the pathogen has been cleared and also protects the host from autoimmune disorders (61). Indeed, dysfunctional NLRX1 has been associated with several autoimmune diseases including lupus, multiple sclerosis, and inflammatory bowel disease (Table 1) and is expressed in a multitude of cell and tissue types associated with these maladies (2, 7, 11, 19, 21, 22, 62).

Many of the mechanisms ascribed to NLRX1 and multiprotein complex formation have been based on other better characterized NLRs. For example, other NLRs have also been shown to form multiprotein complexes with MAVS to regulate IFN signaling following virus infection (12). Following either RSV or VSV exposure, NOD2 interacts with MAVS and this interaction is required for proper IFN signaling in both hematopoietic and non-hematopoietic cells (63). However, consistent with their positive and negative regulatory functions, the NOD2-MAVS interaction exacerbates IFN signaling and inflammation; whereas, the NLRX1-MAVS interaction attenuates these processes (2, 12). The regulation of MAVS is complex, as other molecules like PSMA7, FAF1, STING, PB1-F2, and PKR might function concurrently with NLRX1 to impact innate immunity. A subunit of the proteasome PSMA7 functions similarly to NLRX1, decreasing IFN-I production by inhibiting MAVS (64). Likewise, NLRX1 further hinders IFN-I production by binding to STING, a component of MAVS signaling, to disrupt the STING-TBK1 interaction (30, 65). On the other hand, FAF1 disrupts the NLRX1-MAVS complex, freeing MAVS to activate pro-inflammatory pathways and produce IFN-I (66). NLRX1 also competes with PKR to initiate an antiviral response by protecting IRF1 function (67). This mechanism appears to be specific as NLRX1 prevents IRF3 expression to inhibit MAVS, but allows IRF1 activation (67). Contrastingly, some believe that NLRX1 does not associate with MAVS, but rather interacts directly with viral proteins, like PB1-F2 on the influenza A virus (33). It is possible, and even likely, that other unidentified proteins

interact with NLRX1 to negatively regulate inflammation and anti-viral host responses. The complexity of this regulation contributes to the confounding data seen related to NLRX1 and MAVS. Indeed, there are many aspects of these mitochondrial mechanisms that are still undefined, including the temporal dynamics of the interactions, other proteins that may participate either directly or indirectly in potential NLRX1 multi-protein complex formation, and cell or microbial signals necessary to trigger either positive or negative regulation.

In addition to its role in modulating MAVS signaling on the outer membrane of the mitochondria, NLRX1 has also been shown to be localized within the mitochondria on the inner membrane and matrix (3, 4). Internalized NLRX1 interacts with the protein UQCRC2 in the electron transport chain (4). This interaction has been suggested to potentiate the production of ROS from the mitochondria (4). NLRX1 mediated modulation of ROS production by the mitochondria has significant implications in multiple biological functions, including anti-viral immunity and cancer. ROS production results in the activation of multiple transcription factors, including NF-κB, and is a potent damage associated molecular pattern that is sensed by several pattern recognition receptors, such as NLRP3 (68, 69). Increased oxidative stress is also a key driver of cell death through JNK signaling activation and a significant contributing factor in tumorigenesis, cisplatin-induced ototoxicity, and bacterial infections (3, 16, 70–73). Thus, while the negative regulatory effects of NLRX1 on inflammation are well-documented, this unique NLR also acts to augment ROS production that can promote inflammation. While this may seem counterintuitive, it is likely that the biological impact of the increased ROS production is to facilitate apoptosis, which is a typical host-defense mechanism following virus infection and during tumorigenesis, rather than drive inflammation. Specifically, studies have suggested NLRX1 does so by activating JNK signaling through the production of ROS, and interactions with Caspase-8 (3, 72, 74). For example, NLRX1 has been shown to be required for rhinovirus-mediated disruptions to the airway epithelial barrier (43). In this study, NLRX1 silencing resulted in the elimination of both virus-associated and poly(I:C)-associated ROS production and was shown to be essential for rhinovirus induced NOX-1 expression in polarized airway epithelial cells (43). This attenuation of NLRX1 and

subsequent elimination in mitochondrial ROS production was associated with improved cell survival, tight junction formation, and barrier function (43). Contrastingly, NLRX1 reportedly exerts protective effects against apoptosis in chondrocytes and tubular epithelial cells, and the modulation of apoptosis may be dependent on its interactions with yet another protein, SARM1 (37, 41, 75).

NLRX1 REGULATES MULTIPLE BIOLOGICAL FUNCTIONS THROUGH THE MODULATION OF AUTOPHAGY

Beyond the diverse roles discussed thus far, NLRX1 has also been shown to modulate autophagy. Autophagy is a critical biological process associated with cell death, inflammation, and tumorigenesis. In the context of viral pathogenesis, autophagy upregulation is associated with improved virus clearance. Intracytoplasmic virions can be captured within the autophagy pathway and transferred to lysosomes for eventual breakdown and/or pattern recognition receptor sensing, resulting in the activation of innate and adaptive immune responses (76). NLRX1's promotion and regulation of autophagy has been reported in several instances within the context of virus exposure (59, 60). These studies reveal that NLRX1 is capable of augmenting autophagy pathways by associating with the TUFM protein (59). TUFM is a molecule that not only potently suppresses RIG-I signaling, but is also associated with the autophagy complex ATG12–ATG5–ATG16L1. NLRX1 and TUFM appear to act together to keep IFN-I production in check and also prevent decreases in autophagy (59, 60). The ATG12–ATG5 complex can also interact directly with MAVS to inhibit IFN-I. For example, its absence has been shown to lead to accumulation of MAVS on the mitochondria and elevation of IFN-I (60). Thus, while NLRX1 seems to enhance autophagy, this may actually augment its negative regulation of IFN-I.

In addition to interactions with TUFM during virus infection, NLRX1 has also been shown to modulate autophagy though interactions with the Beclin 1-UVRAG complex. This complex is critical for regulating autophagy following bacteria exposure (77). In studies with Group A Streptococcus, cell invasion was significantly increased in the absence of NLRX1 (77). This was associated with a decrease in autophagosome and

autolysome formation (77). Mechanistically, NLRX1 was shown to interact with Beclin 1 through its NACHT domain and function as a negative regulator to inactivate the Beclin 1-UVRAG complex following bacteria invasion (77). Presumably, the negative regulation of this inhibitory complex actually enhances the binding capacity of Beclin 1 with additional proteins, such as Atg14L. This shift from a Beclin 1-UVRAG complex to a Beclin 1-Atg14L complex is predicted to promote autophagy and increase endolysosomal trafficking (78).

Furthermore, intriguing data has recently revealed that NLRX1 also plays a role in mitophagy in the context of both infectious disease and cancer (15, 35). Mitophagy is a process cells use to purge damaged or unnecessary mitochondria. Pathogens often exploit this mechanism to evade host recognition and killing. For example, the virulence factor listeriolysin O from *L. monocytogenes* induces mitophagy in macrophages (35). NLRX1 was shown to promote *L. monocytogenes*-induced mitophagy (35). NLRX1 is the only NLR family member with a MTS that contains an LC3-interacting region that directly associates with LC3 (35). This oligomerization was induced by listeriolysin O, resulting in mitophagy (35). Conversely, NLRX1 deficiency was found to increase mitochondrial production of ROS and reduced bacteria survival (35). Additionally, the interaction with LC3 modulates proinflammatory cytokine production by macrophages in response to fungal infection (79). In the context of cancer, NLRX1 plays a role in TNF induced mitochondria-lysosomal crosstalk in mammary tumors (15). NLRX1 appears to maintain the crosstalk between mitochondrial metabolism and lysosomal function to modulate key cancer hallmarks (15). When NLRX1 is deleted, lysosomal function is impaired and turnover of damaged mitochondria through mitophagy is reduced (15). This results in decreased OxPhos-dependent cell proliferation and breast cancer cell migration ability in the presence of TNF (15). Together, these studies show the importance of NLRX1 in mitophagy and further identify it as a potential target for future therapeutic interventions.

CONCLUSIONS

There is significantly more to the NLR family beyond the formation of the inflammasome. Over the last two decades, our understanding of the regulatory NLR family

members that function to either augment or attenuate signaling associated with other families of pattern recognition receptors has greatly increased our overall understanding of immune system regulation. The recent characterization of NLRs that function as negative regulators, which participate in the attenuation of inflammation and promote resolution underscore the point that many NLR family members have yet to be significantly characterized. Even among NLRs that have been relatively well-studied, including NLRX1, conflicting data in the literature is common. However, there is a general consensus regarding the broad mechanisms associated with this unique NLR, including regulation of NF-κB, IFN-I signaling, autophagy, and ROS production. However, more mechanistic insight is certainly needed to better define the high-resolution details of its role in each of these biological processes and signaling pathways. As NLRX1 potentially contributes to a multitude of human diseases (Table 1), it is critical to better characterize this enigmatic NLR to propel the field forward and bolster the development of novel disease treatments.

AUTHOR CONTRIBUTIONS

MN-S, HM, and IA conducted literature reviews, analyzed and interpreted data, prepared the figures, and wrote the manuscript. IA provided content expertise and overall direction. All authors have read and approved the manuscript.

CONFLICT OF INTEREST

The authors declare that the research was conducted in the absence of any commercial or financial relationships that could be construed as a potential conflict of interest.

FUNDING

Figures were generated using BioRender. This work was supported by the Virginia-Maryland College of Veterinary Medicine (IA) and the Virginia Tech Institute for Critical Technology and Applied Science (MN-S and IA).

REFERENCES

1. Schroder K, Tschopp J. The inflammasomes. *Cell.* (2010) 140:821–32. doi: 10.1016/j.cell.2010.01.040
2. Moore CB, Bergstralh DT, Duncan JA, Lei Y, Morrison TE, Zimmermann AG, et al. NLRX1 is a regulator of mitochondrial antiviral immunity. *Nature.* (2008) 451:573–7. doi: 10.1038/nature06501
3. Tattoli I, Carneiro LA, Jehanno M, Magalhaes JG, Shu Y, Philpott DJ, et al. NLRX1 is a mitochondrial NOD-like receptor that amplifies NF-kappaB and JNK pathways by inducing reactive oxygen species production. *EMBO Rep.* (2008) 9:293–300. doi: 10.1038/sj.embor.7401161
4. Arnoult D, Soares F, Tattoli I, Castanier C, Philpott DJ, Girardin SE. An N-terminal addressing sequence targets NLRX1 to the mitochondrial matrix. *J Cell Sci.* (2009) 122(Pt 17):3161–8. doi: 10.1242/jcs.051193
5. Song X, Li W, Xie X, Zou Z, Wei J, Wu H, et al. NLRX1 of black carp suppresses MAVS-mediated antiviral signaling through its NACHT domain. *Dev Comp Immunol.* (2019) 96:68–77. doi: 10.1016/j.dci.2019.03.001
6. Reubold TF, Hahne G, Wohlgemuth S, Eschenburg S. Crystal structure of the leucine-rich repeat domain of the NOD-like receptor NLRP1: implications for binding of muramyl dipeptide. *FEBS Lett.* (2014) 588:3327–32. doi: 10.1016/j.febslet.2014.07.017
7. Allen IC, Moore CB, Schneider M, Lei Y, Davis BK, Scull MA, et al. NLRX1 protein attenuates inflammatory responses to infection by interfering with the RIG-I-MAVS and TRAF6-NF-kappaB signaling pathways. *Immunity.* (2011) 34:854–65. doi: 10.1016/j.immuni.2011.03.026
8. Koblansky AA, Truax AD, Liu R, Montgomery SA, Ding S, Wilson JE, et al. The innate immune receptor NLRX1 functions as a tumor suppressor by reducing colon tumorigenesis and key tumor-promoting signals. *Cell Rep.* (2016) 14:2562–75. doi: 10.1016/j.celrep.2016.02.064
9. Allen IC. Non-inflammasome forming NLRs in inflammation and tumorigenesis. *Front Immunol.* (2014) 5:169. doi: 10.3389/fimmu.2014.00169
10. Xia X, Cui J, Wang HY, Zhu L, Matsueda S, Wang Q, et al. NLRX1 negatively regulates TLR-induced NF-kappaB signaling by targeting TRAF6 and IKK. *Immunity.* (2011) 34:843–53. doi: 10.1016/j.immuni.2011.02.022
11. Shao WH, Shu DH, Zhen Y, Hilliard B, Priest SO, Cesaroni M, et al. Prion-like aggregation of mitochondrial antiviral signaling protein in lupus patients is associated with increased levels of type I interferon. *Arthritis Rheumatol.* (2016) 68:2697–707. doi: 10.1002/art.39733
12. Coutermarsh-Ott S, Eden K, Allen IC. Beyond the inflammasome: regulatory NOD-like receptor modulation of the host immune response following virus exposure. *J Gen Virol.* (2016) 97:825–38. doi: 10.1099/jgv.0.000401
13. Schneider M, Zimmermann AG, Roberts RA, Zhang L, Swanson KV, Wen H, et al. The innate immune sensor NLRC3 attenuates Toll-like receptor signaling via modification of the signaling adaptor TRAF6 and transcription factor NF-kappaB. *Nat Immunol.* (2012) 13:823–31. doi: 10.1038/ni.2378
14. Li H, Zhang S, Li F, Qin L. NLRX1 attenuates apoptosis and inflammatory responses in myocardial ischemia by inhibiting MAVS-dependent NLRP3

inflammasome activation. *Mol Immunol.* (2016) 76:90–7. doi: 10.1016/j.molimm.2016.06.013
15. Singh K, Roy M, Prajapati P, Lipatova A, Sripada L, Gohel D, et al. NLRX1 regulates TNF-alpha-induced mitochondria-lysosomal crosstalk to maintain the invasive and metastatic potential of breast cancer cells. *Biochim Biophys Acta Mol Basis Dis.* (2019) 1865:1460–76. doi: 10.1016/j.bbadis.2019.02.018
16. Abdul-Sater AA, Said-Sadier N, Lam VM, Singh B, Pettengill MA, Soares F, et al. Enhancement of reactive oxygen species production and chlamydial infection by the mitochondrial Nod-like family member NLRX1. *J Biol Chem.* (2010) 285:41637–45. doi: 10.1074/jbc.M110.137885
17. Kang MJ, Yoon CM, Kim BH, Lee CM, Zhou Y, Sauler M, et al. Suppression of NLRX1 in chronic obstructive pulmonary disease. *J Clin Invest.* (2015) 125:2458–62. doi: 10.1172/JCI71747
18. Kang MJ, Shadel GS. A mitochondrial perspective of chronic obstructive pulmonary disease pathogenesis. *Tuberc Respir Dis.* (2016) 79:207–13. doi: 10.4046/trd.2016.79.4.207
19. Leber A, Hontecillas R, Tubau-Juni N, Zoccoli-Rodriguez V, Abedi V, Bassaganya-Riera J. NLRX1 modulates immunometabolic mechanisms controlling the host-gut microbiota interactions during inflammatory bowel disease. *Front Immunol.* (2018) 9:363. doi: 10.3389/fimmu.2018.00363
20. Yang Q, Sun G, Cao Z, Yin H, Qi Q, Wang J, et al. The expression of NLRX1 in C57BL/6 mice cochlear hair cells: possible relation to aging- and neomycin-induced deafness. *Neurosci Lett.* (2016) 616:138–46. doi: 10.1016/j.neulet.2015.11.053
21. Eitas TK, Chou WC, Wen H, Gris D, Robbins GR, Brickey J, et al. The nucleotide-binding leucine-rich repeat (NLR) family member NLRX1 mediates protection against experimental autoimmune encephalomyelitis and represses macrophage/microglia-induced inflammation. *J Biol Chem.* (2014) 289:4173–9. doi: 10.1074/jbc.M113.533034
22. Gharagozloo M, Gris KV, Mahvelati T, Amrani A, Lukens JR, Gris D. NLR-dependent regulation of inflammation in multiple sclerosis. *Front Immunol.* (2017) 8:2012. doi: 10.3389/fimmu.2017.02012
23. Mahmoud S, Gharagozloo M, Simard C, Amrani A, Gris D. NLRX1 enhances glutamate uptake and inhibits glutamate release by astrocytes. *Cells.* (2019) 8:E400. doi: 10.3390/cells8050400
24. Qin Y, Xue B, Liu C, Wang X, Tian R, Xie Q, et al. NLRX1 mediates MAVS degradation to attenuate hepatitis C virus-induced innate immune response through PCBP2. *J Virol.* (2017) 91:e01264–17. doi: 10.1128/JVI.01264-17
25. Castano-Rodriguez N, Kaakoush NO, Goh KL, Fock KM, Mitchell HM. The NOD-like receptor signalling pathway in *Helicobacter pylori* infection and related gastric cancer: a case-control study and gene expression analyses. *PLoS ONE.* (2014) 9:e98899. doi: 10.1371/journal.pone.0098899
26. Wang X, Yang C, Liao X, Han C, Yu T, Huang K, et al. NLRC and NLRX gene family mRNA expression and prognostic value in hepatocellular carcinoma. *Cancer Med.* (2017) 6:2660–72. doi: 10.1002/cam4.1202

27. Hu B, Ding GY, Fu PY, Zhu XD, Ji Y, Shi GM, et al. NOD-like receptor X1 functions as a tumor suppressor by inhibiting epithelial-mesenchymal transition and inducing aging in hepatocellular carcinoma cells. *J Hematol Oncol.* (2018) 11:28. doi: 10.1186/s13045-018-0573-9
28. Coutermarsh-Ott S, Simmons A, Capria V, LeRoith T, Wilson JE, Heid B, et al. NLRX1 suppresses tumorigenesis and attenuates histiocytic sarcoma through the negative regulation of NF-kappaB signaling. *Oncotarget.* (2016) 7:33096–110. doi: 10.18632/oncotarget.8861
29. Costford SR, Tattoli I, Duan FT, Volchuk A, Klip A, Philpott DJ, et al. Male mice lacking NLRX1 are partially protected from high-fat diet-induced hyperglycemia. *J Endocr Soc.* (2018) 2:336–47. doi: 10.1210/js.2017-00360
30. Mar KB, Schoggins JW. NLRX1 helps HIV avoid a STING operation. *Cell Host Microbe.* (2016) 19:430–1. doi: 10.1016/j.chom.2016.03.011
31. Nasi M, De Biasi S, Bianchini E, Digaetano M, Pinti M, Gibellini L, et al. Analysis of inflammasomes and antiviral sensing components reveals decreased expression of NLRX1 in HIV-positive patients assuming efficient antiretroviral therapy. *AIDS.* (2015) 29:1937–41. doi: 10.1097/QAD.0000000000000830
32. Barouch DH, Ghneim K, Bosche WJ, Li Y, Berkemeier B, Hull M, et al. Rapid inflammasome activation following mucosal SIV infection of rhesus monkeys. *Cell.* (2016) 165:656–67. doi: 10.1016/j.cell.2016.03.021
33. Jaworska J, Coulombe F, Downey J, Tzelepis F, Shalaby K, Tattoli I, et al. NLRX1 prevents mitochondrial induced apoptosis and enhances macrophage antiviral immunity by interacting with influenza virus PB1-F2 protein. *Proc Natl Acad Sci USA.* (2014) 111:E2110–9. doi: 10.1073/pnas.1322118111
34. Ma Z, Hopcraft SE, Yang F, Petrucelli A, Guo H, Ting JP, et al. NLRX1 negatively modulates type I IFN to facilitate KSHV reactivation from latency. *PLoS Pathog.* (2017) 13:e1006350. doi: 10.1371/journal.ppat.1006350
35. Zhang Y, Yao Y, Qiu X, Wang G, Hu Z, Chen S, et al. Listeria hijacks host mitophagy through a novel mitophagy receptor to evade killing. *Nat Immunol.* (2019) 20:433–46. doi: 10.1038/s41590-019-0324-2
36. Wang YG, Fang WL, Wei J, Wang T, Wang N, Ma JL, et al. The involvement of NLRX1 and NLRP3 in the development of nonalcoholic steatohepatitis in mice. *J Chin Med Assoc.* (2013) 76:686–92. doi: 10.1016/j.jcma.2013.08.010
37. Ma D, Zhao Y, She J, Zhu Y, Zhao Y, Liu L, et al. NLRX1 alleviates lipopolysaccharide-induced apoptosis and inflammation in chondrocytes by suppressing the activation of NF-kappaB signaling. *Int Immunopharmacol.* (2019) 71:7–13. doi: 10.1016/j.intimp.2019.03.001
38. Ebersole JL, Kirakodu S, Novak MJ, Exposto CR, Stromberg AJ, Shen S, et al. Effects of aging in the expression of NOD-like receptors and inflammasome-related genes in oral mucosa. *Mol Oral Microbiol.* (2016) 31:18–32. doi: 10.1111/omi.12121
39. Jing H, Song T, Cao S, Sun Y, Wang J, Dong W, et al. Nucleotide-binding oligomerization domain-like receptor X1 restricts porcine reproductive and respiratory syndrome virus-2 replication by interacting with viral Nsp9. *Virus Res.* (2019) 268:18–26. doi: 10.1016/j.virusres.2019.05.011

40. Bryant AH, Bevan RJ, Spencer-Harty S, Scott LM, Jones RH, Thornton CA. Expression and function of NOD-like receptors by human term gestation-associated tissues. *Placenta.* (2017) 58:25–32. doi: 10.1016/j.placenta.2017.07.017
41. Stokman G, Kors L, Bakker PJ, Rampanelli E, Claessen N, Teske GJD, et al. NLRX1 dampens oxidative stress and apoptosis in tissue injury via control of mitochondrial activity. *J Exp Med.* (2017) 214:2405–20. doi: 10.1084/jem.20161031
42. Kim HW, Kwon YJ, Park BW, Song JJ, Park YB, Park MC. Differential expressions of NOD-like receptors and their associations with inflammatory responses in rheumatoid arthritis. *Clin Exp Rheumatol.* (2017) 35:630–7.
43. Unger BL, Ganesan S, Comstock AT, Faris AN, Hershenson MB, Sajjan US. Nod-like receptor X-1 is required for rhinovirus-induced barrier dysfunction in airway epithelial cells. *J Virol.* (2014) 88:3705–18. doi: 10.1128/JVI.03039-13
44. Zhang Y, Chen Y, Gu T, Xu Q, Zhu G, Chen G. Effects of *Salmonella enterica* serovar Enteritidis infection on egg production and the immune response of the laying duck Anas platyrhynchos. *PeerJ.* (2019) 7:e6359. doi: 10.7717/peerj.6359
45. Theus MH, Brickler T, Meza AL, Coutermarsh-Ott S, Hazy A, Gris D, et al. Loss of NLRX1 exacerbates neural tissue damage and NF-kappaB signaling following brain injury. *J Immunol.* (2017) 199:3547–58. doi: 10.4049/jimmunol.1700251
46. Zeng C, Zhou Z, Han Y, Wen Z, Guo C, Huang S, et al. Interactions of TRAF6 and NLRX1 gene polymorphisms with environmental factors on the susceptibility of type 2 diabetes mellitus vascular complications in a southern Han Chinese population. *J Diabetes Complicat.* (2017) 31:1652–7. doi: 10.1016/j.jdiacomp.2017.08.013
47. Scantlebery AML, Uil M, Butter LM, Poelman R, Claessen N, Girardin SE, et al. NLRX1 does not play a role in diabetes nor the development of diabetic nephropathy induced by multiple low doses of streptozotocin. *PLoS ONE.* (2019) 14:e0214437. doi: 10.1371/journal.pone.0214437
48. Benko S, Magalhaes JG, Philpott DJ, Girardin SE. NLRC5 limits the activation of inflammatory pathways. *J Immunol.* (2010) 185:1681. doi: 10.4049/jimmunol.0903900
49. Meissner TB, Li A, Biswas A, Lee KH, Liu YJ, Bayir E, et al. NLR family member NLRC5 is a transcriptional regulator of MHC class I genes. *Proc Natl Acad Sci USA.* (2010) 107:13794–9. doi: 10.1073/pnas.1008684107
50. Orlandi C, Forlani G, Tosi G, Accolla RS. Molecular and cellular correlates of the CIITA-mediated inhibition of HTLV-2 Tax-2 transactivator function resulting in loss of viral replication. *J Transl Med.* (2011) 9:106. doi: 10.1186/1479-5876-9-106
51. Tosi G, Forlani G, Andresen V, Turci M, Bertazzoni U, Franchini G, et al. Major histocompatibility complex class II transactivator CIITA is a viral restriction factor that targets human T-cell lymphotropic virus type 1 Tax-1 function and inhibits viral replication. *J Virol.* (2011) 85:10719–29. doi: 10.1128/JVI.00813-11
52. Kufer TA, Kremmer E, Adam AC, Philpott DJ, Sansonetti PJ. The pattern-recognition molecule Nod1 is localized at the plasma membrane at sites of

bacterial interaction. *Cell Microbiol.* (2008) 10:477–86. doi: 10.1111/j.1462-5822.2007.01062.x
53. Arthur JC, Lich JD, Aziz RK, Kotb M, Ting JP. Heat shock protein 90 associates with monarch-1 and regulates its ability to promote degradation of NF-kappaB-inducing kinase. *J Immunol.* (2007) 179:6291–6. doi: 10.4049/jimmunol.179.9.6291
54. Yue S, Zhu J, Zhang M, Li C, Zhou X, Zhou M, et al. The myeloid heat shock transcription factor 1/beta-catenin axis regulates NLR family, pyrin domain-containing 3 inflammasome activation in mouse liver ischemia/reperfusion injury. *Hepatology.* (2016) 64:1683–98. doi: 10.1002/hep.28739
55. Gutierrez-Lopez TY, Orduna-Castillo LB, Hernandez-Vasquez MN, Vazquez-Prado J, Reyes-Cruz G. Calcium sensing receptor activates the NLRP3 inflammasome via a chaperone-assisted degradative pathway involving Hsp70 and LC3-II. *Biochem Biophys Res Commun.* (2018) 505:1121–7. doi: 10.1016/j.bbrc.2018.10.028
56. Swaroop S, Mahadevan A, Shankar SK, Adlakha YK, Basu A. HSP60 critically regulates endogenous IL-1beta production in activated microglia by stimulating NLRP3 inflammasome pathway. *J Neuroinflamm.* (2018) 15:177. doi: 10.1186/s12974-018-1355-6
57. Wang Y, Sedlacek AL, Pawaria S, Xu H, Scott MJ, Binder RJ. Cutting Edge: the heat shock protein gp96 activates inflammasome-signaling platforms in APCs. *J Immunol.* (2018) 201:2209–14. doi: 10.4049/jimmunol.1800505
58. Singh K, Sripada L, Lipatova A, Roy M, Prajapati P, Gohel D, et al. NLRX1 resides in mitochondrial RNA granules and regulates mitochondrial RNA processing and bioenergetic adaptation. *Biochim Biophys Acta Mol Cell Res.* (2018) 1865:1260–76. doi: 10.1016/j.bbamcr.2018.06.008
59. Lei Y, Wen H, Yu Y, Taxman DJ, Zhang L, Widman DG, et al. The mitochondrial proteins NLRX1 and TUFM form a complex that regulates type I interferon and autophagy. *Immunity.* (2012) 36:933–46. doi: 10.1016/j.immuni.2012.03.025
60. Lei Y, Wen H, Ting JP. The NLR protein, NLRX1, and its partner, TUFM, reduce type I interferon, and enhance autophagy. *Autophagy.* (2013) 9:432–3. doi: 10.4161/auto.23026
61. Fekete T, Bencze D, Szabo A, Csoma E, Biro T, Bacsi A, et al. Regulatory NLRs control the RLR-mediated type I interferon and inflammatory responses in human dendritic cells. *Front Immunol.* (2018) 9:2314. doi: 10.3389/fimmu.2018.02314
62. Leber A, Hontecillas R, Tubau-Juni N, Zoccoli-Rodriguez V, Hulver M, McMillan R, et al. NLRX1 regulates effector and metabolic functions of CD4(+) T cells. *J Immunol.* (2017) 198:2260–8. doi: 10.4049/jimmunol.1601547
63. Sabbah A, Chang TH, Harnack R, Frohlich V, Tominaga K, Dube PH, et al. Activation of innate immune antiviral responses by Nod2. *Nat Immunol.* (2009) 10:1073–80. doi: 10.1038/ni.1782
64. Jia Y, Song T, Wei C, Ni C, Zheng Z, Xu Q, et al. Negative regulation of MAVS-mediated innate immune response by PSMA7. *J Immunol.* (2009) 183:4241–8. doi: 10.4049/jimmunol.0901646

65. Guo H, Konig R, Deng M, Riess M, Mo J, Zhang L, et al. NLRX1 sequesters STING to negatively regulate the interferon response, thereby facilitating the replication of HIV-1 and DNA viruses. *Cell Host Microbe.* (2016) 19:515–28. doi: 10.1016/j.chom.2016.03.001
66. Kim JH, Park ME, Nikapitiya C, Kim TH, Uddin MB, Lee HC, et al. FAS-associated factor-1 positively regulates type I interferon response to RNA virus infection by targeting NLRX1. *PLoS Pathog.* (2017) 13:e1006398. doi: 10.1371/journal.ppat.1006398
67. Feng H, Lenarcic EM, Yamane D, Wauthier E, Mo J, Guo H, et al. NLRX1 promotes immediate IRF1-directed antiviral responses by limiting dsRNA-activated translational inhibition mediated by PKR. *Nat Immunol.* (2017) 18:1299–309. doi: 10.1038/ni.3853
68. Gloire G, Legrand-Poels S, Piette J. NF-kappaB activation by reactive oxygen species: fifteen years later. *Biochem Pharmacol.* (2006) 72:1493–505. doi: 10.1016/j.bcp.2006.04.011
69. Allen IC, Scull MA, Moore CB, Holl EK, McElvania-TeKippe E, Taxman DJ, et al. The NLRP3 inflammasome mediates *in vivo* innate immunity to influenza A virus through recognition of viral RNA. *Immunity.* (2009) 30:556–65. doi: 10.1016/j.immuni.2009.02.005
70. Klaunig JE, Xu Y, Isenberg JS, Bachowski S, Kolaja KL, Jiang J, et al. The role of oxidative stress in chemical carcinogenesis. *Environ Health Perspect.* (1998) 106:289–95. doi: 10.1289/ehp.98106s1289
71. Circu ML, Aw TY. Reactive oxygen species, cellular redox systems, and apoptosis. *Free Radic Biol Med.* (2010) 48:749–62. doi: 10.1016/j.freeradbiomed.2009.12.022
72. Yin H, Sun G, Yang Q, Chen C, Qi Q, Wang H, et al. NLRX1 accelerates cisplatin-induced ototoxity in HEI-OC1 cells via promoting generation of ROS and activation of JNK signaling pathway. *Sci Rep.* (2017) 7:44311. doi: 10.1038/srep44311
73. Yin H, Yang Q, Cao Z, Li H, Yu Z, Zhang G, et al. Activation of NLRX1-mediated autophagy accelerates the ototoxic potential of cisplatin in auditory cells. *Toxicol Appl Pharmacol.* (2018) 343:16–28. doi: 10.1016/j.taap.2018.02.007
74. Singh K, Poteryakhina A, Zheltukhin A, Bhatelia K, Prajapati P, Sripada L, et al. NLRX1 acts as tumor suppressor by regulating TNF-alpha induced apoptosis and metabolism in cancer cells. *Biochim Biophys Acta.* (2015) 1853:1073–86. doi: 10.1016/j.bbamcr.2015.01.016
75. Killackey SA, Rahman MA, Soares F, Zhang AB, Abdel-Nour M, Philpott DJ, et al. The mitochondrial Nod-like receptor NLRX1 modifies apoptosis through SARM1. *Mol Cell Biochem.* (2019) 453:187–96. doi: 10.1007/s11010-018-3444-3
76. Shoji-Kawata S, Levine B. Autophagy, antiviral immunity, and viral countermeasures. *Biochim Biophys Acta.* (2009) 1793:1478–84. doi: 10.1016/j.bbamcr.2009.02.008
77. Aikawa C, Nakajima S, Karimine M, Nozawa T, Minowa-Nozawa A, Toh H, et al. NLRX1 negatively regulates group A streptococcus invasion and autophagy

induction by interacting with the Beclin 1-UVRAG complex. *Front Cell Infect Microbiol.* (2018) 8:403. doi: 10.3389/fcimb.2018.00403
78. Wu S, He Y, Qiu X, Yang W, Liu W, Li X, et al. Targeting the potent Beclin 1-UVRAG coiled-coil interaction with designed peptides enhances autophagy and endolysosomal trafficking. *Proc Natl Acad Sci USA.* (2018) 115:E5669–78. doi: 10.1073/pnas.1721173115
79. Huang JH, Liu CY, Wu SY, Chen WY, Chang TH, Kan HW, et al. NLRX1 facilitates histoplasma capsulatum-induced LC3-associated phagocytosis for cytokine production in macrophages. *Front Immunol.* (2018) 9:2761. doi: 10.3389/fimmu.2018.02761

FIGURE LEGENDS

Figure 1: NLRX1 regulates immune system signaling. The Nod-like receptor NLRX1 has many diverse, multifaceted roles in innate immune system signaling, and cellular localization plays a key role in determining NLRX1's function. Localized on and within the mitochondria, NLRX1 interacts with a multitude of pathways. NLRX1 interacts with the complex III associated protein UQCRC2 to promote the production of reactive oxygen species (ROS). ROS in turn activates the JNK pathway, which promotes apoptosis. NLRX1 attenuates MAVS signaling through disruption of RIG-I activation via interactions with poly(rC) binding protein 2 (PCBP2). This negatively regulates the production of IL-6, IFN-1, and possibly NLRP3 inflammasome formation. When associated with the mitochondrial immune signaling complex (MISC) and TUFM, NLRX1 promotes autophagy. Lastly, in the presence of TNF, NLRX1 interacts with Caspase-8 to induce TNF-induced apoptosis, and this interaction may inhibit Complex I and III of the Electron Transport Chain. In the cytosol, NLRX1 inhibits NF-κB signaling by interacting with IκB kinase (IKK). Likewise, cytosolic NLRX1 may promote TRAFasome formation, which in turn inhibits NF-κB signaling. Lastly, NLRX1 may also inhibit the MAPK pathway.

FIGURES

Figure 1:

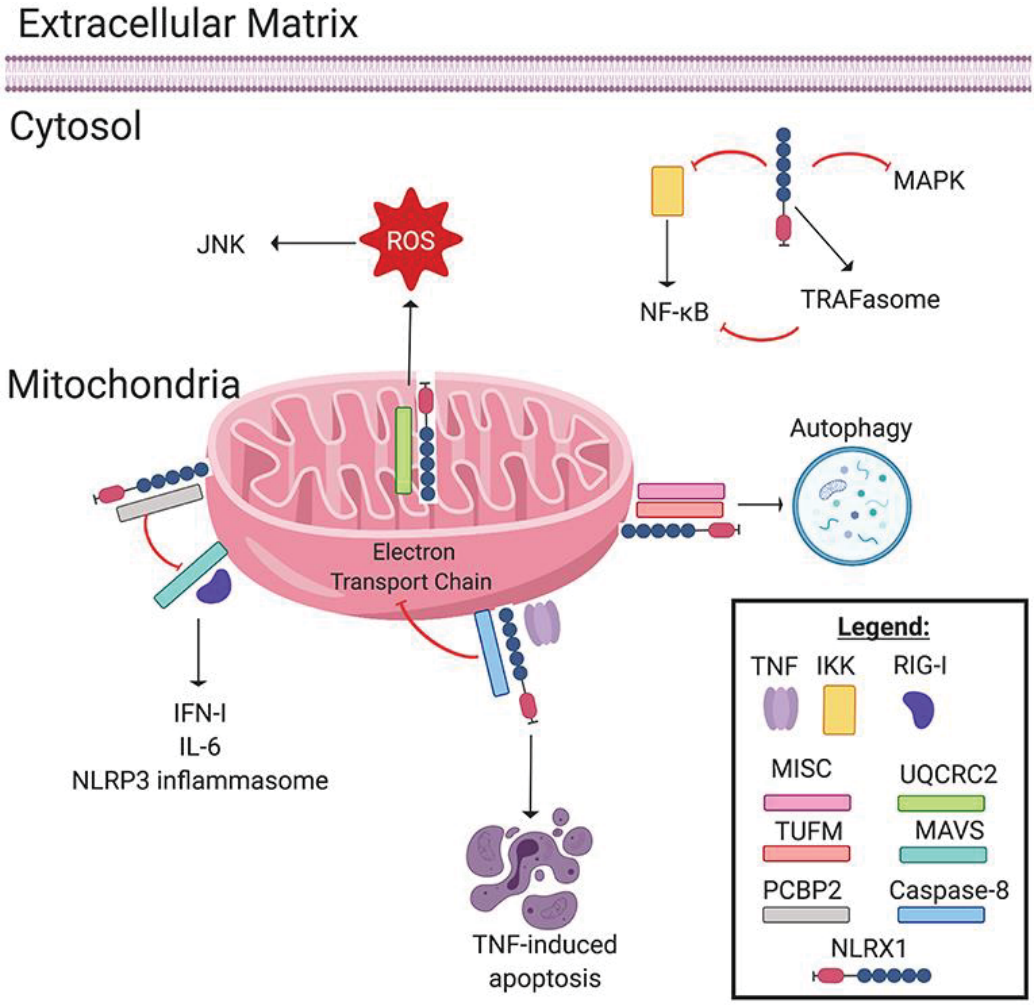

TABLE LEGENDS

Table 1: NLRX1 modulates diverse diseases and host-pathogen interactions.

TABLES

Table 1:

Disease/infection	Mechanism	References
Acute myocardial ischemia (AMI)	NLRX1 has a protective role in myocardial ischemic injury by inhibiting inflammation and hypoxia-induced apoptosis.	(14)
Breast cancer	NLRX1 modulates mitochondrial functions to suppress tumorigenesis in solid tumors, but may facilitate aggressive breast cancer metastasis.	(15)
Chlamydia trachomatis	ROS production induced by NLRX1 creates optimal conditions for Chlamydial growth.	(16)
Chronic Obstructive Pulmonary Disease (COPD)	NLRX1 expression is suppressed in murine models of CS-induced activation of the inflammasome and lungs of human COPD patients. NLRX1 likely inhibits CS-induced pulmonary inflammation by regulating MAVS.	(17, 18)
Colitis-associated cancer/Sporadic Colon Cancer	In *Nlrx1*$^{-/-}$ CAC murine models, mice were more susceptible to CAC pathogenesis. Increased signaling of common cancer-promoting pathways including NF-κB, MAPK, STAT3, and IL-6 were observed.	(8)
Colitis/Inflammatory Bowel Disease (IBD)	NLRX1 has a protective role against IBD due to its effect on the microbiome and negative regulation of inflammation.	(19)
Deafness (aging and neomycin induced)	NLRX1 aggravates apoptosis of cochlear hairs and may play a role in hair cell maturity.	(20)
Experimental Autoimmune Encephalomyelitis (EAE)/Multiple Sclerosis (MS)	NLRX1 is protective against neurological diseases by negatively regulating inflammation. NLRX1 may be protective against additional neurological diseases, including Parkinson's and Alzeihmer's diseases, by maintaining glutamate homeostasis in the central nervous system.	(21–23)
Hepatitis C (HCV)	NLRX1 promotes HCV infection by interacting with PCBP2 to inhibit MAVS via K48-linked polyubiquitination.	(24)
Helicobacter pylori	*Helicobacter pylori* infection promotes inflammation and can lead to gastric cancer. NLRX1 expression is decreased in Chinese gastric cancer patients.	(25)
Hepatocellular carcinoma (HCC)	NLRX1 expression is decreased in human HCC patients.	(26, 27)
Histiocytic sarcoma	NLRX1 may suppress tumorigenesis by inhibiting NF-κB signaling in mice.	(28)
Hyperglycemia	Decreased expression of NLRX1 may be protective against diet-induced hyperglycemia due to decreased pancreatic lipid accumulation.	(29)
Human immunodeficiency virus (HIV)	NLRX1 expression affects HIV infections, but seems to act controversially. NLRX1 expression is decreased in human HIV patients, but NLRX1 promotes establishment of latent HIV-1 reservoirs in mice.	(30–32)
Influenza A Virus (IAV)	NLRX1 interacts with the influenza PB1-F2 protein to protect macrophages from apoptosis, but also downregulates IFN-β and IL-6 production.	(7, 33)
Kaposi's sarcoma-associated herpesvirus (KSHV)	NLRX1 decreases IFN-1 production, which encourages KSHV to reactivate out of the latency stage.	(34)
Listeria monocytogenes	NLRX1 promotes *L. monocytogenes*- induced mitophagy, helping *L. monocytogenes* to evade killing.	(35)
Nonalcoholic steatohepatitis (NASH)	NLRX1 expression is decreased in NASH mouse models.	(36)
Osteoarthritis (OA)	NLRX1 has a protective role in OA. When upregulated, NLRX1 inhibits NF-κB signaling, which inhibits LPS-induced apoptosis and inflammation in chondrocytes that contribute to OA.	(37)
Periodontitis	NLRX1 expression is increased in human adult periodontitis patient samples.	(38)
Porcine Reproductive and Respiratory Syndrome Virus (PRRSV)	NLRX1 interacts with Nsp9 to restrict viral replication.	(39)
Preterm birth	NLRX1 is expressed in human placenta, amnion, and choriodecidua samples, suggesting that it may play a role in preterm birth-related inflammation.	(40)
Renal ischemia-reperfusion injury	NLRX1 is protective in mouse models of renal ischemia-reperfusion injury, and NLRX1 expression is reduced in human kidney samples with ischemic injury.	(41)
Rheumatoid arthritis (RA)	NLRX1 expression is significantly decreased in human RA patient synovial tissue samples.	(42)
Rhinovirus	NLRX1 interaction with Rhinovirus RNA promotes ROS production, leading to the disruption of epithelial barrier function in the airway.	(43)
Salmonella enterica serovar Enteritidis (SE)	NLRX1 is significantly upregulated in the follicles of ducks that are susceptible to SE and SE-infected ducks. NLRX1 is believed to increase recognition of SE by the host.	(44)
Shigella flexneri	NLRX1 promotes ROS production activated by *Shigella* infection, which promotes signaling pathways dependent on NF-κB and Jun amino-terminal kinases (JNK).	(3)
Systemic Lupus Erythematosus (SLE)	NLRX1 expression did not affect MAVS aggregation, but cytosolic NLRX1 was found in SLE patients.	(11)
Traumatic brain injury (TBI)	*Nlrx1*$^{-/-}$ murine models have significantly increased NF-κB signaling, which contributes to increased numbers of microglia and macrophages in cortical lesions. NLRX1 is significantly decreased in human post-aneurysm brain injury patients.	(45)
Type 2 Diabetes Mellitus (T2DM)/Diabetic Nephropathy (DM)	NLRX1 polymorphism rs4245191 is a risk factor for T2DM complications including macrovascular complications and cerebral infarction due to its mutated form. Interestingly, NLRX1 does not have a role in DN.	(46, 47)

CHAPTER THREE

Using Computer-based Image Analysis to Improve Quantification of Lung Metastasis in the 4T1 Breast Cancer Model

Margaret A. Nagai-Singer[1], Alissa Hendricks-Wenger[1,2,3], Rebecca M. Brock[1,2], Holly A. Morrison[1], Juselyn D. Tupik[1], Sheryl Coutermarsh-Ott[1], Irving C. Allen[1,2,4]

[1]Department of Biomedical Sciences and Pathobiology, Virginia-Maryland College of Veterinary Medicine
[2]Graduate Program in Translational Biology, Medicine and Health, Virginia Polytechnic Institute and State University
[3]Department of Biomedical Engineering and Mechanics, Virginia Polytechnic Institute and State University
[4]Department of Basic Science Education, Virginia Tech Carilion School of Medicine, Virginia Polytechnic Institute and State University

Reprinted with the permission of the Journal of Visualized Experiments (JoVE). This is adapted from: Nagai-Singer, M. A., Hendricks-Wenger, A., Brock, R. M., Morrison, H. A., Tupik, J. D., Coutermarsh-Ott, S., Allen, I. C. Using Computer-based Image Analysis to Improve Quantification of Lung Metastasis in the 4T1 Breast Cancer Model. J. Vis. Exp. (164), e61805, doi:10.3791/61805 (2020).

ABSTRACT

Breast cancer is a devastating malignancy, accounting for 40,000 female deaths and 30% of new female cancer diagnoses in the United States in 2019 alone. The leading cause of breast cancer related deaths is the metastatic burden. Therefore, preclinical models for breast cancer need to analyze metastatic burden to be clinically relevant. The 4T1 breast cancer model provides a spontaneously-metastasizing, quantifiable mouse model for stage IV human breast cancer. However, most 4T1 protocols quantify the metastatic burden by manually counting stained colonies on tissue culture plates. While this is sufficient for tissues with lower metastatic burden, human error in manual counting causes inconsistent and variable results when plates are confluent and difficult to count. This method offers a computer-based solution to human counting error. Here, we evaluate the protocol using the lung, a highly metastatic tissue in the 4T1 model. Images of methylene blue-stained plates are acquired and uploaded for analysis in Fiji-ImageJ. Fiji-ImageJ then determines the percentage of the selected area of the image that is blue, representing the percentage of the plate with metastatic burden. This computer-based approach offers more consistent and expeditious results than manual counting or histopathological evaluation for highly metastatic tissues. The consistency of Fiji-ImageJ results depends on the quality of the image. Slight variations in results between images can occur, thus it is recommended that multiple images are taken and results averaged. Despite its minimal limitations, this method is an improvement to quantifying metastatic burden in the lung by offering consistent and rapid results.

INTRODUCTION

One in eight women will be diagnosed with breast cancer in her lifetime, and yet despite multiple treatment options breast cancer is the second leading cause of cancer-related deaths in American women[1]. These women are not dying from the primary tumor in their breast. Instead, the metastatic burden is responsible for the mortality of this disease as it commonly spreads to the lung, bone, brain, liver, and lymph nodes[2]. Because of this, breast cancer models need to evaluate metastasis to contribute to curbing the mortality of this disease. The 4T1 murine breast cancer model is a superb protocol to accomplish this. The method described here offers an improvement to the 4T1 model by using Fiji-ImageJ to quantify lung metastasis, producing consistent and expeditious results.

The 4T1 model is well-established, with most labs using protocols such as those described by Pulaski and Ostrand-Rosenberg in 2001[3]. The 4T1 cell line is 6-Thioguanine (6TG) resistant and representative of stage IV, triple negative breast cancer[3,4,5]. It is clinically relevant as it is an orthotopic model and spontaneously metastasizes to the same organs as in human breast cancer[3,4]. The 4T1 cells spontaneously metastasize at a predictable rate based on the quantity of cells injected[3,4]. Importantly, genetic differences between mice used here caused expected inter-individual variability in metastatic burden. To evaluate metastasis, tissues are harvested to collect and quantify cancer cells in distant sites using 6TG selection and methylene blue staining. The result is a collection of tissue culture plates with blue dots representing metastatic colonies. However, the Pulaski and Ostrand-Rosenberg protocol quantifies metastatic colonies by manually counting them, and therefore this has been the standard means of evaluating metastasis in this model. While this is easy for tissues with low metastatic burden, tissues like the lungs are often laden with metastases. As lung plates can be highly confluent, accurately and precisely quantifying metastatic colonies by manual counting is difficult and prone to human error. To better quantify metastatic burden, we describe using Fiji-ImageJ for a computer-based solution to human counting error. Histopathological analysis with hematoxylin and eosin (H&E) staining is another means to quantify lung metastases, and interestingly has also been improved with Fiji-ImageJ software[6,7]. However, because histopathological analysis observes a single slice of the lung, it can be inaccurate and unrepresentative. This is because the 4T1 model causes several metastatic lesions throughout the organ that are not evenly distributed. While overall trends between histopathological analysis and manual counting can be similar[8], individual values can differ and therefore histopathological analysis should not be used as the sole means of quantification. We demonstrate the benefit compared to histopathological analysis and the inconsistencies in manual counting between different counters, while also demonstrating the consistency of using Fiji-ImageJ. Additionally, we show that this method can reduce the incubation time from 10-14 days to 5 days, meaning researchers can analyze data from their study much sooner than when relying on manual counting.

This method is a collection of simple adjustments to the Pulaski and Ostrand-Rosenberg protocol[3]. Because the 4T1 model is widely used, and because lung metastasis is a critical parameter to measure in preclinical models, we believe this method can be widely used and is

highly valuable to breast cancer researchers. The only additional supplies needed are a camera and access to a computer with Fiji-ImageJ, a free software used frequently in image analysis[9]. This method specifically focuses on lung metastasis, but it could be used for other tissues with significant metastatic burden.

PROTOCOL

All methods described here have been approved by the Institutional Animal Care and Use Committee (IACUC) of Virginia Tech and in accordance with the National Institutes of Health Guide for the Care and Use of Laboratory Animals. Performing this protocol requires permission from the appropriate institutions and adherence to all appropriate guidelines.

1. Cell Culture

1. Make complete culture media (RPMI + 10% Fetal Bovine Serum +1% Pen Strep). Revive 4T1 cells according to ATCC Protocol[10] and incubate at 37 °C and 5% CO_2 in a T-25 flask until confluent. Change media the day after reviving to remove dead cells, and again if media is spent before cells are confluent enough to passage.

2. Once the T-25 flask is confluent, passage cells to a T-75 flask by discarding media, washing flask with 5 mL of 1x Dulbecco's Phosphate Buffered Saline (DPBS), and adding 500 µL of Trypsin-EDTA. Incubate for 5-10 minutes at 37 °C until cells detach.

    1. Once detached, add 5 mL of warmed complete culture media to cells. Aspirate and transfer the 5 mL to a T-75 flask containing 15 mL of warmed complete culture media.

3. Passage cells in T-75 flasks at least four times. Do this once the flask is confluent by washing with 8 mL of 1x DPBS, adding 1 mL of Trypsin-EDTA for detaching cells, adding 10 mL of warmed media to cells, and diluting 1:6-1:8 into a new T-75 flask containing 20 mL of warmed complete culture media.

4. Passage cells up to the appropriate number of T-150 flasks containing 40 mL of warmed complete culture media for the number of mice to be injected. Most studies will require multiple T-150 flasks to ensure enough cells for injection.

5. When mice are ready to be injected (8 weeks old or weighing over 20 g, depending on the IACUC or institutional protocols), harvest cells by discarding media, washing each flask with 10 mL of 1x DPBS and adding 2 mL of trypsin-EDTA. Incubate for 5-10 minutes at 37 °C until cells detach.

6. Wash flask with 10 mL of complete media and transfer all contents (10 mL of media + 2 mL of trypsin-EDTA cell mixture) to the next flask. Continue to wash and collect cells from each flask using the same 10 mL of media to avoid using an excessive amount of media.

    1. Once all flasks have been collected, transfer the contents into a 50 mL centrifuge tube. Collect a 10 µL sample for counting in a microcentrifuge tube and centrifuge the 50 mL conical tube at 125 x *g* for 5 minutes.

7. While cells are being centrifuged, add 10 µL of Trypan blue to 10 µL of cell sample. Count cells using a hemocytometer. Once the total number of cells is determined, calculate the concentration of cells needed to inject mice for 1.2 x 10^6 cells per mouse (per 100 µL).

8. After centrifugation, decant media and resuspend cell pellet in correct amount of sterile 1x DPBS for 1.2 x 10^6 cells per 100 µL. Split cell/DPBS mixture into microcentrifuge tubes for easy access with the syringe when aspirating cells for injection. Keep cells on ice and inject soon thereafter as cells will begin to die after being on ice for extended periods of time.

2. Injections

1. Prepare cells for injection by tapping or gently mixing the microcentrifuge tube to resuspend the cells, and then aspirate 600 µL into a 1 mL syringe. Turn the syringe upwards and pull the plunger down to bring cells away from the syringe opening. Tap the syringe to rid it of air bubbles.

2. Attach the needle bevel up and dispense cells back into the microcentrifuge tube until only 500 µL remain in the syringe. Put syringe flat on ice.
NOTE: 4T1 cells fall out of suspension quickly. Therefore, it is important to mix cells back into suspension by tapping frequently.

3. Anesthetize 8 week old/>20 g female BALB/c mouse using isoflurane or other approved anesthetic agent. Monitor the mouse's breathing to assess depth of anesthesia.

4. Once the mouse is properly anesthetized as indicated by lack of corneal reflex, place the mouse on its back. Using the thumb, pointer, and middle finger, gently hold down the mouse. Use the pointer and middle fingers to hold down the mouse's upper body and thumb for its rear left leg. Be gentle but firm.

5. With the bevel of the needle up, inject 100 µL of cells subcutaneously into the mouse's left abdominal mammary fat pad. Monitor for a good bleb and any leakage, and ensure the mouse wakes up and moves easily after injection.

    1. Change needles between each mouse.
    NOTE: Do not allow needle to enter the peritoneal cavity. This would cause the cancer to spread quickly and not be representative of the model. To ensure a subcutaneous injection, gently pull upwards on the needle when inserted in the left abdominal mammary fat pad. If the needle is easily lifted upwards, it is correctly positioned subcutaneously.

3. Monitoring

1. Monitor mice at least 3 times a week for weight, body condition score, tumor size, tumor condition, respiration, activity level, appearance, and movement. Once the tumor reaches 0.7-0.8 cm in diameter, begin to monitor daily.

    1. Consider euthanasia when tumor size reaches 1.5 cm, or weight loss reaches 20%, or severe clinical decline in body condition score, tumor condition, respiration, activity level, appearance, or movement are observed based on institutional guidelines.
    NOTE: Body condition score is crucial to monitor as body weight may increase as the tumor increases in size, negating body condition loss due to disease burden. Exact monitoring protocols will depend on the approved IACUC or institutional protocols.

4. Necropsy

1. Euthanize mouse using CO_2 following institutional guidelines.
2. Spray mouse with 70% ethanol to disinfect. Make an incision up the ventral midline of the mouse to expose the body cavity.
3. Remove the kidney. Continue cutting up the midline until the diaphragm is visible. Use scissors to puncture the diaphragm to deflate the lungs. Trim the diaphragm to get better access to the cavity.
4. Use blunt scissors to cut up the center of the ribcage. Pin ribcage back to expose the lung and heart.
5. Perfuse the heart with 2 mL of non-sterile 1x DPBS by inserting a needle into the apex of the heart until it pools in the abdominal cavity where the kidney was removed.
6. To remove the heart and lungs, use blunt scissors to cut the esophagus and trachea directly above the heart. Using forceps, begin to pull the heart away from the body and cut away at any connective tissue keeping it attached. The lungs will come out with the heart.
7. Identify the multi-lobed (right) and single-lobed (left) lungs. Keep heart attached for reference, but once lungs are identified, cut the heart away.
8. Label a 12 well plate containing 1x Hank's Balanced Saline Solution (HBSS) in each well. Each mouse needs 2 wells. Place the multi-lobed (right) lung in the 12 well plate for metastasis evaluation and keep on ice. Keep the neighboring well empty for now. NOTE: It is important to use the same lung (multi-lobed) from every mouse to ensure each sample is close in size. The single-lobed lung can then be used for other analysis, like histopathology.
   NOTE: Samples are stable on ice or at 4 °C for a few hours.

5. Processing Tissues

NOTE: All steps in this section should be done using sterile technique.

1. Label 1 15 mL conical tube per mouse and add 2.5 mL of type IV collagenase mixture and 30 units of elastase to each tube. To make type IV collagenase mixture, dissolve 2 mg of

type IV collagenase per mL 1x HBSS and sterile filter. This can be stored up to 12 months at -20 °C and thawed when needed.

2. Transfer the lung to the second, clean 1x HBSS well for that sample. Swirl using forceps to remove any remaining blood. Transfer clean lung to empty 3.5 cm tissue culture plate. Mince lung with scissors. Rinse plate with 2.5 mL of 1x HBSS, transfer 1x HBSS and lung pieces into a 15 mL conical tube already containing collagenase/elastase cocktail (5 mL total).

3. Incubate for 75 minutes at 4 °C. Continue mixing samples during this time, so place tubes on a rocker or rotating wheel. During this incubation step, label 50 mL centrifuge tubes and 10 cm tissue culture plates for each mouse. If doing a dilution, label enough 10 cm tissue culture plates for the dilutions.
NOTE: Label the lid of the tissue culture plates. If labeling the plate itself, the writing will interfere with Fiji-ImageJ analysis.

4. Bring volume of each tube up to 10 mL total with 1x HBSS. Pour contents over a 70 μm cell strainer into a 50 mL conical tube for each sample. Use the plunger of a 1 mL syringe to gently grind the sample through the strainer to allow more cells to filter through.

5. Centrifuge for 5 minutes at 350 x *g* at room temperature (RT). Discard the supernatant and wash pellet with 10 mL of 1x HBSS. Repeat this step twice.

6. Resuspend pellet in 10 mL of 60 μM 6TG complete culture media, either RPMI or IMDM. Plate samples in 10 cm cell culture plates, using a dilution scheme if desired. Incubate at 37 °C, 5% CO_2 for 5 days.
NOTE: 1:2, 1:10, and 1:100 are common dilutions that will need to be empirically determined based on study parameters.
CAUTION: 6TG is toxic. Use caution when handling and follow all Environmental Health and Safety guidelines for disposal.

6. Staining plates

1. Pour culture media off plates into appropriate waste container. Fix cells by adding 5 mL of undiluted methanol per plate and incubate for 5 minutes at RT, making sure to swirl

methanol so that it covers the entire plate. CAUTION: Methanol is hazardous if ingested, inhaled, or is on skin. Use a fume hood for this step.

2. Pour methanol off plates into appropriate waste container. Rinse plates with 5 mL of distilled water per plate and pour water into appropriate waste container. Add 5 mL of 0.03% methylene blue per plate and incubate for 5 minutes at RT, making sure to swirl methylene blue solution so that it covers the entire plate.

3. Pour methylene blue into appropriate waste container. Rinse plates again with 5 mL of distilled water per plate. Turn plates upside down and blot against a paper towel to remove excess liquid. Place plate on its lid and let air dry overnight at RT. NOTE: Metastatic colonies will be blue. Once plates are dried, they can be stored at RT indefinitely.

7. Image analysis

1. Remove labeled lids from plates, taking care to ensure clear identification of samples. Line up all stained lung plates on a clean, light surface to take a picture of all of the plates in one image.

2. Take a picture of the collection of plates in a well-lit area, making sure to minimize reflections as the plates are very reflective. Reflections in the plates will influence image analysis and therefore need to be avoided. NOTE: Fiji-ImageJ has an upper limit of 2 gigapixels. Most modern smart phones will have sufficient cameras. Do not use a camera less than 8 megapixels. The camera used in this experiment was a 12.2 megapixel on a Google Pixel 2.

3. Crop the image to include the plates, but exclude the lids or anything else in the background of the image. Upload the cropped image into Fiji-ImageJ.

4. Change the image to black and white using the following commands: Image, Adjust, Color Threshold, Thresholding method: Default, Threshold color: B&W, Threshold space: Lab. Unselect the Dark background box. The image should now be black and white. Black represents the light background, and white represents the blue metastatic colonies.

5. Using the Circle tool on the Fiji-ImageJ toolbar, select the area to be analyzed. Draw one circle to use for all of the plates to ensure each plate is analyzed for the same-sized area. Choose a size that maximizes analyzed area on the plates while minimizing the background noise that appears on the edge of the plates. The size appears in the toolbar as it is drawn, so it is possible to make a perfect circle by monitoring the height and the width as the circle is drawn.

6. Analyze the selected circle to determine what percentage of the area is white, which represents the area of the plate that has blue metastatic colonies. Use the following commands:
   Analyze, Analyze Particles, Size (pixel^2): 0-Infinity, Circularity: 0.00-1.00, Show: Nothing, and check the Summarize box. Hit OK.

7. Record the % Area result. This is the percentage of the selected area that is white, and therefore represents the metastatic burden.
   NOTE: It is recommended to either save the results in Fiji-ImageJ or copy/paste the entire results page into a separate document. If % Area results are unexpected or suspicious, it is then possible to see if any of the other measurements were also suspicious or if % Area was recorded incorrectly.

8. Move the circle, without altering its size by grabbing it in its center, to the next plate in the picture. Repeat steps 7.6 and 7.7 for all plates in the picture.

9. Repeat steps 7.1 – 7.8 on at least two more images. Once all plates and images have been analyzed, average the % Area results between different images for each plate to mitigate any inconsistencies between pictures.

REPRESENTATIVE RESULTS

This method contains simple adjustments from the Pulaski and Ostrand-Rosenberg 4T1 protocol[3] and can be visualized in **Figure 1**. When 3 separate researchers manually counted metastatic colonies for 12 lung plates (1:10 dilution), the results were very inconsistent between different counters (**Figure 2A**). All researchers were directed to "count the metastatic colonies that appear as blue dots", yet the inconsistencies demonstrate the issue with manually counting highly-

metastatic plates. The researchers had varying levels of experience with the 4T1 model. A board-certified veterinary pathologist analyzed H&E stained lung slides for metastasis as another method to compare to Fiji-ImageJ lung plate analysis (**Figure 2B**).

Using the Fiji-ImageJ analysis, 3 separate researchers analyzed 3 separate images of the collection of 12 plates (1:2 dilution). Images were taken in two separate lab spaces with slightly different lighting. The arrangement of the plates or the angle from which the picture was taken were different between each image. In contrast to the manual counting results, the Fiji-ImageJ results were consistent between counters for each of the 3 images (**Figure 3A**). To determine if there were inconsistencies between the 3 images, the results from the 3 images and the 3 counters were combined per lung plate (**Figure 3B**). There are differences between images for some plates, but the overall trends are similar and it offers more consistency than manual counting. To account for the variations between the 3 different images, results from each image were averaged for each plate (**Figure 3C**). These averages provided consistent results between counters that accurately and precisely analyze metastatic burden. Therefore, this protocol suggests taking at least 3 images of the plate collection in different arrangements, from different angles, or in slightly different light settings, and then analyzing and averaging the results. The contrast between manual counting and Fiji-ImageJ analysis is visualized when comparing **Figure 2A** to **Figure 3C**.

Another way to demonstrate the improvements offered by this protocol is comparing the ranking of the plates from most to least metastatic burden between counters, based on the counts from **Figure 2** and **Figure 3**. Manual counting agreed on the most confluent plate, but all following ranks were inconsistent between counters (**Figure 4A**). Contrastingly, the ranks from Fiji-ImageJ analysis for each image were much more consistent between counters (**Figure 4B**). The consistency is also seen when results from each image for each plate were averaged (**Figure 4C**). We acknowledge that this protocol does not offer complete consistency between counters, but it is an improvement from manual counting when comparing **Figure 4A** to **Figure 4C**. Histopathological analysis differed from both manual and Fiji-ImageJ counting (**Figure 4D**).
To demonstrate the importance of avoiding reflections in the images, an image with a reflection of a hand and its subsequent Fiji-ImageJ analysis is shown (left) opposed to the same plate without a reflection (right) (**Figure 5A**). Other dark blemishes from a dirty background surface or blood

sample residue on the plates can negatively impact Fiji-ImageJ analysis too. The blood plate in **Figure 5B** only has 2 metastatic colonies (noted by white arrows), but the dark residue (noted by black arrows) caused Fiji-ImageJ to consider it as 31.6% metastatic. Therefore, it is important to have a clean, light surface and to not use this method for blood samples as blood samples will typically leave residual dark spots on the plate that are not metastatic colonies.

DISCUSSION

As demonstrated, manually counting the metastatic colonies on each lung plate can be an inaccurate and imprecise method to quantify lung metastasis, demonstrating the need for a better means of quantification (**Figure 2**). Histopathological analysis differed slightly from both manual counting and Fiji-ImageJ analysis (**Figure 2B and 4D**), likely because the H&E slides are not a representative sample of the entire organ. The protocol harvests an entire lung, and therefore is more representative of total lung metastasis, and is more consistent than manual counting. Several different approaches to Fiji-ImageJ analysis were attempted and are discussed below, but the protocol outlined above appears to be the superior method.

Lung, blood, and brain samples were collected for this study. However, the blood and brain samples had very few metastatic colonies, if any at all. We determined that manually counting the metastatic colonies is optimal for these less-metastatic tissues, and therefore blood and brain data were not included. When the metastatic burden is easy to manually count (e.g., ten or twenty metastatic colonies as opposed to thousands), the original issue of human error is not relevant, and therefore this protocol is not needed. Also, blood samples can leave dark spots on the plates after fixation, which interferes with the Fiji-ImageJ analysis (**Figure 5**). Importantly, the quantity of cells injected can influence the metastatic burden. For instance, if fewer cells are injected and the mice can survive longer, the cancer has more time to spread to the traditionally less-metastatic sites like the brain[3,4]. Therefore, this protocol could be modified to include the metastatic burden of other tissues if they are given time to become highly-metastatic. If trying the 4T1 model for the first time or changing the quantity of cells injected, we recommend trying at least two dilutions when plating cells. For this study, we used a 1:2 and 1:10 dilution. The 1:2 dilution would have been difficult to count manually, but was counted easily in Fiji-ImageJ. The 1:10 dilution was still

difficult to count manually and therefore led to inconsistent results. Dilutions can be modified based on the specific study parameters.

Pictures were taken of individual lung plates and the 12 lung plates together. Individual plates were analyzed in two ways: either cropping the image to a central square of the plate prior to uploading to Fiji-ImageJ, or using the circle selection tool in Fiji-ImageJ to select the central circle of the plate in the uncropped image. We found that using the circle selection tool in Fiji-ImageJ offered the easiest, most consistent way to create a same-sized area for analysis for all plates. Furthermore, analyzing the entire collection of lung plates in the same image was superior to analyzing individual images of single lung plates. Having all of the lung plates in the same image allows for the same-sized circle to be used easily between the lung plates. It ensures all lung plates are the same distance from the camera and therefore the same-sized circle for analysis should be the correct size for all lung plates in the image. It also makes analysis quicker as redrawing the circle is not necessary between plates. It is simply dragged to the next plate in the image without changing its size, which guarantees the same size is used for all plates in the picture. When selecting the size of the circle, it is important to make it large enough to analyze the majority of the plate while small enough to avoid the background noise from the edges of the plate. Furthermore, in an attempt to save reagents, cells were also plated in 6 well plates and compared to the 10 cm tissue culture plates. The Fiji-ImageJ results from the 6 well plates were less consistent and did not correlate to the 10 cm dishes (data not shown). One explanation is the smaller surface area provides a smaller area to analyze, leading to less representative data. Another is that reducing the surface area allows the cells to grow more quickly as they are closer to other surviving cells. Therefore, we do not recommend using any tissue culture reagents other than what we have described in the protocol.

As mentioned before, avoiding reflections and having a clean, light background are absolutely critical to this method. **Figure 5A** demonstrates how a reflection is analyzed in Fiji-ImageJ and therefore shows the critical importance of avoiding reflections. As tissue culture plates are highly reflective, it is beneficial to take the picture at a slight angle to avoid reflections from either yourself taking the picture or from the light sources above. The lighting conditions of the specific work area will need to be accounted for. We suggest taking multiple pictures of the plates

to be analyzed, trying slightly different arrangements and/or angles, in a well-lit area. Study the pictures intensely for any reflections. If there are inconsistencies in the analysis, it is likely due to a picture quality issue. To troubleshoot, compare the normal picture to the black and white picture. If areas that are not blue in the normal picture are appearing as white in the black and white picture, there is likely a reflection or blemish that is altering the results.

In addition to consistency, another notable benefit of this method is that it produces data much more quickly than manual counting. Manually counting multiple plates is very time-consuming, while Fiji-ImageJ analysis can be done quickly. It also allows for a shorter incubation time. Pulaski and Ostrand-Rosenberg recommend a 10-14 day incubation period for the plated cells, adding a substantial amount of time to the study[3]. The 10-14 day incubation period allows for larger, easier-to-count colonies to form. However, many lung plates can become confluent before then. Instead, 5 days of incubation gives enough time for the 6TG selection to kill non-cancerous cells (proven by healthy control mice not having any colonies on their lung plates, data not shown), and for the cells to grow enough to be easily quantified with Fiji-ImageJ. This significantly decreases the time between the mice being sacrificed and analyzing essential metastatic data.

To conclude, the benefits of this method far outweigh the limitations. We acknowledge this method does not offer perfect consistency. While this is not the ideal method for less-metastatic tissues, those tissues can easily be counted manually. While getting a picture without reflections can require some careful photography, the consistency gained with this method is significant. It is possible that this method could be used for other tissues that are highly-metastatic and other protocols that require counting stained objects. The study design could also allow for analyzing the rate of metastasis or effect of anti-cancer treatments on metastasis. This method will provide highly-consistent, reliable metastasis data and represents a significant refinement to the 4T1 model. The application of this model to upcoming breast cancer metastasis research is of utmost importance in arming researchers with tools to battle against breast cancer mortality.

DISCLOSURES

The authors have nothing to disclose.

ACKNOWLEDGEMENTS

This work was supported by the Virginia-Maryland College of Veterinary Medicine (IA), the Virginia Tech Institute for Critical Technology and Applied Science Center for Engineered Health (IA), and National Institutes of Health R21EB028429 (IA).

REFERENCES

1. American Cancer Society. Cancer Facts & Figures. *American Cancer Society*. (2019).
2. Yousefi, M., *et al.* Organ-specific metastasis of breast cancer: molecular and cellular mechanisms underlying lung metastasis. *Cellular Oncology*. **41**, (2), 123-140 (2018).
3. Pulaski, B. A., Ostrand-Rosenberg, S. Mouse 4T1 breast tumor model. *Current Protocols in Immunology*. Chapter 20, Unit 20.22 (2001).
4. Pulaski, B. A., Ostrand-Rosenberg, S. Reduction of established spontaneous mammary carcinoma metastases following immunotherapy with major histocompatibility complex class II and B7.1 cell-based tumor vaccines. *Cancer Research*. **58**, (7), 1486-1493 (1998).
5. Aslakson, C. J., Miller, F. R. Selective events in the metastatic process defined by analysis of the sequential dissemination of subpopulations of a mouse mammary tumor. *Cancer Research*. **52**, (6), 1399-1405 (1992).
6. Sikpa, D., *et al.* Automated detection and quantification of breast cancer brain metastases in an animal model using democratized machine learning tools. *Scientific Reports*. **9**, (1), 17333 (2019).
7. Valkonen, M., *et al.* Metastasis detection from whole slide images using local features and random forests. *Cytometry A*. **91**, (6), 555-565 (2017).
8. Coutermarsh-Ott, S. L., Broadway, K. M., Scharf, B. E., Allen, I. C. Effect of Salmonella enterica serovar Typhimurium VNP20009 and VNP20009 with restored chemotaxis on 4T1 mouse mammary carcinoma progression. *Oncotarget*. **8**, (20), 33601-33613 (2017).
9. Schindelin, J., *et al.* Fiji: an open-source platform for biological-image analysis. *Nature Methods*. **9**, (7), 676-682 (2012).
10. ATCC. A.T.C.C. 4T1 (ATCC CRL2539) Product Sheet. *ATCC*. (2020).

TABLE LEGENDS:

Materials table.

TABLES:

Name	Company	Catalog Number	Comments
Anesthesia chamber	See comments	See comments	Use approved materials in your institution's policies
Anesthetic agent	See comments	See comments	Use approved materials in your institution's policies
BALB/c Female Mice	The Jackson Laboratory	000651	
Blunt scissors	Roboz	RS-6700	
Calculator	Any	Any	
Camera	Any	Any	Minimum of 8 megapixels
Centrifuge	Any	Any	Needs to be capable of 125 x g and 300 x g
CO2 euthanasia setup	See comments	See comments	Use approved materials in your institution's policies
Cold room, refrigerator, cold storage	Any	Any	
Computer with Fiji-ImageJ	Any	Any	Needs to be capable of running Fiji-ImageJ
Counting Chamber	Fisher Scientific	02-671-10	

Curved scissors	Roboz	RS-5859	
Distilled water	Any	Any	
Elastase	MP Biomedicals	100617	
Electronic scale	Any	Any	
Fetal Bovine Serum (FBS)	R&D Systems	S11150	
Forceps	Roboz	RS-8100	
Ice	N/A	N/A	
Incubator	See comments	See comments	Needs to be capable of 5% CO_2 and 37 °C
Methanol	Fisher Scientific	A412SK-4	
Methylene blue	Sigma-Aldrich	03978-250ML	
Penicillin Streptomycin	ATCC	30-2300	
Pins or needles	Any	Any	For pinning down mice during necropsy
Plastic calipers	VWR	25729-670	
RMPI-1640 Medium	ATCC	30-2001	
Rocker or rotating wheel	Any	Any	
Sharp scissors	Roboz	RS-6702	

Sterile disposable filter with PES membrane	ThermoFisher Scientific	568-0010	
T-150 Flasks	Fisher Scientific	08-772-48	
T-25 Flasks	Fisher Scientific	10-126-10	
T-75 Flasks	Fisher Scientific	13-680-65	
Tri-cornered plastic beaker	Fisher Scientific	14-955-111F	Used to weigh mice
Trypan blue	VWR	97063-702	
Trypsin-EDTA	ATCC	30-2101	
Type IV collagenase	Sigma-Aldrich	C5138	
3.5 cm tissue culture plates	Nunclon	153066	
1 mL syringe	BD	309659	
1.7 mL microcentrifuge tubes	VWR	87003-294	
10 cm tissue culture plates	Fisher Scientific	08-772-22	
12 well plate	Corning	3512	
15 mL centrifuge tube	Fisher Scientific	14-959-70C	

1X Dulbecco's Phostphate Buffered Saline (DPBS)	Fisher Scientific	SH30028FS	
1X Hank’s Balanced Saline Solution (HBSS)	Thermo Scientific	SH3026802	
27 g 1/2 in needles	Fisher Scientific	14-826-48	
4T1 (ATCC® CRL2539™)	ATCC	CRL-2539	
50 mL centrifuge tube	Fisher Scientific	14-959-49A	
6-Thioguanine	Sigma-Aldrich	A4882	
70 μM cell strainer	Fisher Scientific	22-363-548	
70% ethanol	Sigma Aldrich	E7023	Dilute to 70% with DI water

FIGURE LEGENDS

Figure 1: Protocol Schematic. This protocol focuses solely on analyzing lung metastasis in the 4T1 model. The general flow of this protocol includes growing 4T1 cells in culture, injecting BALB/c female mice with 4T1 cells in the left abdominal mammary fat pad, monitoring mice according to IACUC and institutional protocols, sacrificing mice and collecting the lung, collecting cells from the lung samples, plating and incubating cells in 6TG selection media, fixing and staining cells after 5 days, taking pictures of the plates, and analyzing using Fiji-ImageJ.

Figure 2: Manually counting metastatic cells and histopathological analysis have inconsistent results. A. 12 lung plates with a 1:10 dilution were manually counted by 3 separate researchers instructed to count metastatic colonies the same way, although experience with the model varied between researchers. The number of metastatic colonies counted varied greatly between researchers. **B.** Histopathological analysis identified and quantified individual tumor cell aggregates, classified as metastases, present in H&E stained lung slides. High, medium, and low magnification images of one representative slide are shown.

Figure 3: Fiji-ImageJ analysis is accurate and precise in determining metastatic burden. A. 12 lung plates with a 1:2 dilution were analyzed by 3 separate researchers in 3 separate images of the 12 lung plates. **B.** Results from each of the 3 images by each of the 3 researchers were combined. **C.** Results from each lung plate from the 3 images were averaged. One-way ANOVA with Tukey's multiple comparison test determined no significant differences between counters for each lung plate. Data are shown as mean + SD.

Figure 4: Fiji-ImageJ analysis provides more consistent ranking of metastatic burden compared to manual counting and histopathological analysis. A. The same lung plates from Figure 2 were ranked from most to least metastatic based on the manual counts from Figure 2. **B.** The same 12 lung plates from Figure 3 were ranked from most to least metastatic based on the Fiji-ImageJ analysis from Figure 3A. **C.** The averages from Figure 3C were ranked from most to least metastatic. **D.** Lung slides were ranked from most to least metastatic based on histopathological evaluation.

Figure 5: Reflections and non-metastatic dark spots will negatively impact results. A. An image with a reflection of a hand taking the picture disrupts the Fiji-Image J analysis, as shown in comparing the reflection Fiji-ImageJ analysis (left) to the correct Fiji-ImageJ analysis (right) **B.** Blood plates often leave leftover stains (black arrows) on the plates that are not metastatic colonies (white arrows).

FIGURES

Figure 1:

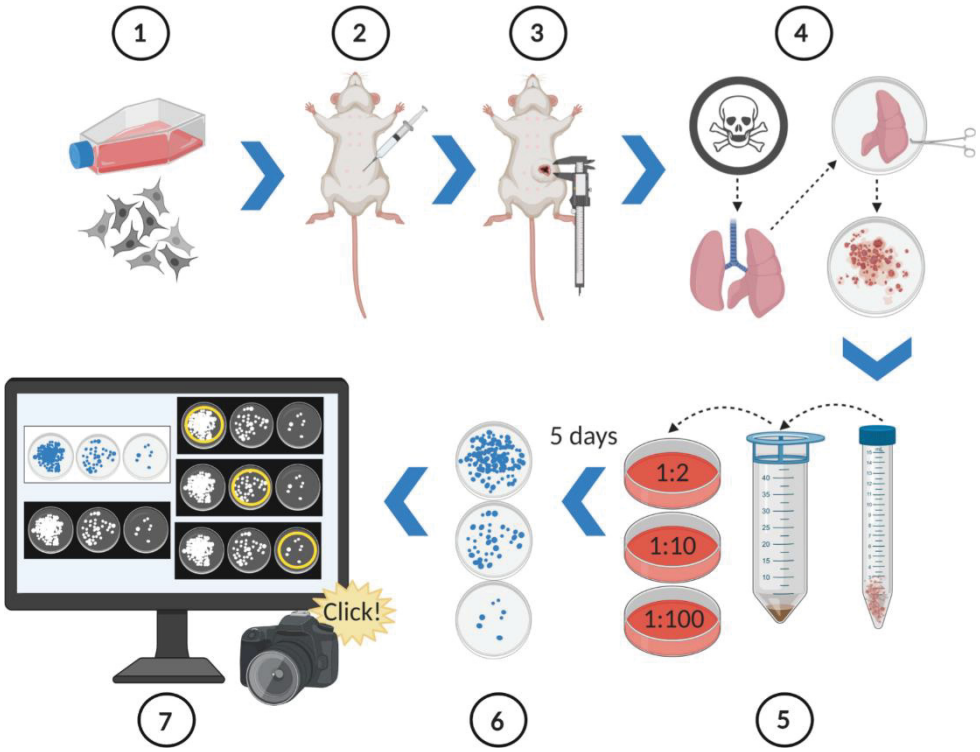

Figure 2:

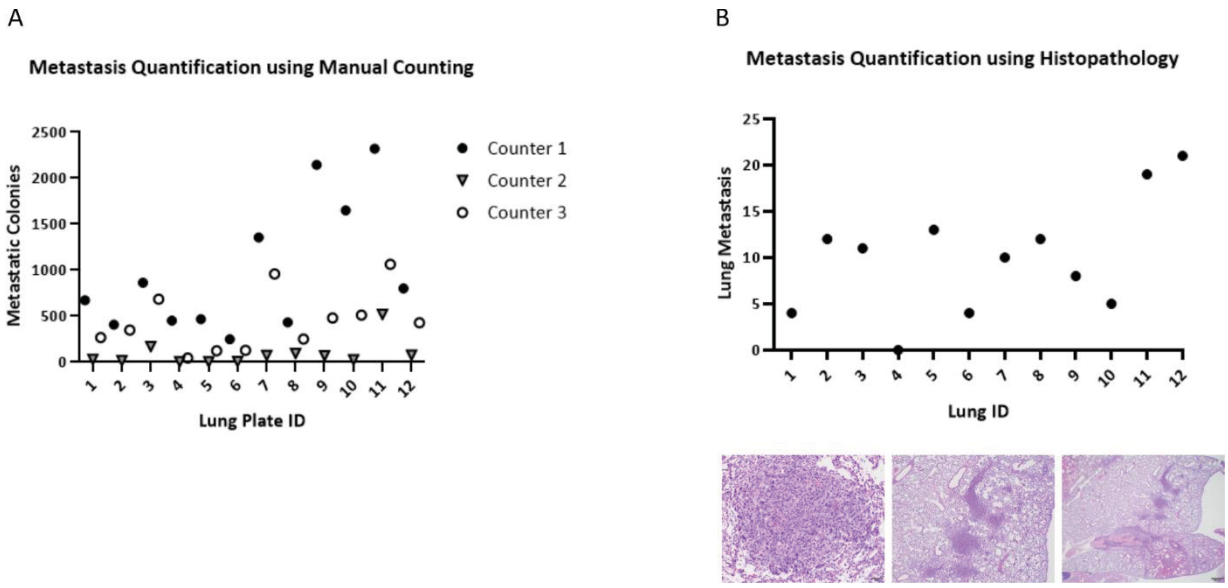
A
Metastasis Quantification using Manual Counting
Metastatic Colonies
2500
2000
1500
1000
500
0
Counter 1
Counter 2
Counter 3
1 2 3 4 5 6 7 8 9 10 11 12
Lung Plate ID
B
Metastasis Quantification using Histopathology
Lung Metastasis
25
20
15
10
5
0
1 2 3 4 5 6 7 8 9 10 11 12
Lung ID

Figure 3:

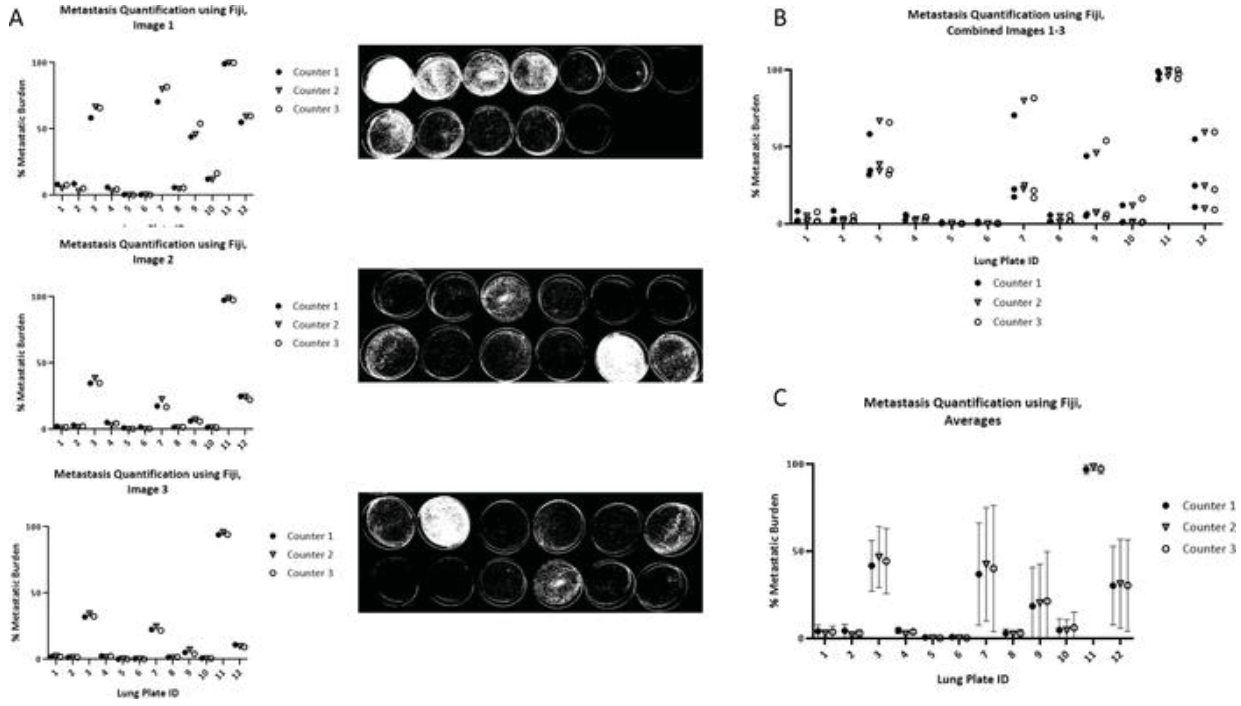
A
Metastasis Quantification using Fiji,
Image 1
% Metastatic Burden
Counter 1
Counter 2
Counter 3
Metastasis Quantification using Fiji,
Image 2
% Metastatic Burden
Counter 1
Counter 2
Counter 3
Metastasis Quantification using Fiji,
Image 3
% Metastatic Burden
Counter 1
Counter 2
Counter 3
Lung Plate ID
B
Metastasis Quantification using Fiji,
Combined Images 1-3
% Metastatic Burden
Lung Plate ID
Counter 1
Counter 2
Counter 3
C
Metastasis Quantification using Fiji,
Averages
% Metastatic Burden
Lung Plate ID
Counter 1
Counter 2
Counter 3

Figure 4:

A

	Counter 1	Counter 2	Counter 3
Most	11	11	11
	9	3	7
	10	8	3
	7	12	10
	3	7	9
	12	9	12
	1	1	2
	5	10	1
	4	2	8
	8	6	6
	2	4	5
Least	6	5	4

B

	Image 1			Image 2			Image 3		
	Counter 1	Counter 2	Counter 3	Counter 1	Counter 2	Counter 3	Counter 1	Counter 2	Counter 3
Most	11	11	11	11	11	11	11	11	11
	7	7	7	3	3	3	3	3	3
	3	3	3	12	12	12	7	7	7
	12	12	12	7	7	7	12	12	12
	9	9	9	9	9	9	9	9	9
	10	10	10	4	4	4	4	1	4
	2	1	1	2	2	2	1	4	1
	1	8	8	1	8	8	8	2	8
	4	2	2	6	10	1	2	8	2
	8	4	4	8	1	10	10	10	10
	5	6	6	10	6	6	6	5	5
Least	6	5	5	5	5	5	5	6	6

C

	Counter 1	Counter 2	Counter 3
Most	11	11	11
	3	3	3
	7	7	7
	12	12	12
	9	9	9
	10	10	10
	4	1	4
	2	4	1
	1	8	2
	8	2	8
	6	6	6
Least	5	5	5

D

	Histopathology
Most	12
	11
	5
	2
	8
	3
	7
	9
	10
	1
	6
Least	4

Figure 5:

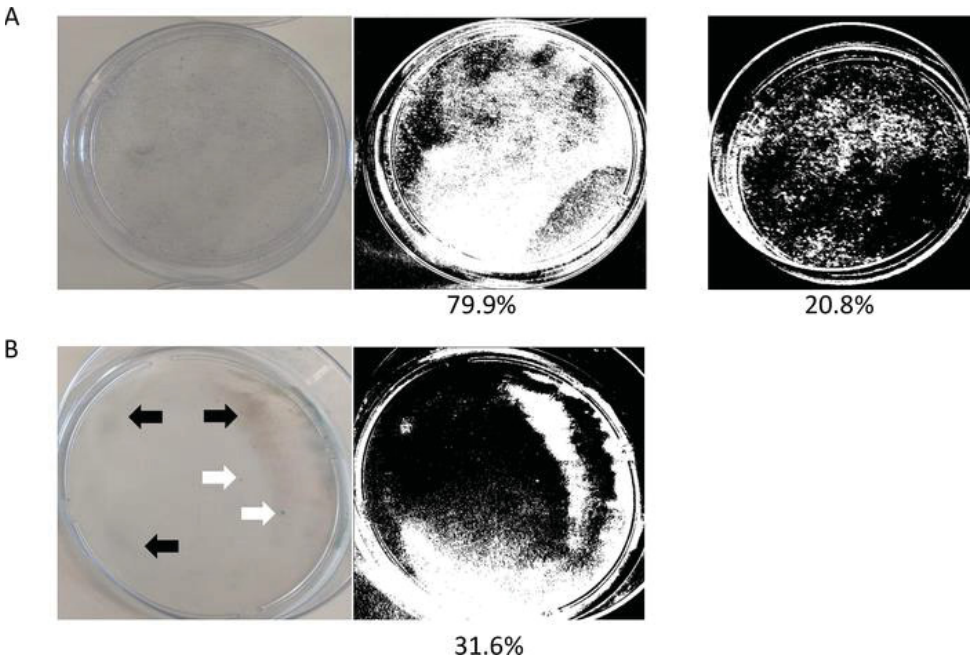

CHAPTER FOUR

The Dichotomous Role of NLRX1 in Triple-Negative Breast Cancer is Dictated by Cellular Context

Margaret A. Nagai-Singer[1], Mackenzie K. Woolls[1], Katerina Leedy[1], Alissa Hendricks-Wenger[2], Rebecca M. Brock[2], Sheryl Coutermarsh-Ott[1], Holly A. Morrison[1], Khan Mohammad Imran[2], Juselyn D. Tupik[1], Endia J. Fletcher[3], David A. Brown[4], Irving C. Allen[1]

[1] Department of Biomedical Sciences and Pathobiology, Virginia-Maryland College of Veterinary Medicine, Virginia Tech, Blacksburg, VA, United States.

[2] Graduate Program in Translational Biology, Medicine and Health, Virginia Tech, Roanoke, VA, United States

[3] Postbaccalaureate Research Education Program, Virginia Tech, Blacksburg, VA, United States

[4] Stealth BioTherapeutics, Needham, MA, United States

Running Title: NLRX1 differentially impacts 4T1 tumor progression

Keywords: NOD-like receptors, 4T1, breast cancer, epithelial-mesenchymal transition, metastasis

Funding: This work was funded by the National Institutes of Health, National Cancer Institute R01CA269811 and the National Institute of Biomedical Imaging and Bioengineering R21EB027979. The content is solely the responsibility of the authors and does not necessarily represent the official views of the National Institutes of Health. This work was also supported by the Virginia Maryland College of Veterinary Medicine, the Virginia Tech Center for Engineered Health, the Virginia Tech Institute for Critical Technology and Applied Science, and the Virginia Tech Center for Drug Discovery.

ABSTRACT

Triple-negative breast cancer (TNBC) is an aggressive, deadly, and difficult-to-treat malignancy. Prior studies have defined multiple, yet inconsistent, roles for NLRX1 in regulating biological functions that are important for driving a variety of cancer hallmarks. Here, we explore the role of NLRX1 in the murine triple-negative 4T1 mammary tumor model. Using novel *Nlrx1*$^{-/-}$ mice engrafted with 4T1 tumors, we demonstrate that NLRX1 functions as a tumor suppressor when expressed in healthy host cells by attenuating tumor growth and metastasis through regulating epithelial-mesenchymal transition (EMT), tumor associated eosinophil recruitment, and the lung metastatic niche. Conversely, using gain- and loss-of-function studies in 4T1 cells, we demonstrate that NLRX1 functions as a tumor promoter when expressed in the cancer cells. Attenuation of NLRX1 expression in 4T1 cells results in attenuated malignant properties *in vitro* and *in vivo*. These effects are partially restored when NLRX1 is overexpressed. In addition to EMT, we show that NLRX1 impacts these phenotypes through regulating cell death, migration, superoxide production, and mitochondrial respiration. Together, we provide critical insight into NLRX1 function in TNBC and establish cellular context as a regulator of NLRX1 function.

INTRODUCTION

One in eight females will be diagnosed with breast cancer in their lifetime, making it one of the most prevalent and deadly malignancies in the United States.[1] Triple-negative breast cancer (TNBC), which is characterized by the absence of the estrogen receptor (ER), progesterone receptor (PR), and HER2, is deadlier and more aggressive than other types of breast cancer with a 5-year survival rate of 12% if the cancer has metastasized to distant sites. TNBC tends to affect females who are less than 40 years of age, are Black, and/or have the *Brca1* mutation.[2] Many biological pathways and processes that are important to the initiation and progression of cancers, including TNBC, are regulated in part through proteins housed in the innate immune system known as pattern recognition receptors (PRRs). PRRs allow cells to sense pathogens, cellular damage, and stress and are often the first to respond to microenvironmental changes in tissue homeostasis which are highly relevant to tumorigenesis and disease burden.[3]

Specifically, PRRs recognize damage- and/or pathogen- associated molecular patterns (DAMPS and PAMPs, respectively) to initiate or regulate the subsequent immune response,

typically through the formation of multiprotein complexes. NOD-like receptors (NLRs) are a group of cytosolic PRRs that are best known for their ability to form a multiprotein complex known as the inflammasome, which initiates inflammation through the activation of caspase-1 and subsequent production of mature IL-18 and IL-1β.[4,5] While the inflammasome-forming NLRs are the best characterized and most recognizable, many NLR proteins do not directly participate in inflammasome formation.[6,7] These non-inflammasome forming NLRs are classified as regulatory NLRs, which function to either augment or attenuate various biological signaling pathways.[6] The majority of studies to date have focused on the role of these regulatory NLR family members in the regulation of inflammation, typically in the context of infectious diseases where they appear to regulate signaling associated with other PRRs, including Toll-like Receptor (TLR) and Rig-I-Like Helicase Receptor (RLR) signaling.[8–14] Consistent with the inflammasome-forming NLRs, the regulatory NLRs also appear to function through the formation of multiprotein complexes, such as the "NODosome" involving NOD1 (NLRC1) or NOD2 (NLRC2).[15] However, unlike the inflammasome-forming NLRs, the mechanisms underlying the majority of regulatory NLR functions are generally undefined and under-studied.[6,7]

NLRX1 is a unique and enigmatic regulatory NLR that generally functions to attenuate inflammation.[16,17] This has been best described in the context of host-pathogen immune signaling, where NLRX1 negatively regulates the interaction between RIG-I and MAVS to attenuate type-I interferon signaling and overzealous inflammation, which facilitates inflammation resolution following viral pathogen clearance.[10,11,18,19] Likewise, NLRX1 also attenuates pro-inflammatory canonical NF-κB signaling through the formation of a multiprotein complex that includes TRAF3 and TRAF6.[7,8,10] NLRX1 functions through a mechanism that is highly similar to two other regulatory NLRs, NLRC3 and NLRP12, that also attenuate inflammation through targeting canonical and noncanonical NF-κB signaling, respectively.[9,13,20] Each of these NLRs appear to independently limit NF-κB signaling through the formation of a multiprotein complex that includes TRAF molecules and has been dubbed the "TRAFasome", which modulates downstream ubiquitination events.[7–10,13,20]

In addition to attenuating RIG-I and NF-κB signaling, NLRX1 has also been shown to regulate other major signaling pathways that involve STAT, MAPK, JNK, and AKT signaling,

albeit through mechanisms that are not entirely defined.[21,22,22–27] Likewise, NLRX1 has also been shown to modulate reactive oxygen species (ROS) production, autophagy, and metabolism under specific biological conditions that are also not fully understood.[26–37] The regulation of these numerous and diverse pathways by NLRX1 suggests NLRX1 potentially contributes to a wide range of human diseases, including cancer.[7,16,17] Thus, it is critical to better characterize NLRX1 and define the mechanisms underlying its functions, especially in different disease models and cellular contexts.

The role of NLRX1 in several cancer models has proven to be enigmatic due in large part to conflicting data in the field between different types and subtypes of cancer. For example, NLRX1 has been suggested to function as a tumor suppressor in several models of colon cancer, including spontaneous and azoxymethane/dextran sodium sulfate (AOM/DSS) mouse models and human RKO colon cancer cells engrafted into mice.[21,25,28] NLRX1 also appears to protect against disease burden in histiocytic sarcoma and hepatocellular carcinoma models.[22,24] Interestingly, many of these phenotypes seem to be driven by pathways including ERK, STAT3, NF-κB, MAPK, and AKT signaling and through the non-hematopoietic compartment. Conversely, conflicting data have been reported that demonstrate NLRX1 can instead function as a tumor promoter. In an AOM-only model of colorectal cancer, the loss of NLRX1 improved disease outcome.[38] Additionally, similar findings were reported for HPV-associated head and neck squamous cell carcinoma where NLRX1 suppressed detection of HPV by inhibiting STING/IFN-I and CD8+ T cell function.[39] Together, these studies illustrate that in all models, genetic modification of NLRX1 clearly results in robust phenotypes; however, the tumor suppressing or tumor promoting role of NLRX1 is complex and nuanced.

The complexity of NLRX1 function extends to breast cancer, where its role remains understudied and conflicting. The role of NLRX1 in breast cancer appears to be impacted by the aggressiveness and type of breast cancer cell. For example, NLRX1 is upregulated in TNBC cell lines which lack ER and PR, compared to non-TNBC cell lines expressing ER and PR.[28,37] Likewise, in human tumors, NLRX1 is upregulated in ER/PR negative tumors and metastatic tumors compared to ER/PR positive tumors and early-stage tumors.[37] *In vitro,* NLRX1 overexpression in MCF-7 human breast cancer cells (ER/PR positive) demonstrated decreased

clonogenicity and migration. This observation was attributed to increased cleavage of caspase-8, mitochondrial ROS production, and decreased ATP production and suggested NLRX1 is tumor-suppressing.[28] Conversely, NLRX1 knockdown in MDA-MB-231 human TNBC cells (ER/PR negative) demonstrated decreased proliferation and migration. In this TNBC cell line, the phenotype was associated with the regulation of OXPHOS, mitochondrial ROS production, autophagy, mitochondrial turnover, and lysosomal function, and overall suggested NLRX1 is tumor-promoting.[37] These previous studies have clearly shown a role for NLRX1 in the modulation of biological functions during breast cancer. However, they lack *in vivo* studies and loss- and gain-of-function studies within a consistent cell line, limiting the exploration of NLRX1 on disease burden and restricting more comprehensive mechanistic studies.

To address these issues, we generated novel *Nlrx1*$^{-/-}$ mice on the BALB/cJ background, which is the strain required for the commonly-used 4T1 mouse mammary tumor model. We also generated 4T1 cell lines to conduct critical loss-of-function and gain-of-function studies within the same parental cell line both *in vitro* and *in vivo*. Here, using these unique mice and cell lines in combination, we show that the biological effects of NLRX1 in TNBC are cell type specific and highly dependent on the cellular context. Using *Nlrx1*$^{-/-}$ mice, we show that NLRX1 functions as a tumor suppressor in healthy host cells where it attenuates tumor progression and decreases metastasis by limiting epithelial-mesenchymal transition (EMT), the recruitment of pro-tumor eosinophils, and the formation of the metastatic niche in the lung. However, in the tumor cells themselves, NLRX1 augments tumor progression by increasing malignant properties, mitochondrial dysregulation, and metastasis through promoting EMT. Together, our data demonstrate a functional dichotomy between NLRX1 in healthy host cells versus in mammary tumor cells. By using *in vitro* and *in vivo* models that can be evaluated together and in parallel, our studies offer an explanation for at least some of the conflicting data generated to date related to NLRX1 and potentially other NLR family members.

MATERIALS AND METHODS

Cell Culture and Transfection

4T1 cells were obtained from ATCC and were cultured in RPMI 1640 (ATCC) supplemented with 10% fetal bovine serum (R&D Systems) and 1% penicillin streptomycin

(Thermo Fisher Scientific). Cells were incubated at 37°C and 5% CO_2. 4T1 cells were transduced to either knock down or overexpress murine NLRX1 using lentiviral shRNA technology (Origene) and ORF technology (Origene) according to the manufacturer's protocols, respectively. Antibiotic selection with 3 μg/mL puromycin (Santa Cruz Biotechnology) was used to select for transduced cells and successful overexpression or knockdown was confirmed by western blot for murine NLRX1 (Abcam). Cells were authenticated using morphology checks by microscope and commercial *Mycoplasma* testing (Charles River Research Animal Diagnostic Services) and were discarded before 30 passages.

Cell Migration Assay

Transduced 4T1 cells were seeded at 5 x 10^6 cells per well in a 6 well plate in complete media and incubated overnight. Media was then switched to 1% FBS media and incubated for 24 hours to allow cells to adjust to the decreased serum content. A 200 μL pipette tip was used to make 3 scratches per well for a "scratch" or "wound healing" assay. Initial images of each scratch were acquired directly following the scratch induction (Invitrogen EVOS M5000). At 5- and 8-hours post-scratch, images of each scratch were acquired at the same location of the initial image. Images were uploaded to Fiji-ImageJ and the width of the scratch was measured several times per image. Rate of migration was calculated as pixels per hour.

Proliferation Assay

Transduced 4T1 cells were seeded at 1 x 10^4 cells per well in a 96 well plate in complete media and incubated overnight. Media was then replaced with experimental media of complete media, +/- 10 ng/mL TNF (PeproTech), +/- 10 ng/mL TGF-β (R&D Systems) and allowed to incubate for 48 hours. An MTT assay was performed according to manufacturer's protocols (Abcam).

Cell Death Assay

Transduced 4T1 cells were seeded at 1 x 10^4 cells per well in a 96 well plate in complete media and incubated overnight. Media was then replaced with complete media, +/- 100 mM H_2O_2 (Fisher Chemical) and allowed to incubate for 6 hours. An LDH assay was performed according to manufacturer's protocols (Thermo Fisher Scientific).

Mitochondrial ROS Production

Transduced 4T1 cells were seeded at 1 x 10^5 cells per well in a 24 well plate in complete media and incubated overnight. Media was then replaced with complete media, +/- 10 ng/mL TNF (PeproTech) and incubated for 4 hours. MitoSOX (Thermo Fisher Scientific) and NucBlue (Thermo Fisher Scientific) were added to the wells per manufacturer's protocols. Several images per well were acquired with a fluorescent microscope (Invitrogen EVOS M5000). Fluorescent intensity of each image was measured using Fiji-ImageJ and corrected for background fluorescence in unstained samples.

Metabolism Assays

Transduced 4T1 cells were seeded at 1 x 10^4 cells per well in a 96 well Seahorse XF96 cell culture microplate (Agilent) in complete media and allowed to attach for 3 hours. Media was then replaced with experimental media of complete media, +/- 10 ng/mL TNF (PeproTech), +/- 10 ng/mL TGF-β (R&D Systems) and incubated for 24 hours. A Seahorse XF96 Mito Stress test (Agilent) was performed according to manufacturer's protocols at the Virginia Tech Metabolism Core. Respiratory capacity was calculated as (Maximal Respiration – Basal Respiration) of the final timepoint of each injection step and corrected for non-mitochondrial respiration.

Western Blotting

Protein was extracted from cells or tissues in a protein lysis buffer of 2% SDS, 100mM Tris HCl, 100mM NaCl, 1X protease inhibitor (Thermo Fisher Scientific) and quantified using a BCA assay (Thermo Fisher Scientific) according to manufacturer's protocols. Samples were loaded at 20 μg/mL with reducing sample buffer (Thermo Fisher Scientific) in pre-cast 4 to 12%, Bis-Tris Mini Protein Gels (Thermo Fisher Scientific), transferred to a PVDF membrane in 1X TGE + 20% methanol, and blocked in 5% milk in TBS + 0.1% Tween-20 (TBST). All antibodies were diluted 1:1000 in 5% BSA or 5% milk and incubated overnight at 4°C (CST and Abcam). TBST was used for all wash steps. Images were obtained with iBright (Thermo Fisher Scientific) or Odyssey XF (LI-COR) imaging systems using an HRP-conjugated secondary antibody (CST) and SuperSignal West Pico, Dura, or Femto Chemiluminescent Substrates (Thermo Fisher Scientific).

Flow Cytometry

Tumors and lungs were collected in cold RPMI and mechanically and/or enzymatically digested. Cells were counted with Trypan Blue and diluted to 1 x 10^7 cells per mL. 100 µL of each sample were collected in a microcentrifuge tube and fixed (Invitrogen) for 15 minutes in the dark. Fixed cells were resuspended in PBS and stored at 4°C in the dark until staining. Permeabilization was conducted on samples in Panel 2 (Invitrogen). Staining was conducted and samples were submitted to the Flow Cytometry Core at Virginia Tech. The flow cytometry panel can be found in **Supplemental Figure S1**.

Generation of BALB/cJ Nlrx1$^{-/-}$ Mice

BALB/cJ *Nlrx1*$^{-/-}$ mice were generated through 12 generations of backcrossing. C57/BL6J *Nlrx1*$^{-/-}$ mice (provided by Dr. Jenny Ting, UNC Chapel Hill) were crossed with WT BALB/cJ mice purchased from Jackson Laboratories to create *Nlrx1*$^{+/-}$ offspring.[10] Each generation of *Nlrx1*$^{+/-}$ offspring was crossed with WT BALB/cJ mice for 12 generations. F12 *Nlrx1*$^{+/-}$ mice were crossed with each other to generate the first BALB/cJ *Nlrx1*$^{-/-}$ offspring, which established the colony of BALB/cJ *Nlrx1*$^{-/-}$ mice. WT and *Nlrx1*$^{-/-}$ mice were maintained as separate colonies. All mice were housed under specific pathogen free (SPF) conditions and all experiments were conducted under the approval of the Virginia Tech Institutional Animal Care and Use Committee (IACUC) and the NIH Guide for the Care and Use of Laboratory Animals.

Genotyping

We confirmed the genotype of all mice generated from backcrossing. Tail snips were collected for DNA extraction. DNA extraction was performed using 25 mM NaOH/0.2 mM EDTA and 40 mM Tris-HCl. MyTaq (BioLine) and 3 *Nlrx1* primers (5' CCAGGCTCAGCATAATTTGTT 3', 5' AGCCGGAAGTCAAGGTTGAGG 3', and 5' AGCGCATCGCCTTCTATCGCCTTC 3') were used for PCR. PCR product was loaded into a 2% LE Agarose Gel with Ethidium Bromide and set to run for 60 minutes at 150 volts. Gel images were obtained with iBright (Thermo Fisher Scientific) or Odyssey XF (LI-COR) imaging systems.

In Vivo 4T1 Models

Experimental mice were all females between 2 and 5 months of age. Mice were anesthetized and injected with 1.2 x 10^6 4T1 cells (4T1, $4T1^{OE}$, $4T1^{OE\text{-}CTL}$, $4T1^{KD}$, or $4T1^{KD\text{-}CTL}$) in 100 µL sterile PBS in the left abdominal mammary fat pad. Tumor size was measured as the square root of tumor length x tumor width. Tumors were collected for final tumor volume, calculated as (3.14159/6) x length x width x height as previously described.[40] Sections of the tumors were fixed in 10% formalin for H&E analysis, flash frozen for RNA/protein extraction, or harvested for flow cytometry. Lungs were collected for metastasis quantification as previously described [41,42], as well as flash frozen for RNA/protein extraction or harvested for flow cytometry. Whole blood was collected for metastasis quantification as previously described.[42] All experiments were conducted with IACUC approval and in accordance with the NIH Guide for the Care and Use of Laboratory Animals.

Gene Expression and Transcriptomics

RNA was extracted from flash frozen tumors using a RNeasy Isolation Kit per the manufacturer's protocols (Qiagen). Total RNA from 4T1 tumors were pooled per genotype (WT and *Nlrx1*$^{-/-}$). Gene expression was evaluated with a murine breast cancer RT^2 Profiler PCR Array (Qiagen). Ingenuity Pathway Analysis (IPA) was used to determine pathways impacted by differentially expressed genes. For transcriptomics analysis, total RNA was pooled for 4T1, $4T1^{OE}$, or $4T1^{OE\text{-}CTL}$ tumors from each genotype (WT and *Nlrx1*$^{-/-}$) and gene expression was evaluated using microarray analysis (Clariom S, Applied Biosystems, Thermo Fisher Scientific). Data were analyzed using Transcriptome Analysis Console (Applied Biosystems, Thermo Fisher Scientific).

Statistical Analysis

Animal numbers were justified by a power analysis. Comparisons were analyzed using a two-way unpaired t-test or an ANOVA followed by Tukey's post-test for multiple comparisons as appropriate. Survival was analyzed using a Log-Rank Mantel-Cox test. All figures and analyses were completed in GraphPad Prism. Outlier tests were conducted to identify and remove any outliers in the data when appropriate.

Data Availability

The data generated in this study will be publicly available upon publication.

RESULTS

NLRX1 Expressed in Healthy Host Cells Attenuates Tumor Progression and Metastasis

NLRX1 is considered to be ubiquitously expressed in the majority of cells and tissues.[43] To determine the role of NLRX1 in healthy host cells on mammary tumor progression, we generated novel BALB/cJ *Nlrx1*$^{-/-}$ mice compatible with the 4T1 mammary tumor model. These mice were generated through 12 generations of backcrossing and were confirmed to lack a functional *Nlrx1* gene (**Supplemental Fig. S2A & B**). *Nlrx1*$^{-/-}$ and WT BALB/cJ mice were injected with 1.2 x 10^6 4T1 cells in a single mammary fat pad and were monitored for tumor growth, morbidity, and mortality. Additional WT and *Nlrx1*$^{-/-}$ mice were injected with sterile PBS for tumor-free controls (data not shown). During the course of the study, there were minimal differences in tumor growth (**Fig. 1A**) and no differences in morbidity (**Fig. 1B**) or mortality (**Fig. 1C**). However, because tumor measurements throughout the study only account for the length and width of the tumor, we additionally calculated final tumor volume of excised tumors so that tumor depth was included in the disease burden considerations. This revealed that *Nlrx1*$^{-/-}$ mice developed significantly larger tumors compared to the WT mice (**Fig. 1D**). *Nlrx1*$^{-/-}$ mice also exhibited a significant increase in metastatic burden in the lung compared to WT animals (**Fig. 1E-F**). *Nlrx1*$^{-/-}$ mice had increased blood metastasis that were approximately six times the levels found in WT animals; however, this assessment was highly variable in the *Nlrx1*$^{-/-}$ mice and results were not statistically significant ($p = 0.2$) (**Fig. 1G**). Histological analysis by a board-certified pathologist (SC-O) revealed no histopathologic or morphologic differences between 4T1 tumors from *Nlrx1*$^{-/-}$ mice and WT animals (**Fig. 1H**). Together, these data revealed phenotypes that suggest NLRX1 is protective against disease burden, specifically lung metastasis and tumor volume, when it is expressed by healthy host cells.

NLRX1 Expressed in Healthy Host Cells Decreases Metastasis by Limiting Epithelial-Mesenchymal Transition (EMT) and Eosinophil Recruitment

To begin uncovering the mechanism(s) responsible for NLRX1-mediated tumor suppression, we next evaluated gene expression using rt-PCR arrays and microarray analysis. Total RNA was extracted from 4T1 tumors collected from WT and *Nlrx1*$^{-/-}$ mice. Using a commercially-available and pathway-focused quantitative RT^2 Profiler PCR Array and whole transcriptome Clariom S microarrays, we performed pathway-focused evaluations and unbiased analyses to

identify genes and pathways altered in 4T1 tumors engrafted into WT and *Nlrx1*$^{-/-}$ mice. The unbiased microarray analysis identified the top 20 pathways significantly altered in tumors from *Nlrx1*$^{-/-}$ mice versus tumors from WT mice based on the number of differentially expressed genes (DEGs) in each pathway (**Fig. 2A**). This analysis revealed that many pathways associated with the pro-metastatic process of epithelial-mesenchymal transition (EMT) were significant (**Fig. 2A**). Specifically, in the absence of NLRX1, genes associated with EGFR1 signaling, focal adhesion, PI3K-Akt-mTOR, Kit receptor signaling, and TGF-β receptor signaling were all significantly upregulated compared to tumors generated in WT mice (**Fig. 2B**). Subsequent analysis of the DEGs in each of these EMT-related pathways revealed that the loss of NLRX1 was associated with gene transcription profiles correlated with the promotion of EMT in the 4T1 tumors (**Fig. 2B**). In total, we identified 12 DEGs that are highly relevant to EMT and appear to be regulated, at least in part, by the expression of NLRX1 in healthy host cells (**Fig. 2C, Supplemental Fig. S3A**).[44] To further validate that NLRX1 is indeed regulating EMT, we next analyzed protein levels of the epithelial marker E-Cadherin, which is commonly found to be downregulated in cells undergoing EMT.[45] The western blot data revealed a decrease in E-Cadherin in tumors from *Nlrx1*$^{-/-}$ mice compared to tumors from WT animals (**Fig. 2D, Supplemental Fig. S3B**). We also analyzed protein levels of TGF-β and MMP9, both of which promote EMT.[46] We found that tumors from *Nlrx1*$^{-/-}$ mice express more MMP9 and TGF-β, further suggesting a protective role for NLRX1 against EMT when expressed by healthy host cells (**Fig. 2E, Supplemental Fig. S3B**). Ingenuity Pathway Analysis (IPA) of the rt-PCR array data confirmed significantly upregulated pathways associated with EMT in the absence of NLRX1 and identified specific interactions most likely to result in the phenotypes observed in the *Nlrx1*$^{-/-}$ mice (**Fig. 2F, Supplemental Fig. S3C-D**). From these combined gene expression, transcriptomics, and western blot experiments, our data suggest that NLRX1 in healthy host cells acts in the mammary tumor to limit EMT by suppressing TGF-β, C-kit, and EGF receptors and therefore suppressing PI3K-AKT, ERK1/2, and β-Catenin pathways (**Fig. 2F, Supplemental Fig. S3C-D**). At the transcription factor level, *Zeb2* appears to be downregulated in the presence of NLRX1, which may also attenuate EMT. Together, these pathways converge on the regulation of E-Cadherin, which is significantly downregulated in the tumors from *Nlrx1*$^{-/-}$ mice (**Fig. 2F**).

Immune cells provide a critical niche that can facilitate tumor progression, invasion, and metastasis through the modulation of the EMT.[47,48] Thus, we next sought to define the tumor microenvironment immune niche using flow cytometry on the 4T1 tumors from WT and *Nlrx1*$^{-/-}$ mice. Using a well-defined panel of cell surface markers (**Supplemental Fig. S1**), no significant differences were identified in macrophage, M-MDSC, G-MDSC, cDC1, cDC2, inflammatory DC, B cell, natural killer cell, T reg, CD8+ T cell, CD4+ T cell, or double negative T cell populations in the tumor microenvironment (**Supplemental Fig. S3E**). However, tumors from *Nlrx1*$^{-/-}$ mice contained significantly more eosinophils (CD45+ CD11b+ CD11c- Ly6G- Ly6C-) than tumors from WT animals (**Fig. 2G-H**). Eosinophils can significantly impact the tumor microenvironment and drive EMT through the secretion of MMP9 and release growth factors like TGF-β.[49] This would be consistent with the increase in MMP9 and TGF-β observed in tumors from *Nlrx1*$^{-/-}$ mice (**Fig. 2E**). Additionally, CXCL9 is known to inhibit recruitment of eosinophils and here, *Cxcl9* is the most significantly downregulated gene in tumors from *Nlrx1*$^{-/-}$ mice (**Fig. 2I**).[50] CXCL9 has also been found to be dysregulated in the absence of NLRX1 in other models, such as in invasive pulmonary aspergillosis and HPV+ head and neck squamous cell carcinoma.[39,51] Likewise, CXCL9 is regulated by AKT, ERK, and STING signaling through mechanisms previously shown to be regulated by NLRX1 in other models.[21,22,24,39,52] Thus, our data suggest that NLRX1, when expressed in the healthy host cells, attenuates tumor progression and metastasis through the regulation of CXCL9, limiting the recruitment of pro-EMT eosinophils, and attenuating the subsequent production of MMP9 and TGF-β to ultimately suppress EMT.

NLRX1 Expressed in Healthy Cells Attenuates Lung Metastasis Through Limiting the Formation of the Metastatic Niche

Increased EMT is a critical hallmark of cancer metastasis that allows tumor cells to migrate more freely from the primary tumor, and prior studies in the 4T1 model have shown that sublines of 4T1 cells with significant EMT demonstrate increased metastasis.[53] The priming of distal organs to make them favorable environments for metastatic seeding (the "metastatic niche") allows tumor cells that have undergone EMT to find a hospitable location outside of the tumor.[54] Indeed, there is some evidence of crosstalk between the metastatic niche and tumor cells undergoing EMT.[55] NLRX1 has been implicated in several hallmarks of the metastatic niche, including inflammation, angiogenesis, immune suppression, and ECM remodeling.[16,17,22,56] Thus, we next sought to

determine if NLRX1 impacts the distant site organs typically targeted for breast cancer metastasis in the 4T1 model. We focused our assessments on the lungs, which are commonly evaluated in this model, and because our *in vivo* data demonstrated a protective role of NLRX1 against lung metastasis (**Fig. 1E-F**).[53,57–59]

Here, we evaluated the evolution of the metastatic niche in the WT and *Nlrx1*$^{-/-}$ mice throughout the 4T1 disease progression using western blot analysis at pre-metastasis and post-metastasis timepoints. Given the concentration of 4T1 cells injected in our studies, we expect the cells to become metastatic by Day 8 post-injection.[59] At the pre-metastasis timepoint, lungs from *Nlrx1*$^{-/-}$ mice contained increased levels of Lox, Fibronectin, MMP9, IL-6, and TGF-β compared to lungs from WT animals (**Fig. 3A, Supplemental Fig. 4A**). Increased levels of these proteins have been previously correlated with increased metastasis in various cancer models and are commonly used to define the metastatic niche.[55] A slight decrease in CD31, a marker for angiogenesis, was also observed (**Fig. 3A, Supplemental Fig. S4A**). Thus, these data suggest that NLRX1 attenuates the formation of the pre-metastatic niche through suppressing inflammation and ECM remodeling in the lung. At the post-metastasis timepoint, lungs from *Nlrx1*$^{-/-}$ mice still demonstrated increased levels of MMP9 and IL-6, but had decreased expression of TGF-β, Fibronectin, and Lox, and an increase in CD31 expression compared to lungs from WT animals (**Fig. 3B, Supplemental Fig. S4B**). These data suggest the lung metastatic niche shifts as the tumor cells begin to colonize, but that NLRX1 still remains protective against lung metastatic niche formation through ECM remodeling, inflammation, and angiogenesis (**Fig. 3C**).

To define how NLRX1 impacts the immune cells involved in metastatic niche formation, we evaluated the immune cell populations in the lungs at the pre- and post-metastasis timepoints. There were no significant differences in eosinophil, macrophage, M-MDSC, G-MDSC, cDC1, cDC2, B cell, T reg, or CD8+ T cell populations between WT and *Nlrx1*$^{-/-}$ mice at the pre-metastasis timepoint (**Supplemental Fig. S4C**). However, lungs from *Nlrx1*$^{-/-}$ mice had significantly fewer double-negative T cells (CD45+ CD3+ CD19- CD4- CD8-) and CD4+ T cells (CD45+ CD3+ CD19- CD4+ CD8-), and significantly increased inflammatory dendritic cells (CD45+ CD11b+ CD11c+ Ly6G - Ly6C+) and natural killer cells (CD45+ CD3- NK1.1+ CD19-) compared to WT lungs (**Fig. 3 D-G, Supplemental Fig. S4D-F**). At the post-metastasis

timepoint, there were no significant differences in any of the immune cell populations (**Supplemental Fig. S4G**). Together, these data suggest a role for NLRX1 impacting the immune cell populations in the lung pre-metastatic niche that may further attenuate 4T1 metastasis (**Fig. 3C**).

NLRX1 Expressed in 4T1 Cells Enhances Their Malignant Properties

The experiments above suggest that NLRX1 functions as a tumor suppressor when expressed systemically in the host. We next sought to determine the function of NLRX1 in the 4T1 mammary tumor cells and conduct gain-of-function and loss-of-function studies. Here, we utilized a stable lentiviral transduction method to generate 4T1 cells that either overexpress ($4T1^{OE}$) or knockdown ($4T1^{KD}$) NLRX1, as well as their respective controls ($4T1^{OE\text{-}CTL}$ and $4T1^{KD\text{-}CTL}$) **(Fig. 4A**). Western blot confirmed successful overexpression and knockdown of NLRX1 (**Fig 4A**). In the limited studies done previously to examine NLRX1 in breast cancer, proliferation and cell death have been implicated.[28,37] To examine proliferation, we performed an MTT assay. $4T1^{OE}$ cells trended towards an increase in proliferation compared to $4T1^{OE\text{-}CTL}$ cells ($p = 0.08$), with the $4T1^{OE}$ cells demonstrating approximately a 20% increase over the $4T1^{OE\text{-}CTL}$ cells (**Fig. 4B**). Conversely, the $4T1^{KD}$ cells displayed significantly decreased proliferation compared to $4T1^{KD\text{-}CTL}$ cells, with the knockdown cells undergoing half the proliferation of their controls (**Fig. 4B**). We repeated this experiment using TNF to stimulate NLRX1 function as previously described or TGF-β to stimulate EMT (**Supplemental Fig. S5A**).[28,37] Here, we observed no significant differences in the $4T1^{OE}$ cells, but we did continue to observe significantly decreased proliferation in the $4T1^{KD}$ cells following stimulation with either TNF or TGF-β (**Supplemental Fig. S5A**). Cell death was then evaluated following treatment with H_2O_2 using an LDH assay. NLRX1 overexpression protected the 4T1 cells from H_2O_2-induced cell death, as shown by the significant decrease in the cytotoxicity for the $4T1^{OE}$ cells compared to the $4T1^{OE\text{-}CTL}$ cells (**Fig. 4C**). Conversely, cells lacking NLRX1 were more sensitive to H_2O_2-induced cell death, as evidenced by the significant increase in cytotoxicity observed in $4T1^{KD}$ cells compared to $4T1^{KD\text{-}CTL}$ cells (**Fig 4C**). Together, these data suggest that NLRX1 functions as a tumor promoter in the 4T1 cells by attenuating ROS-mediated cell death and moderately impacting proliferation.

Due to the metastasis phenotype observed *in vivo*, we next evaluated migration potential in the knockdown and overexpression cells using a common wound healing scratch assay. At 5- and 8-hours post-scratch, NLRX1 overexpression in the $4T1^{OE}$ cells resulted in significantly faster rates of migration compared to $4T1^{OE\text{-}CTL}$ cells, migrating approximately three times faster at each timepoint (**Fig. 4D-E**). Conversely, the loss of NLRX1 in the $4T1^{KD}$ cells reduced migration by approximately 40% and 50% compared to $4T1^{KD\text{-}CTL}$ cells at each the 5 hour and 8 hour timepoints, respectively (**Fig 4D-E**). Together these data suggest that in addition to increasing proliferation and reducing cell death, NLRX1 expression in the 4T1 tumor cells also increases their migration potential and metastatic properties.

NLRX1 was originally characterized as being associated with the mitochondria in the context of infectious diseases, although its exact impact on mitochondrial function continues to be an active area of research and debate.[11,16,60] Accordingly, prior studies have implicated NLRX1 in the regulation of ROS.[26–29,35,37,61,62] Tumor cells routinely demonstrate increased ROS production and dysregulated mitochondrial dynamics, both of which can impact the survival and metastatic potential of tumor cells. Thus, we next sought to evaluate the role of NLRX1 in these biological features using the $4T1^{KD}$ and $4T1^{OE}$ cells.

To evaluate superoxide production, we utilized MitoSOX staining. Overexpression of NLRX1 in the $4T1^{OE}$ cells resulted in a significant increase in mitochondrial superoxide production that was almost 6-fold ($\log_2$) higher than the $4T1^{OE\text{-}CTL}$ control cells (**Fig. 4F**). Conversely, the loss of NLRX1 in the $4T1^{KD}$ cells resulted in a significant repression of mitochondrial superoxide production, observed to be approximately 4-fold ($\log_2$) lower than their controls (**Fig. 4F**). Interestingly, superoxide levels in $4T1^{KD\text{-}CTL}$ cells mimic those of $4T1^{OE}$ cells instead of $4T1^{OE\text{-}CTL}$ cells. It is possible that the differences in the knockdown and overexpression lentiviral constructs can cause these differences. However, despite the differences in the controls, the cells with greater NLRX1 expression in both the overexpression and knockdown system comparisons displayed increased superoxide levels. The regulation of ROS levels was retained following TNF stimulation in the knockdown system, but not the overexpression system (**Supplemental Fig. S5B**). These findings are consistent with earlier studies that showed NLRX1 promotes ROS production in HeLa, HEK293, and MCF7 cells through regulation of caspase-8 during TNF-induced apoptosis.[28]

The inclusion of both the loss-of-function and gain-of-function models effectively illustrate that NLRX1 levels have significant effects on mitochondria superoxide levels.

To better define a role for NLRX1 in mitochondria function and energetics, we utilized a Seahorse XF Mito Stress Test. In the gain-of-function studies, no significant differences were observed in mitochondrial respiration (**Fig. 4G**). However, loss of NLRX1 in the $4T1^{KD}$ cells resulted in a significant shift in mitochondrial respiration (**Fig. 4G**). This was most evident in the basal respiration and in the maximal respiration (**Fig. 4G**). We also observed four times more spare respiratory capacity in $4T1^{KD}$ cells compared to the $4T1^{KD\text{-}CTL}$ cells (**Fig. 4H**). Conversely, this coincided with approximately double the spare respiratory capacity in $4T1^{OE\text{-}CTL}$ cells compared to $4T1^{OE}$ cells, but this was not statistically significant ($p = 0.16$). The mitochondrial respiration and spare respiratory capacity phenotypes were also consistent under TNF and TGF-β conditions (**Supplemental Fig. S5C-D**). Together, these data suggest that loss of NLRX1 attenuates several cancer hallmarks in the 4T1 cells, including decreased proliferation, migration, ROS production, and increasing cell death and respiratory capacity. Conversely, the overexpression of NLRX1 generally augments many of these same biological functions.

NLRX1 Expressed in 4T1 Cells Promotes Malignancy and Tumor Growth In Vivo

Our data suggest that NLRX1 suppresses tumor growth and metastasis when expressed in the host and conversely functions as a tumor promoter when expressed in the 4T1 mammary tumor cells. Thus, we next sought to determine if the increase in malignant properties observed *in vitro* was sufficient to increase the disease burden *in vivo*. We injected 1.2×10^6 cells (either $4T1^{OE}$, $4T1^{OE\text{-}CTL}$, $4T1^{KD}$, or $4T1^{KD\text{-}CTL}$) into a singular mammary fat pad of WT and *Nlrx1*$^{-/-}$ mice (**Fig. 5A & F**). Additional WT and *Nlrx1*$^{-/-}$ mice were injected with sterile PBS for tumor-free controls (data not shown). Mice were monitored for morbidity and tumor growth throughout the study and euthanized on Day 14 post-injection, approximately when the tumors reached 1 cm^2, for tissue collection. Minimal differences in tumor growth were observed in any of the groups (**Fig. 5 B & G**), but significant differences became more pronounced upon necropsy. In the mice engrafted with 4T1 cells overexpressing NLRX1 ($4T1^{OE}$), we observed a doubling of final tumor volume compared to mice engrafted with the overexpression control cells ($4T1^{OE\text{-}CTL}$) in both WT and

Nlrx1$^{-/-}$ mice (**Fig. 5C**). However, no differences in final tumor volume were observed in either WT or *Nlrx1*$^{-/-}$ mice engrafted with the knockdown cells or their controls (**Fig. 5H**).

In addition to tumor growth, morbidity was monitored over the course of the study and quantified using a health scoring system with a range of 0-4. By harvesting animals with tumors in the ~1 cm^2 size range, morbidity can be minimized. Consistent with this, we did not observe any major clinical signs of morbidity in any groups of animals (**Fig. 5D & I**). However, we did observe a significant decrease in the health scores – indicating a decrease in morbidity – in WT mice engrafted with the knockdown 4T1 ($4T1^{KD}$) cells on days 12-14 post-injection compared to WT mice engrafted with the knockdown control cells ($4T1^{KD\text{-}CTL}$) (**Fig. 5I**). Upon further investigation, we determined the differences in morbidity were driven by tumor eschar. Tumor eschar, which is necrotic tissue that typically forms an ulcerating lesion around the center of the mammary tumor on the surface of the skin, can occur during the 4T1 model.[59] WT mice engrafted with $4T1^{KD}$ cells displayed significantly less tumor eschar than WT mice engrafted with $4T1^{KD\text{-}CTL}$ cells (**Fig. 5J**). *Nlrx1*$^{-/-}$ mice with $4T1^{KD}$ tumors also displayed less morbidity and less tumor eschar than *Nlrx1*$^{-/-}$ mice with $4T1^{KD\text{-}CTL}$ cells, but this was not statistically significant (**Fig. 5I, Supplemental Fig. 6A**). Additionally, there were no significant differences in morbidity in either WT or *Nlrx1*$^{-/-}$ mice with overexpression cells or their controls (**Fig. 5D**). Thus, while this phenotype could be an artifact of the knockdown construct or delivery method in the $WT^{KD\text{-}CTL}$ animals, the absence of eschar in the *Nlrx1*$^{-/-}$ and WT mice with $4T1^{KD}$ cells may suggest a protective role for NLRX1 in this biological phenomenon.

Consistent with the increased migration observed in the *in vitro* studies (**Fig. 4D & E**), the metastatic burden was significantly increased in mice engrafted with the $4T1^{OE}$ cells in both the WT and *Nlrx1*$^{-/-}$ mice, with 4-fold (log_2) and 3-fold (log_2) increases, respectively (**Fig. 5E**). Consistent with the attenuation of migration observed in the *in vitro* studies (**Fig. 4D & E**) and converse to the observations in the overexpression studies (**Fig. 4D & E, Fig. 5E**), we observed at least three times less lung metastasis in WT mice engrafted with $4T1^{KD}$ cells compared to those engrafted with $4T1^{KD\text{-}CTL}$ cells (**Fig. 5K**). In the *Nlrx1*$^{-/-}$ mice, we also observed at least three times less lung metastasis in mice engrafted with $4T1^{KD}$ cells compared to the $4T1^{KD\text{-}CTL}$ animals, but this was not statistically significant (**Fig. 5K**). Quantification of lung metastasis was acquired

either through percent metastatic burden or a manual count of metastatic colonies, both of which have been previously described.[41,59]

Taking into consideration the results of the *Nlrx1*$^{-/-}$ studies with the parental 4T1 cell line *in vivo* (**Fig. 1**) and the *in vitro* cell line studies (**Fig. 4**), we would predict *Nlrx1*$^{-/-}$ mice engrafted with 4T1^{OE} cells (*Nlrx1*$^{-/-}$ 4T1^{OE}) to have the most severe disease burden. To confirm this, we performed ANOVAs on the tumor growth, morbidity, final tumor volume, and lung metastasis data to compare the results between all four comparisons in each study (**Supplemental Fig. 6B-I**). Indeed, the loss of the protective effects of NLRX1 in healthy host cells combined with the overexpression of NLRX1 in the 4T1^{OE} cells in the *Nlrx1*$^{-/-}$ 4T1^{OE} group resulted in the highest metastatic burden that more than doubled the levels observed in the WT mice with the same 4T1^{OE} cells (**Supplemental Fig. 6H**). No additional significant differences were noted between WT and *Nlrx1*$^{-/-}$ mice engrafted with the same 4T1 cells (**Supplemental Fig. 5B-I**). Together, the *in vivo* overexpression and knockdown studies revealed that NLRX1 appears to augment 4T1 mammary tumor growth and metastasis when expressed in the 4T1 cancer cells, which is a reversal of function compared to the role of NLRX1 expressed in the healthy host cells.

NLRX1 Expressed in 4T1 Cells Augments Lung Metastasis Through Promoting Epithelial-Mesenchymal Transition

NLRX1 modulation of EMT was one of the mechanisms identified in the attenuation of 4T1 tumor progression and metastasis in the *Nlrx1*$^{-/-}$ mice (**Fig. 2**). To explore potential mechanisms associated with the phenotypes observed in the NLRX1 overexpression and knockdown 4T1 cells in the WT and *Nlrx1*$^{-/-}$ animals, we again utilized a transcriptomics approach. Here, we focused our analysis on the NLRX1 overexpression cells due to the *in vivo* phenotypes being more pronounced in the overexpression cell lines compared to the knockdown cell lines (**Fig. 5**). RNA was collected from 4T1^{OE} and 4T1$^{OE\text{-}CTL}$ tumors from WT and *Nlrx1*$^{-/-}$ mice for transcriptomics analysis (Clariom S). An unbiased analysis identified the top 20 pathways that were significantly impacted by NLRX1 overexpression, as dictated by number of DEGs identified for each of the 4 available comparisons. Pathways that consistently ranked in the top 20 in at least 2 of the 4 comparisons were considered to be significant (**Fig. 6A**). This analysis identified 10 pathways that overlapped with pathways identified in the earlier *Nlrx1*$^{-/-}$ studies using unmodified

4T1 cells (**Fig. 2A**), identified here with a star (**Fig. 6A**). Many of the top significant pathways are again important to EMT, including EGFR1 signaling, focal adhesion, PI3K-Akt-mTOR, MAPK, and TGF-β receptor signaling pathways (**Fig. 6A**). Interestingly, all of these EMT-related pathways are more significant between $4T1^{OE}$ and $4T1^{OE\text{-}CTL}$ tumors than between *Nlrx1*$^{-/-}$ and WT mice, suggesting NLRX1 has a larger impact on EMT when expressed by 4T1 cells than by healthy host cells (**Fig. 6A**). We then identified the DEGs in the EMT-related pathways between $4T1^{OE}$ and $4T1^{OE\text{-}CTL}$ tumors in *Nlrx1*$^{-/-}$ (**Fig. 6B**) and WT mice (**Fig. 6C**) and found the signature in $4T1^{OE}$ tumors to be consistent with the promotion of EMT (**Fig. 6B-C**). More specifically, we identified 27 DEGs in tumors from *Nlrx1*$^{-/-}$ mice and 13 DEGs in tumors from WT mice specifically related to EMT that were generally up-regulated in the $4T1^{OE}$ tumors (**Fig. 6D-E**; **Supplemental Fig. S7A**). Consistent with the increased disease burden when NLRX1 is overexpressed in the tumor and lacking in the host, there are more DEGs significantly upregulated in $4T1^{OE}$ tumors from *Nlrx1*$^{-/-}$ mice compared to tumors in the WT animals (**Fig. 6B-E**).

We next analyzed protein levels of the epithelial marker E-Cadherin and found that $4T1^{OE}$ tumors express less E-Cadherin than $4T1^{OE\text{-}CTL}$ tumors in WT and *Nlrx1*$^{-/-}$ mice (**Fig. 6F, Supplemental Fig. S7B**). This is consistent with *in vitro* and *in vivo* data that demonstrate overexpression of NLRX1 in 4T1 cells confers an advantage to the tumor. Conversely, $4T1^{KD}$ tumors retained E-Cadherin while $4T1^{KD\text{-}CTL}$ tumors lost E-Cadherin in both WT and *Nlrx1*$^{-/-}$ mice (**Fig. 6F, Supplemental Fig. S7B**). Again, this is consistent with our *in vitro* and *in vivo* data that indicate the loss of NLRX1 in 4T1 cells confers a loss of aggressiveness and decreased disease burden severity. Pathway analysis of the gene transcription data identified several pathways regulated by NLRX1 that appear to contribute to EMT (**Fig. 6G**). Specifically, NLRX1 in 4T1 cells is predicted to promote EMT through the upregulation of growth factors TGF-β3 and HB-EGF, upregulating C-kit, VEGFR1, and Notch1/2 receptors, and promoting Smad, p38 MAPK, PI3K-AKT, MAPK/ERK, and β-Catenin pathways (**Fig. 6G**). Together, these pathways converge on the transcription factors SNAIL1 and TCF4 resulting in the subsequent upregulation of EMT (**Fig. 6G**).

DISCUSSION

The majority of studies evaluating NLRX1 function have focused on its role in modulating the host immune response following pathogen exposure.[16,17] In this context, the consensus appears to be coalescing around NLRX1 functioning to negatively regulate NF-κB and type-I interferon signaling, modulating autophagy, and facilitating ROS production.[16,17] However, the mechanisms proposed for these functions are still relatively unclear and NLRX1 remains an enigmatic member of the NLR family. Indeed, since its initial discovery and characterization, its signaling, function, and even cellular localization have been heavily debated.[10,11,16–18,26,28,37,38,60] Beyond infectious disease studies, there is significant interest in better defining the role of NLRX1 in cancer.[7] The current literature characterizes NLRX1 as both a tumor promoter and a tumor suppressor.[21,22,24,25,28,38,39] These seemingly contradictory findings have added to NLRX1's intrigue and have resulted in general confusion in the field regarding its biological functions.

The lack of *in vivo* syngeneic tumor models and studies utilizing *Nlrx1*$^{-/-}$ mice have been major limitations with prior studies, especially in breast cancer studies which have focused on *in vitro* characterization in varying cell lines. Here, we circumvented these prior limitations by using both loss-of-function and gain-of-function 4T1 cells and *Nlrx1*$^{-/-}$ mice fully backcrossed onto the BALB/cJ background for syngeneic mammary tumor studies using the same parental cell line. Our data demonstrate that NLRX1 functions differently depending on whether it is expressed in the healthy host cells or in the 4T1 cancer cells. In the healthy host cells, NLRX1 functions as a tumor suppressor where it limits tumor progression and metastasis. Conversely, in the 4T1 mammary tumor cell line, NLRX1 appears to function as a tumor promoter that enhances malignant properties. Together, these data provide insight into some of the controversy and confusion associated with this NLR family member by revealing a dichotomy between NLRX1 functions based on cellular context.

Together, our data revealed several overlapping pathways that were significantly altered following the manipulation of NLRX1. Many of these pathways have previously been found to be regulated by NLRX1 in either infectious disease or cancer studies. For example, NLRX1 negatively regulates AKT, MAPK, and NF-κB signaling in a model of chemical-induced histiocytic sarcoma.[24] This is also consistent with other studies in colorectal cancer where NLRX1

was found to function as a tumor suppressor through the inhibition of NF-κB, MAPK, STAT3, and IL-6 signaling.[21] Complementing these data, *Nlrx1* deficiency on the $Apc^{min/+}$ background resulted in increased proliferation and expression of β-Catenin and Cathepsin B.[21] In general, our data are consistent with these prior findings that identify NLRX1 as a regulator of AKT, MAPK, ERK, IL-6, and β-Catenin. Intriguingly, we did not observe significant dysregulation of NF-κB signaling in the tumors of any of our studies. It is possible that the inflammatory nature of the histiocytic sarcoma and colorectal cancer models were stronger inducers of NF-κB signaling, requiring higher levels of NLRX1 regulation, compared to the relatively immunosuppressive nature of the 4T1 model.[59] Our data also predicted that NLRX1 in both healthy host cells and 4T1 tumor cells impacts EGFR dysregulation and downstream tumor progression, which is consistent with prior studies in head and neck squamous cell carcinoma where NLRX1 appears to form a critical signaling hub that augments autophagy.[57] Additionally, consistent with the well-defined ability for NLRX1 to limit inflammation, we found that NLRX1 in healthy host cells can limit inflammation in the lung to prevent the formation of the metastatic niche. We also revealed a lesser-studied role for NLRX1 in the metastatic niche regarding angiogenesis and immune cell recruitment, both of which are relatively undefined functions of NLRX1, especially in cancer.[31,39,51,56]

While our data reveal differences in function based on the cellular context, our studies converge on NLRX1 regulation of EMT as a potential mechanism underlying the phenotypes observed in both the *Nlrx1*$^{-/-}$ mice engrafted with the unmodified 4T1 cells and in the gain-of-function/loss-of-function 4T1 cell studies. Complementing the transcriptomics pathway analysis findings, our validation studies revealed decreased E-cadherin, increased MMP9, and increased TGF-β following modification of *Nlrx1*. These three events are closely associated with EMT and subsequent metastasis, including in the context of breast cancer.[64–66] Loss of E-cadherin has been observed in highly aggressive and invasive breast tumors and leads to the destabilization of adherens junctions, cancer cell survival, invasiveness, and metastasis.[64,65,67] In the present study, the decrease in E-cadherin observed in the *Nlrx1*$^{-/-}$ 4T1 tumors and the $4T1^{OE}$ tumors was correlated with increased β-catenin, Snail1, Zeb2, and TCF4 gene expression. Each of these transcription factors and co-activators either significantly repress E-cadherin expression or are downregulated by E-cadherin.[67–70] Compounding the decreased E-cadherin, the increase in MMP9

and TGF-β are also predicted to increase tumor progression and metastasis through regulating EMT.[64–66]

Only one previous study has examined the role of NLRX1 in EMT.[22] In the previous study, Hu et al. explored NLRX1 in hepatocellular carcinoma. Using two murine hepatocellular carcinoma cell lines, HCCLM3 and Huh7, the authors overexpressed NLRX1 in HCCLM3 cells and knocked down NLRX1 in Huh7 cells. The study found that NLRX1 overexpression increased E-Cadherin expression and decreased N-Cadherin, Vimentin, Snail1, and Twist1 expression. Conversely, the knockdown of NLRX1 resulted in the opposite expression pattern, suggesting NLRX1 suppresses EMT in hepatocellular carcinoma cells. The authors concluded NLRX1 suppresses EMT by inhibiting the PI3K-AKT pathway and subsequently downregulating Snail1 expression.[22] These previous results counter what we find in the current study, where NLRX1 overexpression in mammary 4T1 tumor cells decreases E-Cadherin and NLRX1 knockdown retains E-Cadherin. However, the importance of AKT signaling is consistent between both the hepatocellular carcinoma model and our mammary tumor model. More work is certainly needed to further define the underlying mechanisms of this regulation in different types of cancer.

Mechanistically, it is possible that NLRX1 directly regulates E-cadherin, MMP9, and TGF-β through the formation of multi-protein complexes similar to the so-called TRAFasomes that have been described for related NLRs that regulate NF-κB signaling.[9] However, it is also possible that NLRX1 regulates these processes indirectly through the modulation of eosinophil influx. The finding that eosinophils are significantly increased in the 4T1 tumor microenvironment of *Nlrx1*$^{-/-}$ mice was unexpected. However, these results are consistent with the significant downregulation of CXCL9. CXCL9 has been shown to inhibit eosinophil responses through a CCR3- and Rac2-dependent mechanism.[50] While we observed increased eosinophils in the more aggressive 4T1 tumors, it should be noted that the role of eosinophils in cancer is itself quite controversial, with data suggesting these cells function through anti-tumor, pro-tumor, and even neutral mechanisms.[49,71] However, eosinophils can be a source of MMP9 and TGF-β in the tumor microenvironment.[49] Thus, the increase in tumor associated eosinophils in the *Nlrx1*$^{-/-}$ mice, driven by the decrease in CXCL9, could potentially serve as the source for these pro-tumor EMT mediators. Increased eosinophils were previously observed in the *Nlrx1*$^{-/-}$ mice in a model of

pulmonary aspergillosis.[51] The mechanism was determined to be partially due to a loss of NLRX1 mediated negative regulation of IL-4 and CCL5, resulting in a more pronounced Th2 immune response.[51] In all studies prior to the present study, *Nlrx1*$^{-/-}$ mice were generated and maintained on the C57Bl/6 background. Due to the use of 4T1 cell engraftment necessitating the use of mice on the BALB/cJ background, the present study is the first to our knowledge to utilize *Nlrx1*$^{-/-}$ mice fully backcrossed onto the BALB/c background. BALB/c mice skew towards Th2 mediated immune responses, which may also contribute to the increase in tumor associated eosinophils observed in our studies.[72]

Beyond the tumor microenvironment and regulation of EMT, we also identified a significant role for NLRX1 in regulating ROS production, migration, and mitochondrial respiration in the 4T1 cells. The relationship between NLRX1 and the mitochondria is well established with studies showing functions associated with the regulation of RIG-I-like helicase signaling through interactions with MAVS on the mitochondria surface.[11,18] NLRX1 interacts with another mitochondrial protein, TUFM, to regulate autophagy, and NLRX1 has been implicated in mitochondria-specific autophagy known as mitophagy.[34–37] In the mitochondrial electron transport chain, NLRX1 was found to interact with Complex I and Complex III to regulate ATP levels, and to interact with UQCRC2 of Complex III to promote ROS production.[28,33] Specifically in MCF-7 human breast carcinoma cells, NLRX1 was acting as a tumor suppressor through inhibiting the activity of the mitochondrial respiratory chain and the generation of ROS.[28] This was suggested to sensitize cells to TNF-α mediated cell death.[28] These MCF-7 results are the opposite of our findings here in 4T1 cells and of previous findings in MDA-MB-231 human TNBC cells that show NLRX1 serving as a tumor promoter.[37] In MDA-MB-231 cells, the tumor promoting phenotypes of NLRX1 were found to be a function of mitochondria-lysosomal crosstalk and NLRX1 appeared to decrease ROS levels.[37] In the current study, dysregulated mitochondrial respiration and increased superoxide levels are at least partially responsible for the tumor promoting phenotypes of NLRX1 in 4T1 cells.

Our data show dramatically increased mitochondrial respiration and respiratory capacity when NLRX1 levels are knocked down, which is moderately reversed when NLRX1 is overexpressed. This finding is consistent with the reduced malignant features observed in the

knockdown cells, both *in vitro* and *in vivo*, and the attenuated superoxide levels. Typically, cancer cells demonstrate reduced respiratory capacity due to the high glycolytic rate.[73] Based on the high spare respiratory capacity in our $4T1^{KD}$ cells, there is a significant improvement for adapting and dealing with stress conditions in these cells.[73] For example, it would be predicted that these cells would have lower ROS and superoxide production as they maximize respiratory rate and ATP synthesis.[74] While these findings are the opposite of the studies in MDA-MB-231 cells, they are consistent with prior studies evaluating the host immune response to *Aspergillus fumigatus*.[51] Here, loss of NLRX1 resulted in a diminished ability to generate superoxide and ROS.[51] An analysis of glycolysis and mitochondrial function led the authors to speculate that NLRX1 was needed to either increase or decrease glycolysis based on the lifecycle of *A. fumigatus* in airway epithelial cells.[51] Importantly, this study demonstrates, similar to our own findings in the 4T1 cells, that the role of NLRX1 can vary significantly between cell types and stimuli.[51]

In conclusion, our data suggest that NLRX1 functions as a tumor promoter in the 4T1 mammary tumor cells, while simultaneously serving as a tumor suppressor in healthy host cells. These findings provide insight into the often-conflicting data generated in studies evaluating not only NLRX1, but many of the NLR family members, where function is likely specific to cell-type, stimuli, situational, and/or temporal factors. For NLRX1 in breast cancer, the dichotomy of effects observed in the tumor cells versus the healthy host cells is of critical importance for the design of future therapeutics. Our data would suggest that activating NLRX1 in healthy host cells or attenuating NLRX1 in cancer cells would be successful in attenuating the disease burden. However, this is cautionary, as any therapeutic that reverses this pattern would likely result in more aggressive disease. While the mechanisms of NLRX1 are still not completely defined, this research has identified several biological functions that are significantly impacted by NLRX1 in mammary tumors and provides novel insights into the role of this enigmatic NLR family member in this malignancy.

ACKNOWLEDGEMENTS

The authors would like to thank Hannah Ivester and Dr. Brie Trusiano for their support and teamwork, Dr. Thomas Cecere and the Cell Morphology Core at the Virginia Maryland College of Veterinary Medicine, the Metabolism Core at Virginia Tech, Melissa Makris and the Flow

Cytometry Core at Virginia Tech, Bettina Heid for her logistical support, and the Animal Care Staff and University Veterinarians at Virginia Tech. We would also like to thank Dr. Jenny Ting of UNC Chapel Hill for the use of her C57/BL6J *Nlrx1*$^{-/-}$ mice in our backcrossing methods. Summary figures were created with BioRender.com. David A. Brown is employed by Stealth BioTherapeutics, a biotechnology company that is developing potential therapeutics for mitochondrial diseases. The authors have no additional conflicting financial interests.

REFERENCES

1. American Cancer Society. Cancer Facts & Figures 2021. **2021**, 72.
2. American Cancer Society. *Triple-negative Breast Cancer | Details, Diagnosis, and Signs*. https://www.cancer.org/cancer/breast-cancer/about/types-of-breast-cancer/triple-negative.html (accessed 2022-04-26).
3. Man, S. M.; Jenkins, B. J. Context-Dependent Functions of Pattern Recognition Receptors in Cancer. *Nat Rev Cancer* **2022**, *22* (7), 397–413. https://doi.org/10.1038/s41568-022-00462-5.
4. Kayagaki, N.; Warming, S.; Lamkanfi, M.; Walle, L. V.; Louie, S.; Dong, J.; Newton, K.; Qu, Y.; Liu, J.; Heldens, S.; Zhang, J.; Lee, W. P.; Roose-Girma, M.; Dixit, V. M. Non-Canonical Inflammasome Activation Targets Caspase-11. *Nature* **2011**, *479* (7371), 117–121. https://doi.org/10.1038/nature10558.
5. Martinon, F.; Burns, K.; Tschopp, J. The Inflammasome: A Molecular Platform Triggering Activation of Inflammatory Caspases and Processing of ProIL-Beta. *Mol Cell* **2002**, *10* (2), 417–426. https://doi.org/10.1016/s1097-2765(02)00599-3.
6. Coutermarsh-Ott, S. *Beyond the inflammasome: regulatory NOD-like receptor modulation of the host immune response following virus exposure | Microbiology Society*. https://www.microbiologyresearch.org/content/journal/jgv/10.1099/jgv.0.000401 (accessed 2022-06-09).
7. Allen, I. C. Non-Inflammasome Forming NLRs in Inflammation and Tumorigenesis. *Frontiers in Immunology* **2014**, *5*.
8. Xia, X.; Cui, J.; Wang, H. Y.; Zhu, L.; Matsueda, S.; Wang, Q.; Yang, X.; Hong, J.; Songyang, Z.; Chen, Z. J.; Wang, R.-F. NLRX1 Negatively Regulates TLR-Induced NF-KB Signaling by Targeting TRAF6 and IKK. *Immunity* **2011**, *34* (6), 843–853. https://doi.org/10.1016/j.immuni.2011.02.022.
9. Schneider, M.; Zimmermann, A. G.; Roberts, R. A.; Zhang, L.; Swanson, K. V.; Wen, H.; Davis, B. K.; Allen, I. C.; Holl, E. K.; Ye, Z.; Rahman, A. H.; Conti, B. J.; Eitas, T. K.; Koller, B. H.; Ting, J. P.-Y. The Innate Immune Sensor NLRC3 Attenuates Toll-like Receptor Signaling via Modification of the Signaling Adaptor TRAF6 and Transcription Factor NF-KB. *Nat Immunol* **2012**, *13* (9), 823–831. https://doi.org/10.1038/ni.2378.
10. Allen, I. C.; Moore, C. B.; Schneider, M.; Lei, Y.; Davis, B. K.; Scull, M. A.; Gris, D.; Roney, K. E.; Zimmermann, A. G.; Bowzard, J. B.; Ranjan, P.; Monroe, K. M.; Pickles, R. J.; Sambhara, S.; Ting, J. P. Y. NLRX1 Protein Attenuates Inflammatory Responses to Infection by Interfering with the RIG-I-MAVS and TRAF6-NF-KB Signaling Pathways. *Immunity* **2011**, *34* (6), 854–865. https://doi.org/10.1016/j.immuni.2011.03.026.
11. Moore, C. B.; Bergstralh, D. T.; Duncan, J. A.; Lei, Y.; Morrison, T. E.; Zimmermann, A. G.; Accavitti-Loper, M. A.; Madden, V. J.; Sun, L.; Ye, Z.; Lich, J. D.; Heise, M. T.; Chen, Z.; Ting, J. P.-Y. NLRX1 Is a Regulator of Mitochondrial Antiviral Immunity. *Nature* **2008**, *451* (7178), 573–577. https://doi.org/10.1038/nature06501.
12. Chen, S.-T.; Chen, L.; Lin, D. S.-C.; Chen, S.-Y.; Tsao, Y.-P.; Guo, H.; Li, F.-J.; Tseng, W.-T.; Tam, J. W.; Chao, C.-W.; Brickey, W. J.; Dzhagalov, I.; Song, M.-J.; Kang, H.-R.; Jung, J. U.; Ting, J. P.-Y. NLRP12 Regulates Anti-Viral RIG-I

Activation via Interaction with TRIM25. *Cell Host Microbe* **2019**, *25* (4), 602-616.e7. https://doi.org/10.1016/j.chom.2019.02.013.
13. Allen, I. C.; Lich, J. D.; Arthur, J. C.; Jania, C. M.; Roberts, R. A.; Callaway, J. B.; Tilley, S. L.; Ting, J. P.-Y. Characterization of NLRP12 during the Development of Allergic Airway Disease in Mice. *PLoS One* **2012**, *7* (1), e30612. https://doi.org/10.1371/journal.pone.0030612.
14. Zhang, L.; Mo, J.; Swanson, K. V.; Wen, H.; Petrucelli, A.; Gregory, S. M.; Zhang, Z.; Schneider, M.; Jiang, Y.; Fitzgerald, K. A.; Ouyang, S.; Liu, Z.-J.; Damania, B.; Shu, H.-B.; Duncan, J. A.; Ting, J. P.-Y. NLRC3, a Member of the NLR Family of Proteins, Is a Negative Regulator of Innate Immune Signaling Induced by the DNA Sensor STING. *Immunity* **2014**, *40* (3), 329–341. https://doi.org/10.1016/j.immuni.2014.01.010.
15. Tattoli, I.; Travassos, L. H.; Carneiro, L. A.; Magalhaes, J. G.; Girardin, S. E. The Nodosome: Nod1 and Nod2 Control Bacterial Infections and Inflammation. *Semin Immunopathol* **2007**, *29* (3), 289–301. https://doi.org/10.1007/s00281-007-0083-2.
16. Nagai-Singer, M. A.; Morrison, H. A.; Allen, I. C. NLRX1 Is a Multifaceted and Enigmatic Regulator of Immune System Function. *Front Immunol* **2019**, *10*, 2419. https://doi.org/10.3389/fimmu.2019.02419.
17. Pickering, R. J.; Booty, L. M. NLR in EXile: Emerging Roles of NLRX1 in Immunity and Human Disease. *Immunology* **2021**, *162* (3), 268–280. https://doi.org/10.1111/imm.13291.
18. Qin, Y.; Xue, B.; Liu, C.; Wang, X.; Tian, R.; Xie, Q.; Guo, M.; Li, G.; Yang, D.; Zhu, H. NLRX1 Mediates MAVS Degradation To Attenuate the Hepatitis C Virus-Induced Innate Immune Response through PCBP2. *J Virol* **2017**, *91* (23), e01264-17. https://doi.org/10.1128/JVI.01264-17.
19. Jiao, Q.; Xu, W.; Guo, X.; Liu, H.; Liao, B.; Zhu, X.; Chen, C.; Yang, F.; Wu, L.; Xie, C.; Peng, L. NLRX1 Can Counteract Innate Immune Response Induced by an External Stimulus Favoring HBV Infection by Competitive Inhibition of MAVS-RLRs Signaling in HepG2-NTCP Cells. *Sci Prog* **2021**, *104* (4), 368504211058036. https://doi.org/10.1177/00368504211058036.
20. Allen, I. C.; Wilson, J. E.; Schneider, M.; Lich, J. D.; Roberts, R. A.; Arthur, J. C.; Woodford, R.-M. T.; Davis, B. K.; Uronis, J. M.; Herfarth, H. H.; Jobin, C.; Rogers, A. B.; Ting, J. P.-Y. NLRP12 Suppresses Colon Inflammation and Tumorigenesis through the Negative Regulation of Noncanonical NF-KB Signaling. *Immunity* **2012**, *36* (5), 742–754. https://doi.org/10.1016/j.immuni.2012.03.012.
21. Koblansky, A. A.; Truax, A. D.; Liu, R.; Montgomery, S. A.; Ding, S.; Wilson, J. E.; Brickey, W. J.; Mühlbauer, M.; McFadden, R.-M. T.; Hu, P.; Li, Z.; Jobin, C.; Lund, P. K.; Ting, J. P.-Y. The Innate Immune Receptor NLRX1 Functions as a Tumor Suppressor by Reducing Colon Tumorigenesis and Key Tumor-Promoting Signals. *Cell Rep* **2016**, *14* (11), 2562–2575. https://doi.org/10.1016/j.celrep.2016.02.064.
22. Hu, B.; Ding, G.-Y.; Fu, P.-Y.; Zhu, X.-D.; Ji, Y.; Shi, G.-M.; Shen, Y.-H.; Cai, J.-B.; Yang, Z.; Zhou, J.; Fan, J.; Sun, H.-C.; Kuang, M.; Huang, C. NOD-like Receptor X1 Functions as a Tumor Suppressor by Inhibiting Epithelial-Mesenchymal Transition and Inducing Aging in Hepatocellular Carcinoma Cells. *J Hematol Oncol* **2018**, *11*, 28. https://doi.org/10.1186/s13045-018-0573-9.

23. Zhang, H.; Xiao, Y.; Nederlof, R.; Bakker, D.; Zhang, P.; Girardin, S. E.; Hollmann, M. W.; Weber, N. C.; Houten, S. M.; van Weeghel, M.; Kibbey, R. G.; Zuurbier, C. J. NLRX1 Deletion Increases Ischemia-Reperfusion Damage and Activates Glucose Metabolism in Mouse Heart. *Front Immunol* **2020**, *11*, 591815. https://doi.org/10.3389/fimmu.2020.591815.
24. Coutermarsh-Ott, S.; Simmons, A.; Capria, V.; LeRoith, T.; Wilson, J. E.; Heid, B.; Philipson, C. W.; Qin, Q.; Hontecillas-Magarzo, R.; Bassaganya-Riera, J.; Ting, J. P.-Y.; Dervisis, N.; Allen, I. C. NLRX1 Suppresses Tumorigenesis and Attenuates Histiocytic Sarcoma through the Negative Regulation of NF-ΛB Signaling. *Oncotarget* **2016**, *7* (22), 33096–33110. https://doi.org/10.18632/oncotarget.8861.
25. Tattoli, I.; Killackey, S. A.; Foerster, E. G.; Molinaro, R.; Maisonneuve, C.; Rahman, M. A.; Winer, S.; Winer, D. A.; Streutker, C. J.; Philpott, D. J.; Girardin, S. E. NLRX1 Acts as an Epithelial-Intrinsic Tumor Suppressor through the Modulation of TNF-Mediated Proliferation. *Cell Reports* **2016**, *14* (11), 2576–2586. https://doi.org/10.1016/j.celrep.2016.02.065.
26. Tattoli, I.; Carneiro, L. A.; Jéhanno, M.; Magalhaes, J. G.; Shu, Y.; Philpott, D. J.; Arnoult, D.; Girardin, S. E. NLRX1 Is a Mitochondrial NOD-like Receptor That Amplifies NF-KB and JNK Pathways by Inducing Reactive Oxygen Species Production. *EMBO Rep* **2008**, *9* (3), 293–300. https://doi.org/10.1038/sj.embor.7401161.
27. Yin, H.; Sun, G.; Yang, Q.; Chen, C.; Qi, Q.; Wang, H.; Li, J. NLRX1 Accelerates Cisplatin-Induced Ototoxity in HEI-OC1 Cells via Promoting Generation of ROS and Activation of JNK Signaling Pathway. *Sci Rep* **2017**, *7* (1), 44311. https://doi.org/10.1038/srep44311.
28. Singh, K.; Poteryakhina, A.; Zheltukhin, A.; Bhatelia, K.; Prajapati, P.; Sripada, L.; Tomar, D.; Singh, R.; Singh, A. K.; Chumakov, P. M.; Singh, R. NLRX1 Acts as Tumor Suppressor by Regulating TNF-α Induced Apoptosis and Metabolism in Cancer Cells. *Biochimica et Biophysica Acta (BBA) - Molecular Cell Research* **2015**, *1853* (5), 1073–1086. https://doi.org/10.1016/j.bbamcr.2015.01.016.
29. Stokman, G.; Kors, L.; Bakker, P. J.; Rampanelli, E.; Claessen, N.; Teske, G. J. D.; Butter, L.; van Andel, H.; van den Bergh Weerman, M. A.; Larsen, P. W. B.; Dessing, M. C.; Zuurbier, C. J.; Girardin, S. E.; Florquin, S.; Leemans, J. C. NLRX1 Dampens Oxidative Stress and Apoptosis in Tissue Injury via Control of Mitochondrial Activity. *J Exp Med* **2017**, *214* (8), 2405–2420. https://doi.org/10.1084/jem.20161031.
30. Leber, A.; Hontecillas, R.; Tubau-Juni, N.; Zoccoli-Rodriguez, V.; Abedi, V.; Bassaganya-Riera, J. NLRX1 Modulates Immunometabolic Mechanisms Controlling the Host–Gut Microbiota Interactions during Inflammatory Bowel Disease. *Frontiers in Immunology* **2018**, *9*.
31. Leber, A.; Hontecillas, R.; Tubau-Juni, N.; Zoccoli-Rodriguez, V.; Hulver, M.; McMillan, R.; Eden, K.; Allen, I. C.; Bassaganya-Riera, J. NLRX1 Regulates Effector and Metabolic Functions of CD4+ T Cells. *J Immunol* **2017**, *198* (6), 2260–2268. https://doi.org/10.4049/jimmunol.1601547.
32. Huang, J.-H.; Liu, C.-Y.; Wu, S.-Y.; Chen, W.-Y.; Chang, T.-H.; Kan, H.-W.; Hsieh, S.-T.; Ting, J. P.-Y.; Wu-Hsieh, B. A. NLRX1 Facilitates Histoplasma Capsulatum-

Induced LC3-Associated Phagocytosis for Cytokine Production in Macrophages. *Frontiers in Immunology* **2018**, *9*.
33. Arnoult, D.; Soares, F.; Tattoli, I.; Castanier, C.; Philpott, D. J.; Girardin, S. E. An N-Terminal Addressing Sequence Targets NLRX1 to the Mitochondrial Matrix. *Journal of Cell Science* **2009**, *122* (17), 3161–3168. https://doi.org/10.1242/jcs.051193.
34. Lei, Y.; Wen, H.; Ting, J. P. Y. The NLR Protein, NLRX1, and Its Partner, TUFM, Reduce Type I Interferon, and Enhance Autophagy. *Autophagy* **2013**, *9* (3), 432–433. https://doi.org/10.4161/auto.23026.
35. Li, S.; Zhou, Y.; Gu, X.; Zhang, X.; Jia, Z. NLRX1/FUNDC1/NIPSNAP1-2 Axis Regulates Mitophagy and Alleviates Intestinal Ischaemia/Reperfusion Injury. *Cell Prolif* **2021**, *54* (3), e12986. https://doi.org/10.1111/cpr.12986.
36. Zhang, Y.; Yao, Y.; Qiu, X.; Wang, G.; Hu, Z.; Chen, S.; Wu, Z.; Yuan, N.; Gao, H.; Wang, J.; Song, H.; Girardin, S. E.; Qian, Y. Listeria Hijacks Host Mitophagy through a Novel Mitophagy Receptor to Evade Killing. *Nat Immunol* **2019**, *20* (4), 433–446. https://doi.org/10.1038/s41590-019-0324-2.
37. Singh, K.; Roy, M.; Prajapati, P.; Lipatova, A.; Sripada, L.; Gohel, D.; Singh, A.; Mane, M.; Godbole, M. M.; Chumakov, P. M.; Singh, R. NLRX1 Regulates TNF-α-Induced Mitochondria-Lysosomal Crosstalk to Maintain the Invasive and Metastatic Potential of Breast Cancer Cells. *Biochimica et Biophysica Acta (BBA) - Molecular Basis of Disease* **2019**, *1865* (6), 1460–1476. https://doi.org/10.1016/j.bbadis.2019.02.018.
38. Soares, F.; Tattoli, I.; Rahman, M. A.; Robertson, S. J.; Belcheva, A.; Liu, D.; Streutker, C.; Winer, S.; Winer, D. A.; Martin, A.; Philpott, D. J.; Arnoult, D.; Girardin, S. E. The Mitochondrial Protein NLRX1 Controls the Balance between Extrinsic and Intrinsic Apoptosis. *J Biol Chem* **2014**, *289* (28), 19317–19330. https://doi.org/10.1074/jbc.M114.550111.
39. Luo, X.; Donnelly, C. R.; Gong, W.; Heath, B. R.; Hao, Y.; Donnelly, L. A.; Moghbeli, T.; Tan, Y. S.; Lin, X.; Bellile, E.; Kansy, B. A.; Carey, T. E.; Brenner, J. C.; Cheng, L.; Polverini, P. J.; Morgan, M. A.; Wen, H.; Prince, M. E.; Ferris, R. L.; Xie, Y.; Young, S.; Wolf, G. T.; Chen, Q.; Lei, Y. L. HPV16 Drives Cancer Immune Escape via NLRX1-Mediated Degradation of STING. *J Clin Invest* **2020**, *130* (4), 1635–1652. https://doi.org/10.1172/JCI129497.
40. Tomayko, M. M.; Reynolds, C. P. Determination of Subcutaneous Tumor Size in Athymic (Nude) Mice. *Cancer Chemother Pharmacol* **1989**, *24* (3), 148–154. https://doi.org/10.1007/BF00300234.
41. Nagai-Singer, M. A.; Hendricks-Wenger, A.; Brock, R. M.; Morrison, H. A.; Tupik, J. D.; Coutermarsh-Ott, S.; Allen, I. C. Using Computer-Based Image Analysis to Improve Quantification of Lung Metastasis in the 4T1 Breast Cancer Model. *JoVE (Journal of Visualized Experiments)* **2020**, No. 164, e61805. https://doi.org/10.3791/61805.
42. *Mouse 4T1 Breast Tumor Model - Pulaski - 2000 - Current Protocols in Immunology - Wiley Online Library*. https://currentprotocols.onlinelibrary.wiley.com/doi/10.1002/0471142735.im2002s39 (accessed 2022-06-09).

43. The Human Protein Atlas. *Tissue expression of NLRX1 - Summary - The Human Protein Atlas*. https://www.proteinatlas.org/ENSG00000160703-NLRX1/tissue (accessed 2022-09-12).
44. Zhao, M.; Kong, L.; Liu, Y.; Qu, H. DbEMT: An Epithelial-Mesenchymal Transition Associated Gene Resource. *Sci Rep* **2015**, *5* (1), 11459. https://doi.org/10.1038/srep11459.
45. Onder, T. T.; Gupta, P. B.; Mani, S. A.; Yang, J.; Lander, E. S.; Weinberg, R. A. Loss of E-Cadherin Promotes Metastasis via Multiple Downstream Transcriptional Pathways. *Cancer Research* **2008**, *68* (10), 3645–3654. https://doi.org/10.1158/0008-5472.CAN-07-2938.
46. Xu, J.; Lamouille, S.; Derynck, R. TGF-β-Induced Epithelial to Mesenchymal Transition. *Cell Res* **2009**, *19* (2), 156–172. https://doi.org/10.1038/cr.2009.5.
47. Wang, G.; Xu, D.; Zhang, Z.; Li, X.; Shi, J.; Sun, J.; Liu, H.-Z.; Li, X.; Zhou, M.; Zheng, T. The Pan-Cancer Landscape of Crosstalk between Epithelial-Mesenchymal Transition and Immune Evasion Relevant to Prognosis and Immunotherapy Response. *npj Precis. Onc.* **2021**, *5* (1), 1–10. https://doi.org/10.1038/s41698-021-00200-4.
48. Taki, M.; Abiko, K.; Ukita, M.; Murakami, R.; Yamanoi, K.; Yamaguchi, K.; Hamanishi, J.; Baba, T.; Matsumura, N.; Mandai, M. Tumor Immune Microenvironment during Epithelial–Mesenchymal Transition. *Clinical Cancer Research* **2021**, *27* (17), 4669–4679. https://doi.org/10.1158/1078-0432.CCR-20-4459.
49. Grisaru-Tal, S.; Itan, M.; Klion, A. D.; Munitz, A. A New Dawn for Eosinophils in the Tumour Microenvironment. *Nat Rev Cancer* **2020**, *20* (10), 594–607. https://doi.org/10.1038/s41568-020-0283-9.
50. Fulkerson, P. C.; Zhu, H.; Williams, D. A.; Zimmermann, N.; Rothenberg, M. E. CXCL9 Inhibits Eosinophil Responses by a CCR3- and Rac2-Dependent Mechanism. *Blood* **2005**, *106* (2), 436–443. https://doi.org/10.1182/blood-2005-02-0489.
51. Kastelberg, B.; Tubau-Juni, N.; Ayubi, T.; Leung, A.; Leber, A.; Hontecillas, R.; Bassaganya-Riera, J.; Kale, S. D. NLRX1 Is a Key Regulator of Immune Signaling during Invasive Pulmonary Aspergillosis. *PLOS Pathogens* **2020**, *16* (9), e1008854. https://doi.org/10.1371/journal.ppat.1008854.
52. Zhang, C.; Li, Z.; Xu, L.; Che, X.; Wen, T.; Fan, Y.; Li, C.; Wang, S.; Cheng, Y.; Wang, X.; Qu, X.; Liu, Y. CXCL9/10/11, a Regulator of PD-L1 Expression in Gastric Cancer. *BMC Cancer* **2018**, *18* (1), 462. https://doi.org/10.1186/s12885-018-4384-8.
53. Guo, W.; Zhang, S.; Liu, S. Establishment of a Novel Orthotopic Model of Breast Cancer Metastasis to the Lung. *Oncology Reports* **2015**, *33* (6), 2992–2998. https://doi.org/10.3892/or.2015.3927.
54. Jinesh, G. G.; Brohl, A. S. Classical Epithelial-Mesenchymal Transition (EMT) and Alternative Cell Death Process-Driven Blebbishield Metastatic-Witch (BMW) Pathways to Cancer Metastasis. *Sig Transduct Target Ther* **2022**, *7* (1), 1–17. https://doi.org/10.1038/s41392-022-01132-6.
55. Liu, Y.; Cao, X. Characteristics and Significance of the Pre-Metastatic Niche. *Cancer Cell* **2016**, *30* (5), 668–681. https://doi.org/10.1016/j.ccell.2016.09.011.
56. Liu, Y.; Tang, N.; Cao, K.; Wang, S.; Tang, S.; Su, H.; Zhou, J. Negative-Pressure Wound Therapy Promotes Wound Healing by Enhancing Angiogenesis Through

Suppression of NLRX1 via MiR-195 Upregulation. *Int J Low Extrem Wounds* **2018**, *17* (3), 144–150. https://doi.org/10.1177/1534734618794856.
57. Coutermarsh-Ott, S. L.; Broadway, K. M.; Scharf, B. E.; Allen, I. C. Effect of Salmonella Enterica Serovar Typhimurium VNP20009 and VNP20009 with Restored Chemotaxis on 4T1 Mouse Mammary Carcinoma Progression. *Oncotarget* **2017**, *8* (20), 33601–33613. https://doi.org/10.18632/oncotarget.16830.
58. Ringel-Scaia, V. M.; Beitel-White, N.; Lorenzo, M. F.; Brock, R. M.; Huie, K. E.; Coutermarsh-Ott, S.; Eden, K.; McDaniel, D. K.; Verbridge, S. S.; Rossmeisl, J. H.; Oestreich, K. J.; Davalos, R. V.; Allen, I. C. High-Frequency Irreversible Electroporation Is an Effective Tumor Ablation Strategy That Induces Immunologic Cell Death and Promotes Systemic Anti-Tumor Immunity. *EBioMedicine* **2019**, *44*, 112–125. https://doi.org/10.1016/j.ebiom.2019.05.036.
59. Pulaski, B. A.; Ostrand-Rosenberg, S. Mouse 4T1 Breast Tumor Model. *Current Protocols in Immunology* **2000**, *39* (1), 20.2.1-20.2.16. https://doi.org/10.1002/0471142735.im2002s39.
60. Soares, F.; Tattoli, I.; Wortzman, M. E.; Arnoult, D.; Philpott, D. J.; Girardin, S. E. NLRX1 Does Not Inhibit MAVS-Dependent Antiviral Signalling. *Innate Immun* **2013**, *19* (4), 438–448. https://doi.org/10.1177/1753425912467383.
61. Abdul-Sater, A. A.; Saïd-Sadier, N.; Lam, V. M.; Singh, B.; Pettengill, M. A.; Soares, F.; Tattoli, I.; Lipinski, S.; Girardin, S. E.; Rosenstiel, P.; Ojcius, D. M. Enhancement of Reactive Oxygen Species Production and Chlamydial Infection by the Mitochondrial Nod-like Family Member NLRX1. *J Biol Chem* **2010**, *285* (53), 41637–41645. https://doi.org/10.1074/jbc.M110.137885.
62. Unger, B. L.; Ganesan, S.; Comstock, A. T.; Faris, A. N.; Hershenson, M. B.; Sajjan, U. S. Nod-Like Receptor X-1 Is Required for Rhinovirus-Induced Barrier Dysfunction in Airway Epithelial Cells. *J Virol* **2014**, *88* (7), 3705–3718. https://doi.org/10.1128/JVI.03039-13.
63. Lei, Y.; Kansy, B. A.; Li, J.; Cong, L.; Liu, Y.; Trivedi, S.; Wen, H.; Ting, J. P.-Y.; Ouyang, H.; Ferris, R. L. EGFR-Targeted MAb Therapy Modulates Autophagy in Head and Neck Squamous Cell Carcinoma through NLRX1-TUFM Protein Complex. *Oncogene* **2016**, *35* (36), 4698–4707. https://doi.org/10.1038/onc.2016.11.
64. Hao, Y.; Baker, D.; ten Dijke, P. TGF-β-Mediated Epithelial-Mesenchymal Transition and Cancer Metastasis. *Int J Mol Sci* **2019**, *20* (11), 2767. https://doi.org/10.3390/ijms20112767.
65. Dongre, A.; Weinberg, R. A. New Insights into the Mechanisms of Epithelial–Mesenchymal Transition and Implications for Cancer. *Nat Rev Mol Cell Biol* **2019**, *20* (2), 69–84. https://doi.org/10.1038/s41580-018-0080-4.
66. Owyong, M.; Chou, J.; van den Bijgaart, R. J.; Kong, N.; Efe, G.; Maynard, C.; Talmi-Frank, D.; Solomonov, I.; Koopman, C.; Hadler-Olsen, E.; Headley, M.; Lin, C.; Wang, C.-Y.; Sagi, I.; Werb, Z.; Plaks, V. MMP9 Modulates the Metastatic Cascade and Immune Landscape for Breast Cancer Anti-Metastatic Therapy. *Life Sci Alliance* **2019**, *2* (6), e201800226. https://doi.org/10.26508/lsa.201800226.
67. Wong, T.-S.; Gao, W.; Chan, J. Y.-W. Transcription Regulation of E-Cadherin by Zinc Finger E-Box Binding Homeobox Proteins in Solid Tumors. *Biomed Res Int* **2014**, *2014*, 921564. https://doi.org/10.1155/2014/921564.

68. Conacci-Sorrell, M.; Simcha, I.; Ben-Yedidia, T.; Blechman, J.; Savagner, P.; Ben-Ze'ev, A. Autoregulation of E-Cadherin Expression by Cadherin-Cadherin Interactions: The Roles of Beta-Catenin Signaling, Slug, and MAPK. *J Cell Biol* **2003**, *163* (4), 847–857. https://doi.org/10.1083/jcb.200308162.
69. Peiró, S.; Escrivà, M.; Puig, I.; Barberà, M. J.; Dave, N.; Herranz, N.; Larriba, M. J.; Takkunen, M.; Francí, C.; Muñoz, A.; Virtanen, I.; Baulida, J.; García de Herreros, A. Snail1 Transcriptional Repressor Binds to Its Own Promoter and Controls Its Expression. *Nucleic Acids Res* **2006**, *34* (7), 2077–2084. https://doi.org/10.1093/nar/gkl141.
70. Wang, Q.; Sun, Z.-X.; Allgayer, H.; Yang, H.-S. Downregulation of E-Cadherin Is an Essential Event in Activating Beta-Catenin/Tcf-Dependent Transcription and Expression of Its Target Genes in Pdcd4 Knockdown Cells. *Oncogene* **2010**, *29* (1), 128–138. https://doi.org/10.1038/onc.2009.302.
71. Varricchi, G.; Galdiero, M. R.; Loffredo, S.; Lucarini, V.; Marone, G.; Mattei, F.; Marone, G.; Schiavoni, G. Eosinophils: The Unsung Heroes in Cancer? *Oncoimmunology* **2018**, *7* (2), e1393134. https://doi.org/10.1080/2162402X.2017.1393134.
72. Charles River. *BALB/c Mice*. https://www.criver.com/products-services/find-model/balbc-mouse?region=3611 (accessed 2022-10-01).
73. Marchetti, P.; Fovez, Q.; Germain, N.; Khamari, R.; Kluza, J. Mitochondrial Spare Respiratory Capacity: Mechanisms, Regulation, and Significance in Non-Transformed and Cancer Cells. *The FASEB Journal* **2020**, *34* (10), 13106–13124. https://doi.org/10.1096/fj.202000767R.
74. Cortassa, S.; O'Rourke, B.; Aon, M. A. Redox-Optimized ROS Balance and the Relationship between Mitochondrial Respiration and ROS. *Biochim Biophys Acta* **2014**, *1837* (2), 287–295. https://doi.org/10.1016/j.bbabio.2013.11.007.

FIGURE LEGENDS

Figure 1. NLRX1 in healthy host cells is protective against mammary tumor progression. **A.** Tumor growth over time was monitored in 2 dimensions, with minimal differences in progression noted between wild type (WT) and *Nlrx1*$^{-/-}$ mice. **B.** Morbidity and **C.** mortality were not significantly impacted by mouse genotype. **D.** The final tumor volume, measured in 3 dimensions, was significantly increased in the *Nlrx1*$^{-/-}$ mice compared to the WT animals. **E-F.** Significant differences between WT and *Nlrx1*$^{-/-}$ mice were observed in **(E)** quantification of lung metastasis and **(F)** representative images of lung metastatic colonies. **G.** Increased blood metastasis was observed in the *Nlrx1*$^{-/-}$ mice compared to the WT animals but was not significant. **H.** Histopathology comparisons using H&E stained tissue sections did not reveal any significant pathological differences between *Nlrx1*$^{-/-}$ and WT tumors. Lung metastasis, blood metastasis, and final tumor volume were analyzed using a two-way unpaired T test. Tumor growth and morbidity were analyzed using multiple T tests – one per row. Survival was analyzed using a Log-Rank Mantel-Cox test. WT (n=5) and *Nlrx1*$^{-/-}$ (n=7) mice. Data are representative of 2 independent experiments. All data displayed as mean ± SE. *$p \leq 0.05$, **$p \leq 0.01$, ***$p \leq 0.001$, **** $p \leq 0.0001$.

Figure 2. NLRX1 in healthy host cells impacts EMT and the tumor microenvironment immune niche. A. Transcriptomic assessments identified pathways significantly altered in tumors harvested from *Nlrx1*$^{-/-}$ mice compared to WT animals, defined by the number of DEGs in the Transcriptomics Analysis Console (TAC) software. Pathways are listed alphabetically as a heat map by TAC significance (*Nlrx1*$^{-/-}$ tumors vs WT tumors). The analysis revealed 5 pathways related to EMT were identified as significantly altered based on animal genotype. **B.** Heat maps of the DEGs from respective pathways in TAC (*Nlrx1*$^{-/-}$ tumors vs WT tumors) were generated. **C.** Heat map of DEGs from EMT-related genes significantly altered in the *Nlrx1*$^{-/-}$ tumors compared to the WT tumors. **D-E.** Differences in protein levels for **(D)** E-Cadherin and **(E)** MMP9 and TGF-β **F**. Ingenuity Pathway Analysis (IPA) and TAC analysis were utilized to generate a working model of the pathways altered by NLRX1 in 4T1 tumor progression and metastasis. **G-H.** Flow cytometry was used to define the immune niche of the tumor microenvironment in tumors harvested from *Nlrx1*$^{-/-}$ and WT mice. **(G)** Representative scatter plots showing an increase in the number of eosinophils present in *Nlrx1*$^{-/-}$ tumors. **(H)** Quantification of flow cytometry data

confirmed a statistically significant increase in eosinophils in tumors collected from *Nlrx1*$^{-/-}$ mice (n=5) compared to the WT tumors (n=5). Data were analyzed using two-way unpaired T test and shown as mean ± SE. **I.** Heat map of five DEGs (*Nlrx1*$^{-/-}$ tumors vs WT tumors) associated with eosinophil recruitment. *p ≤ 0.05, **p ≤ 0.01, ***p ≤ 0.001, **** p ≤ 0.0001.

Figure 3. NLRX1 in healthy host cells attenuates metastatic niche formation. A-B. Western blot analysis of MMP9, IL-6, TGF-β, LOX, Fibronectin, and CD31 in (**A)** pre-metastasis lungs (n = 4 per genotype) and (**B)** post-metastasis lungs (n = 5 per genotype). **C.** Summary schematic of biological effects of NLRX1 on the pre- and post-metastatic niche in the lungs harvested. **D-G.** Quantification of **(D)** Double Negative T cells, **(E)** CD4+ T cells, **(F)** Inflammatory DCs, and **(G)** NK cells in pre-metastasis lungs evaluated using flow cytometry. Western blot images are representative of two experiments and flow cytometry experiments were performed once. n = 4 for both genotypes. All quantification data were analyzed using a two-way unpaired T test and shown as mean ± SE. *p ≤ 0.05, **p ≤ 0.01, ***p ≤ 0.001, **** p ≤ 0.0001.

Figure 4. NLRX1 modulates critical biological functions associated with cancer in 4T1 cells. **A.** Western blot verification of NLRX1 knockdown ($4T1^{KD}$) and overexpression ($4T1^{OE}$) in 4T1 cells with separate control cell line ($4T1^{KD\text{-}CTL}$; $4T1^{OE\text{-}CTL}$, respectively) and schematic of the generated cells and color scheme for data. **B.** Proliferation differences between $4T1^{OE}$ cells and $4T1^{OE\text{-}CTL}$ cells (p=0.08), and between $4T1^{KD}$ cells and $4T1^{KD\text{-}CTL}$ cells. **C.** H_2O_2-induced cell death differences between $4T1^{OE}$ cells and $4T1^{OE\text{-}CTL}$ cells, and $4T1^{KD}$ cells and $4T1^{KD\text{-}CTL}$ cells. **D-E.** Differences in migration rate after **(D)** 5 hours and **(E)** 8 hours between $4T1^{OE}$ cells and $4T1^{OE\text{-}CTL}$ cells, and $4T1^{KD}$ cells and $4T1^{KD\text{-}CTL}$ cells. **F.** Differences in mitochondrial ROS (superoxide) levels between $4T1^{OE}$ cells and $4T1^{OE\text{-}CTL}$ cells, and $4T1^{KD}$ cells and $4T1^{KD\text{-}CTL}$ cells. **G-H.** Differences in (**G**) mitochondrial respiration and **(H)** spare respiratory capacity between $4T1^{OE}$ cells and $4T1^{OE\text{-}CTL}$ cells, and $4T1^{KD}$ cells and $4T1^{KD\text{-}CTL}$ cells. Data were analyzed using two-way unpaired t test. All data are shown as mean ± SE. n = 4-15 for each cell type per study. All data are representative of at least 2 independent studies. *p ≤ 0.05, **p ≤ 0.01, ***p ≤ 0.001, **** p ≤ 0.0001.

Figure 5. NLRX1 in 4T1 cells functions as a tumor promoter in the 4T1 *in vivo* mammary tumor model. A. Schematic of the overexpression study design using WT and *Nlrx1*$^{-/-}$ mice with either 4T1^{OE} or 4T1$^{OE\text{-}CTL}$ cells and color scheme for data. **B-E.** Differences in disease burden between 4T1^{OE} or 4T1$^{OE\text{-}CTL}$ tumors in both WT and *Nlrx1*$^{-/-}$ mice. Data are representative of 2 independent experiments. **(B)** Minimal differences were observed in tumor growth, but significant differences in **(C)** 3-dimensional final tumor volume measurements were present. **(D)** No differences in morbidity were observed. **(E)** Lung metastasis was increased in WT and *Nlrx1*$^{-/-}$ mice with 4T1^{OE} tumors. **F.** Schematic of knockdown study design using WT and *Nlrx1*$^{-/-}$ mice with either 4T1^{KD} or 4T1$^{KD\text{-}CTL}$ cells and color scheme for data. Data representative of one independent experiment. **G-K.** Differences in disease burden between 4T1^{KD} or 4T1$^{KD\text{-}CTL}$ tumors in both WT and *Nlrx1*$^{-/-}$ mice. **(G)** Minimal differences were observed in 2-dimensional tumor growth measurements and **(H)** no differences were observed in 3-dimensional final tumor volume measurements. **(I)** WT mice with 4T1$^{KD\text{-}CTL}$ tumors displayed more severe morbidity than those with 4T1^{KD} tumors, caused by **(J)** more severe tumor eschar as determined by tumor condition score. **(K)** Lung metastasis was increased in WT mice with 4T1$^{KD\text{-}CTL}$ tumors compared to those with 4T1^{KD} tumors. Data were analyzed using two-way unpaired t test and are shown as mean ± SE. n = 3-5 for each group per study. *$p \leq 0.05$, **$p \leq 0.01$, ***$p \leq 0.001$, **** $p \leq 0.0001$.

Figure 6. Overexpression of NLRX1 in 4T1 cells increases epithelial-mesenchymal transition. A. Twenty pathways were identified by the number of DEGs in the Transcriptomics Analysis Console (TAC) software as being significant in at least 2 of the 4 groups compared, listed here alphabetically as a heat map of TAC significance. **B-C.** Heat maps of DEGs from respective pathways in TAC between **(B)** 4T1^{OE} vs 4T1$^{OE\text{-}CTL}$ tumors in *Nlrx1*$^{-/-}$ mice and **(C)** 4T1^{OE} vs 4T1$^{OE\text{-}CTL}$ tumors in WT mice. **D-E.** Heat map of DEGs from EMT-related genes between **(D)** 4T1^{OE} vs 4T1$^{OE\text{-}CTL}$ tumors in *Nlrx1*$^{-/-}$ mice and **(E)** 4T1^{OE} vs 4T1$^{OE\text{-}CTL}$ tumors in WT mice. **F.** Western blot of E-Cadherin from WT and *Nlrx1*$^{-/-}$ mice with either 4T1^{OE}, 4T1$^{OE\text{-}CTL}$, 4T1^{KD}, or 4T1$^{KD\text{-}CTL}$ tumors. **G.** Pathway analysis of transcriptomics data predicts multiple pathways up-regulated by NLRX1 in 4T1 cells that converge to increase EMT.

SUPPLEMENTAL FIGURE LEGENDS

Supplemental Figure S1. Flow cytometry panel. A complete list of the flow cytometry antibodies used and the markers for each cell type.

Supplemental Figure S2. Generation and confirmation of *Nlrx1*$^{-/-}$ BALB/cJ mice. A. Breeding schematic. **B.** Gel electrophoresis image of first *Nlrx1*$^{-/-}$ BALB/cJ mice generated through backcrossing. Knockout mice are indicated with an asterisk.

Supplemental Figure S3. Expansion on NLRX1 in healthy host cells impacts EMT and the tumor microenvironment immune niche. A. Heatmap of the complete list of 100 EMT-related genes (*Nlrx1*$^{-/-}$ tumors vs WT tumors). **B.** Densitometry of E-Cadherin, MMP9, and TGF-β western blots. n = 4-5 per genotype. Data were analyzed with two-way unpaired t tests and are shown as mean ± SE. **C.** Heatmap of the complete list of genes in the murine breast cancer RT^2 Profiler PCR Array (*Nlrx1*$^{-/-}$ tumors vs WT tumors). **D.** Ingenuity Pathway Analysis (IPA) output. **E.** Quantification of immune cell populations in the tumor that were not statistically significant between WT (n=5) and *Nlrx1*$^{-/-}$ (n=5) mice. Data were analyzed with two-way unpaired t tests and are shown as mean ± SE. *$p \leq 0.05$, **$p \leq 0.01$, ***$p \leq 0.001$, **** $p \leq 0.0001$.

Supplemental Figure S4. Expansion on NLRX1 in healthy host cells attenuates metastatic niche formation. A-B. Densitometry of Lox, Fibronectin, IL6, TGF-β, CD31, and MMP9 western blot at the **(A)** pre-metastasis timepoint (n = 4 per genotype) and the **(B)** post-metastasis timepoint (n = 5 per genotype). **C-F.** In the pre-metastatic lungs (n = 4 per genotype), **(C)** quantification of immune cell populations that were not statistically significant between WT and *Nlrx1*$^{-/-}$ mice and **(D)** the representative flow cytometry scatter plots of immune cell populations that were statistically significant, including **(D)** double negative T cells and CD4+ T cells, **(E)** inflammatory DCs, and **(F)** NK cells. **G.** In the post-metastatic lung (n=4 per genotype), quantification of immune cell populations that were not statistically significant between WT and *Nlrx1*$^{-/-}$ mice. Data were analyzed with two-way unpaired t tests and are shown as mean ± SE. *$p \leq 0.05$, **$p \leq 0.01$, ***$p \leq 0.001$, **** $p \leq 0.0001$.

Supplemental Figure S5. Expansion of NLRX1 modulates critical biological functions associated with cancer in 4T1 cells. A. Proliferation differences between $4T1^{OE}$ cells and $4T1^{OE\text{-}CTL}$ cells, and between $4T1^{KD}$ cells and $4T1^{KD\text{-}CTL}$ cells (n = 4 per group) when stimulated with TNF or TGF-β. **B.** Differences in mitochondrial ROS production between $4T1^{OE}$ cells and $4T1^{OE\text{-}CTL}$ cells, and $4T1^{KD}$ cells and $4T1^{KD\text{-}CTL}$ cells (n = 4-6 per group) when stimulated with TNF. Differences in **C.** mitochondrial respiration and **D.** spare respiratory capacity between $4T1^{OE}$ cells and $4T1^{OE\text{-}CTL}$ cells, and $4T1^{KD}$ cells and $4T1^{KD\text{-}CTL}$ cells (n = 7 per group) when stimulated with TNF or TGF-β. Proliferation, ROS production, and respiratory capacity were analyzed using a two-way unpaired T test. Mitochondrial respiration was analyzed using multiple t tests – one per row. All data are shown as mean ± SE. *$p \leq 0.05$, **$p \leq 0.01$, ***$p \leq 0.001$, **** $p \leq 0.0001$.

Supplemental Figure S6. Expansion on NLRX1 in 4T1 cells functions as a tumor promoter in the 4T1 in vivo mammary tumor model. A. Comparison of tumor eschar between $4T1^{KD}$ and $4T1^{KD\text{-}CTL}$ tumors in WT and *Nlrx1*$^{-/-}$ mice. **B-I.** Ordinary one-way ANOVAs with Tukey's multiple comparisons test were performed to compare all four groups within the overexpression studies and the knockdown studies. No differences were observed in tumor growth in the **(B)** overexpression or **(C)** knockdown studies, or in morbidity in the **(D)** overexpression or **(E)** knockdown studies. **(F)** No additional differences were observed in the final tumor volume in the overexpression studies, and **(G)** no significant differences were observed in final tumor volume in the knockdown studies. **(H)** In the overexpression studies, additional insight was gained showing differences in lung metastasis between WT mice and *Nlrx1*$^{-/-}$ mice with $4T1^{OE}$ tumors. **(I)** No significant differences lung metastasis in the knockdown studies were observed. n = 3-5 for each group per study. All data are shown as mean ± SE. *$p \leq 0.05$, **$p \leq 0.01$, ***$p \leq 0.001$, **** $p \leq 0.0001$.

Supplemental Figure S7. Expansion on overexpression of NLRX1 in 4T1 cells increases epithelial-mesenchymal transition. A. Heatmap of the complete list of 100 EMT-related genes ($4T1^{OE}$ vs $4T1^{OE\text{-}CTL}$ tumors). **B.** Densitometry of E-Cadherin western blots from $4T1^{OE}$, $4T1^{OE\text{-}CTL}$, $4T1^{KD}$, and $4T1^{KD\text{-}CTL}$ tumors in WT and *Nlrx1*$^{-/-}$ mice. n = 3-5 per group. All data are shown as mean ± SE. *$p \leq 0.05$, **$p \leq 0.01$, ***$p \leq 0.001$, **** $p \leq 0.0001$.

Figure 1

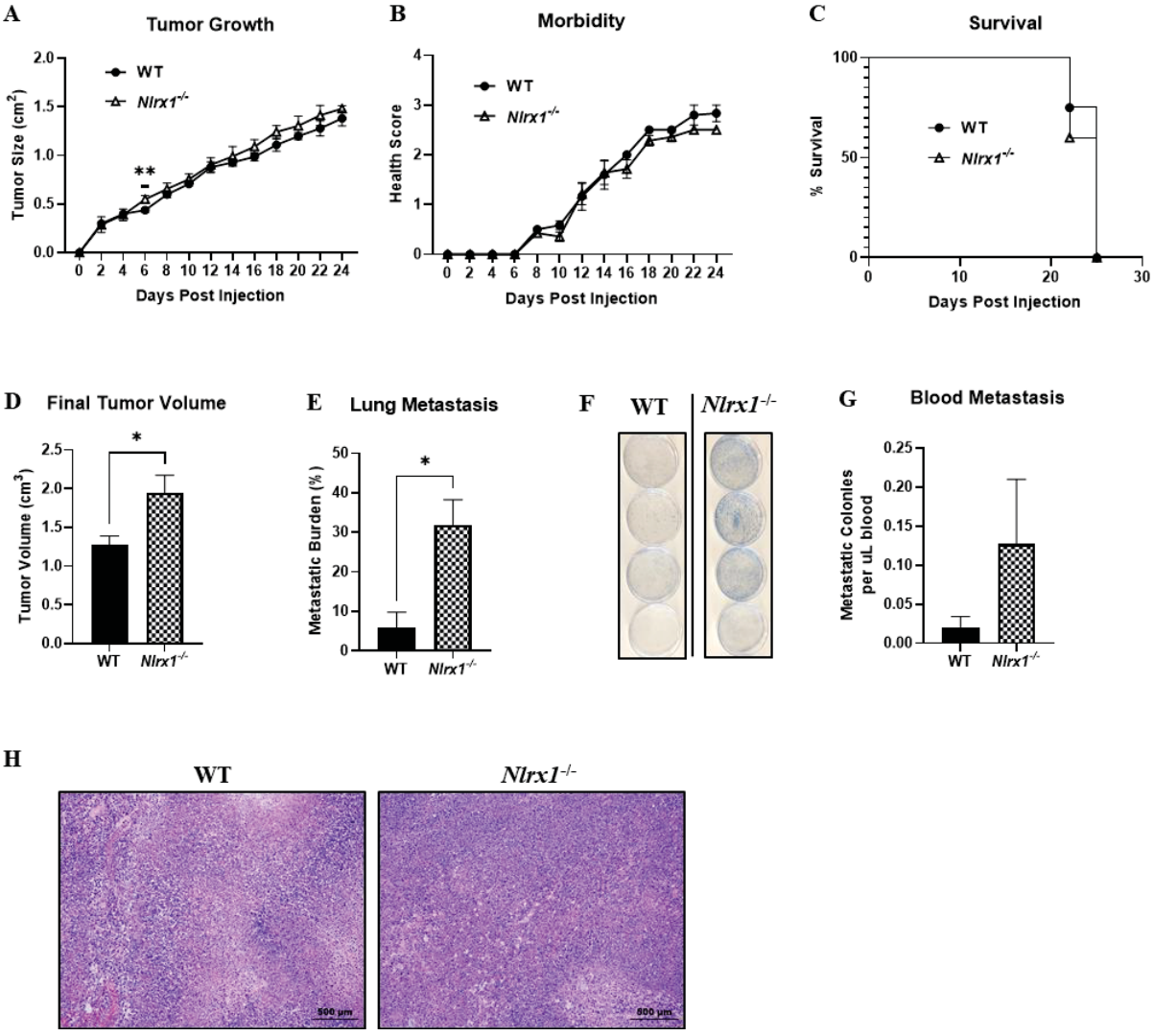
A
Tumor Growth
WT
Nlrx1-/-
Tumor Size (cm2)
Days Post Injection
**
B
Morbidity
Health Score
Days Post Injection
C
Survival
% Survival
Days Post Injection
D
Final Tumor Volume
Tumor Volume (cm3)
*
E
Lung Metastasis
Metastatic Burden (%)
F
WT
Nlrx1-/-
G
Blood Metastasis
Metastatic Colonies per uL blood
H
WT
Nlrx1-/-
500 µm

Figure 2

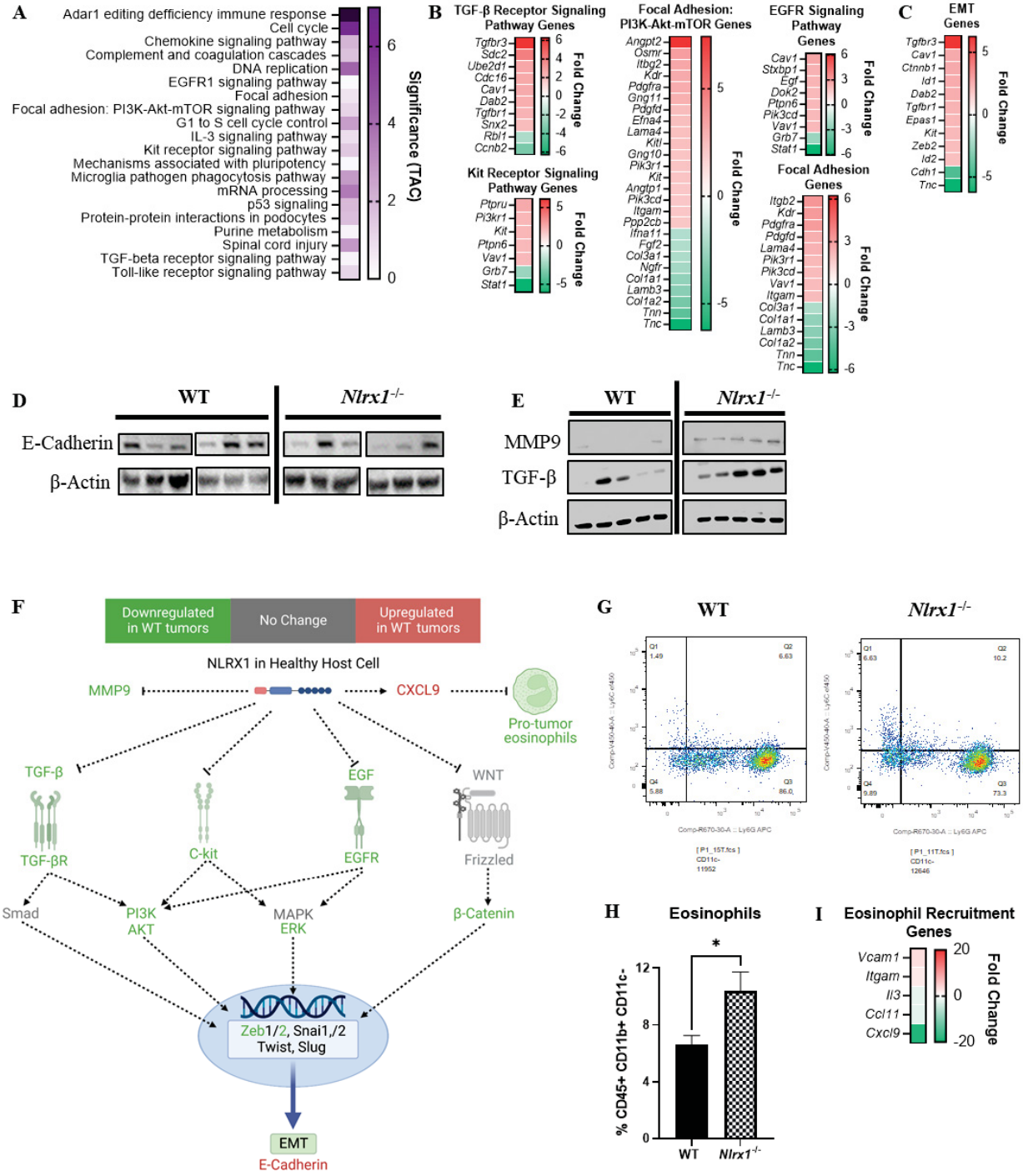
A
Adar1 editing defficiency immune response
Cell cycle
Chemokine signaling pathway
Complement and coagulation cascades
DNA replication
EGFR1 signaling pathway
Focal adhesion
Focal adhesion: PI3K-Akt-mTOR signaling pathway
G1 to S cell cycle control
IL-3 signaling pathway
Kit receptor signaling pathway
Mechanisms associated with pluripotency
Microglia pathogen phagocytosis pathway
mRNA processing
p53 signaling
Protein-protein interactions in podocytes
Purine metabolism
Spinal cord injury
TGF-beta receptor signaling pathway
Toll-like receptor signaling pathway
Significance (TAC)
B
TGF-β Receptor Signaling Pathway Genes
Kit Receptor Signaling Pathway Genes
Focal Adhesion: PI3K-Akt-mTOR Genes
EGFR Signaling Pathway Genes
Focal Adhesion Genes
Fold Change
C
EMT Genes
D
WT
Nlrx1-/-
E-Cadherin
β-Actin
E
WT
Nlrx1-/-
MMP9
TGF-β
β-Actin
F
Downregulated in WT tumors
No Change
Upregulated in WT tumors
NLRX1 in Healthy Host Cell
MMP9
CXCL9
Pro-tumor eosinophils
TGF-β
TGF-βR
C-kit
EGF
EGFR
WNT
Frizzled
Smad
PI3K AKT
MAPK ERK
β-Catenin
Zeb1/2, Snai1,/2 Twist, Slug
EMT
E-Cadherin
G
WT
Nlrx1-/-
H
Eosinophils
% CD45+ CD11b+ CD11c-
WT
Nlrx1-/-
I
Eosinophil Recruitment Genes
Vcam1
Itgam
Il3
Ccl11
Cxcl9
Fold Change

Figure 3

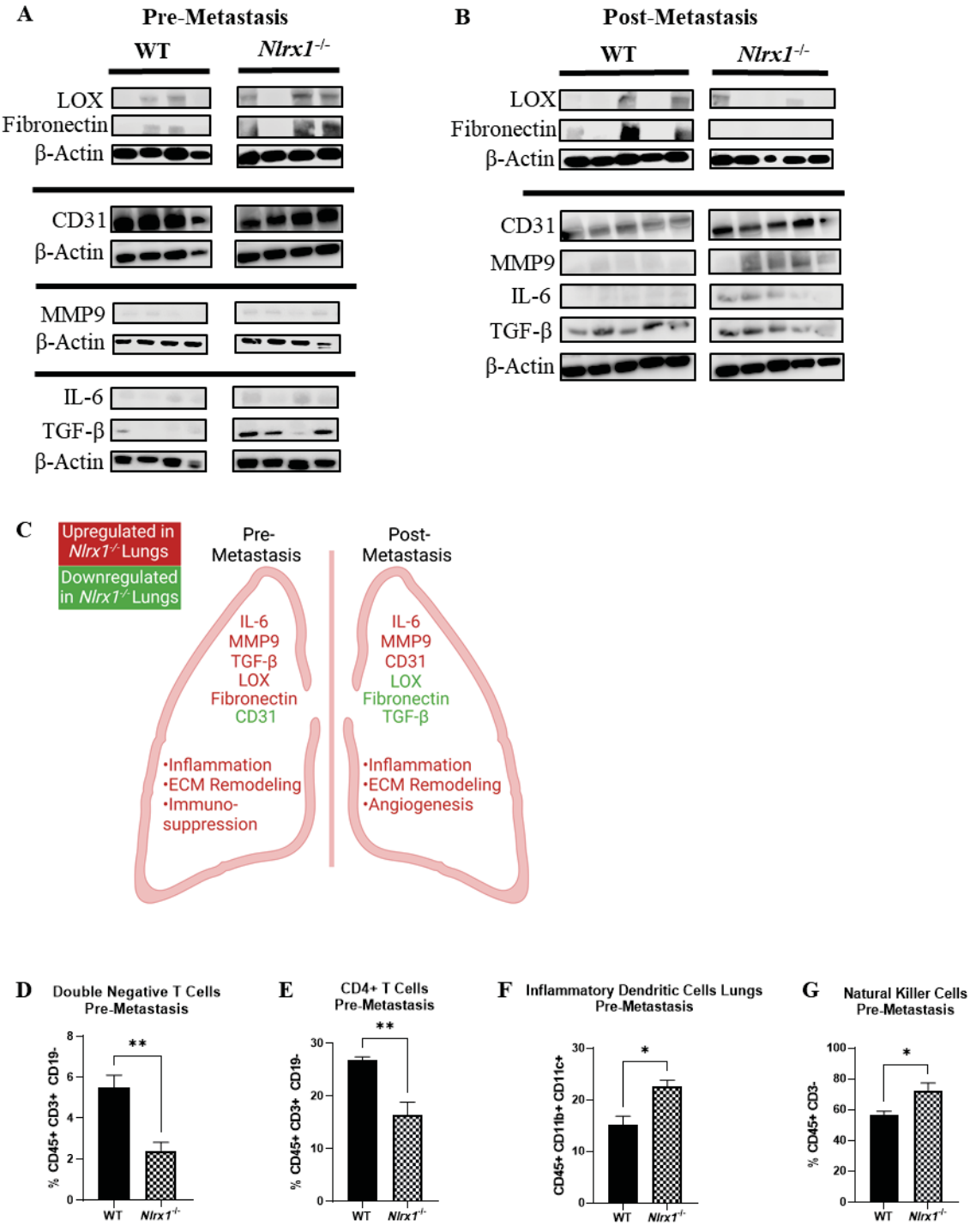
A
Pre-Metastasis
WT
Nlrx1-/-
LOX
Fibronectin
β-Actin
CD31
β-Actin
MMP9
β-Actin
IL-6
TGF-β
β-Actin
B
Post-Metastasis
WT
Nlrx1-/-
LOX
Fibronectin
β-Actin
CD31
MMP9
IL-6
TGF-β
β-Actin
C
Upregulated in Nlrx1-/- Lungs
Downregulated in Nlrx1-/- Lungs
Pre-Metastasis
Post-Metastasis
IL-6
MMP9
TGF-β
LOX
Fibronectin
CD31
•Inflammation
•ECM Remodeling
•Immuno-suppression
IL-6
MMP9
CD31
LOX
Fibronectin
TGF-β
•Inflammation
•ECM Remodeling
•Angiogenesis
D
Double Negative T Cells Pre-Metastasis
% CD45+ CD3+ CD19-
WT
Nlrx1-/-
E
CD4+ T Cells Pre-Metastasis
% CD45+ CD3+ CD19-
WT
Nlrx1-/-
F
Inflammatory Dendritic Cells Lungs Pre-Metastasis
CD45+ CD11b+ CD11c+
WT
Nlrx1-/-
G
Natural Killer Cells Pre-Metastasis
% CD45+ CD3-
WT
Nlrx1-/-

Figure 4

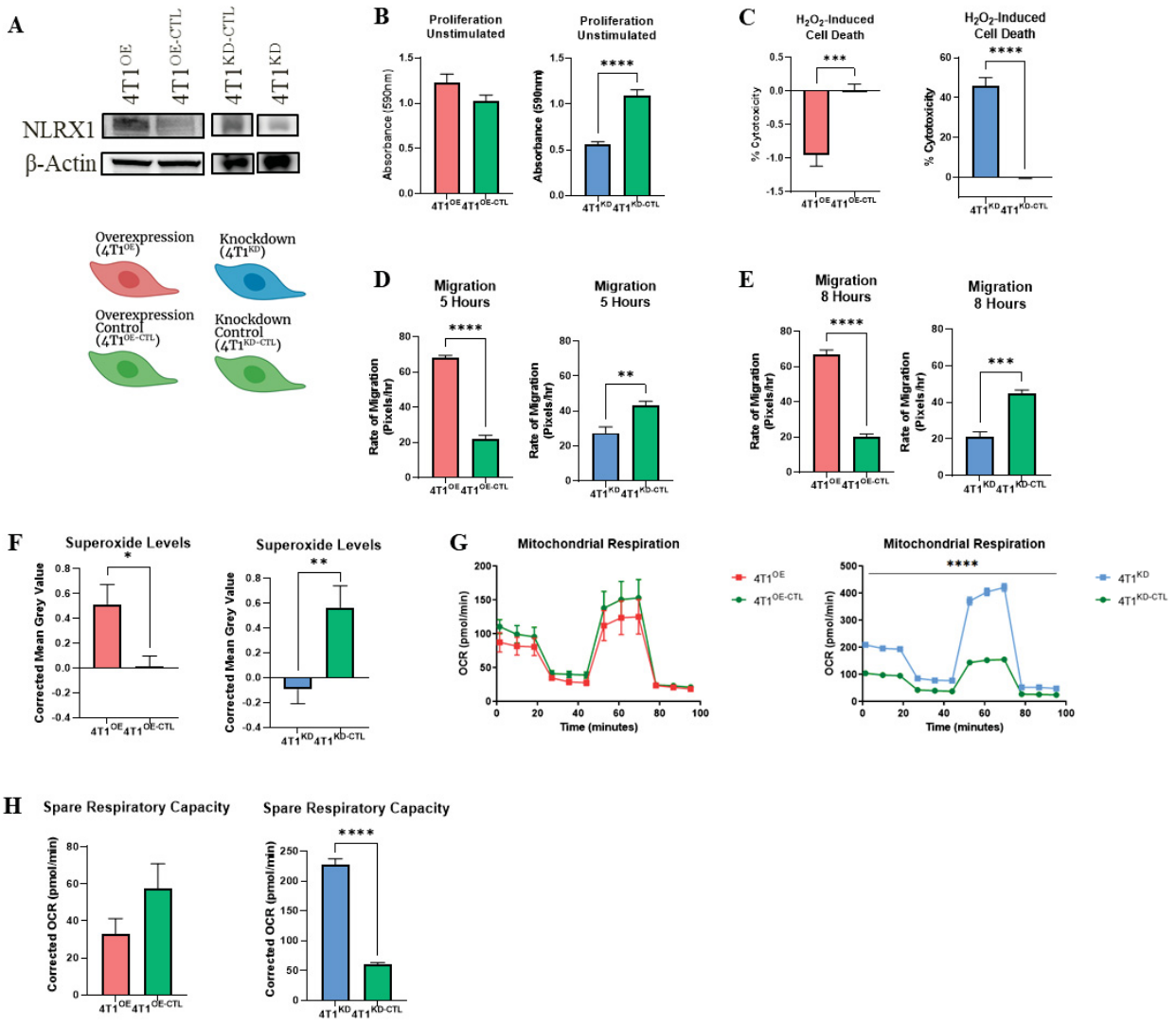
A
4T1OE
4T1OE-CTL
4T1KD-CTL
4T1KD
NLRX1
β-Actin
Overexpression (4T1OE)
Knockdown (4T1KD)
Overexpression Control (4T1OE-CTL)
Knockdown Control (4T1KD-CTL)
B
Proliferation Unstimulated
Absorbance (590nm)
Proliferation Unstimulated
Absorbance (590nm)
C
H2O2-Induced Cell Death
% Cytotoxicity
H2O2-Induced Cell Death
% Cytotoxicity
D
Migration 5 Hours
Rate of Migration (Pixels/hr)
Migration 5 Hours
Rate of Migration (Pixels/hr)
E
Migration 8 Hours
Rate of Migration (Pixels/hr)
Migration 8 Hours
Rate of Migration (Pixels/hr)
F
Superoxide Levels
Corrected Mean Grey Value
Superoxide Levels
Corrected Mean Grey Value
G
Mitochondrial Respiration
OCR (pmol/min)
Time (minutes)
Mitochondrial Respiration
OCR (pmol/min)
Time (minutes)
H
Spare Respiratory Capacity
Corrected OCR (pmol/min)
Spare Respiratory Capacity
Corrected OCR (pmol/min)

Figure 5

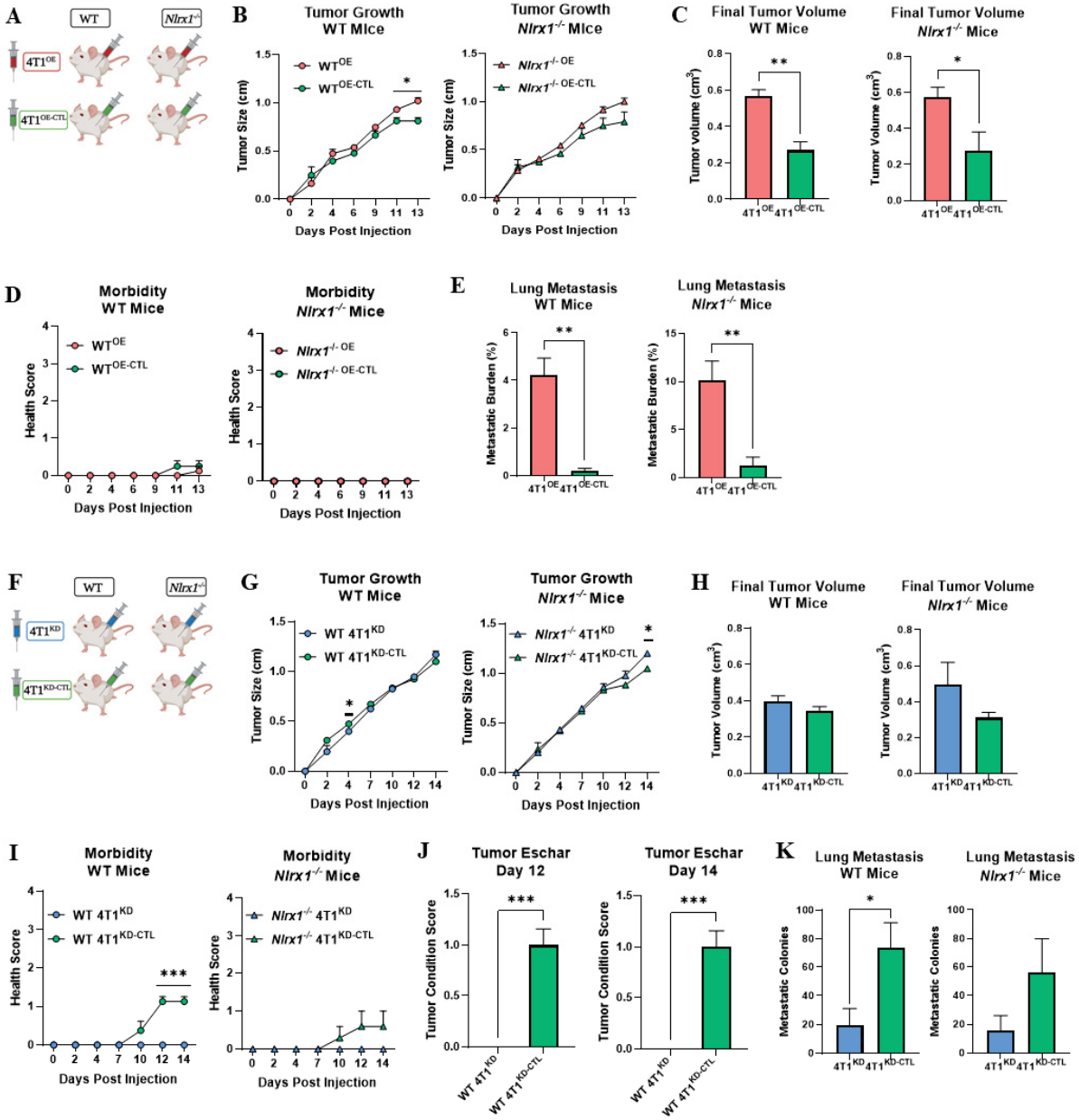
A
WT
Nlrx1-/-
4T1OE
4T1OE-CTL
B
Tumor Growth
WT Mice
WTOE
WTOE-CTL
Tumor Size (cm)
Days Post Injection
Tumor Growth
Nlrx1-/- Mice
Nlrx1-/- OE
Nlrx1-/- OE-CTL
C
Final Tumor Volume
WT Mice
Tumor volume (cm3)
Final Tumor Volume
Nlrx1-/- Mice
D
Morbidity
WT Mice
Health Score
Morbidity
Nlrx1-/- Mice
E
Lung Metastasis
WT Mice
Metastatic Burden (%)
Lung Metastasis
Nlrx1-/- Mice
F
4T1KD
4T1KD-CTL
G
Tumor Growth
WT Mice
WT 4T1KD
WT 4T1KD-CTL
Tumor Growth
Nlrx1-/- Mice
Nlrx1-/- 4T1KD
Nlrx1-/- 4T1KD-CTL
H
Final Tumor Volume
WT Mice
Final Tumor Volume
Nlrx1-/- Mice
I
Morbidity
WT Mice
Morbidity
Nlrx1-/- Mice
J
Tumor Eschar
Day 12
Tumor Condition Score
Tumor Eschar
Day 14
K
Lung Metastasis
WT Mice
Metastatic Colonies
Lung Metastasis
Nlrx1-/- Mice

Figure 6

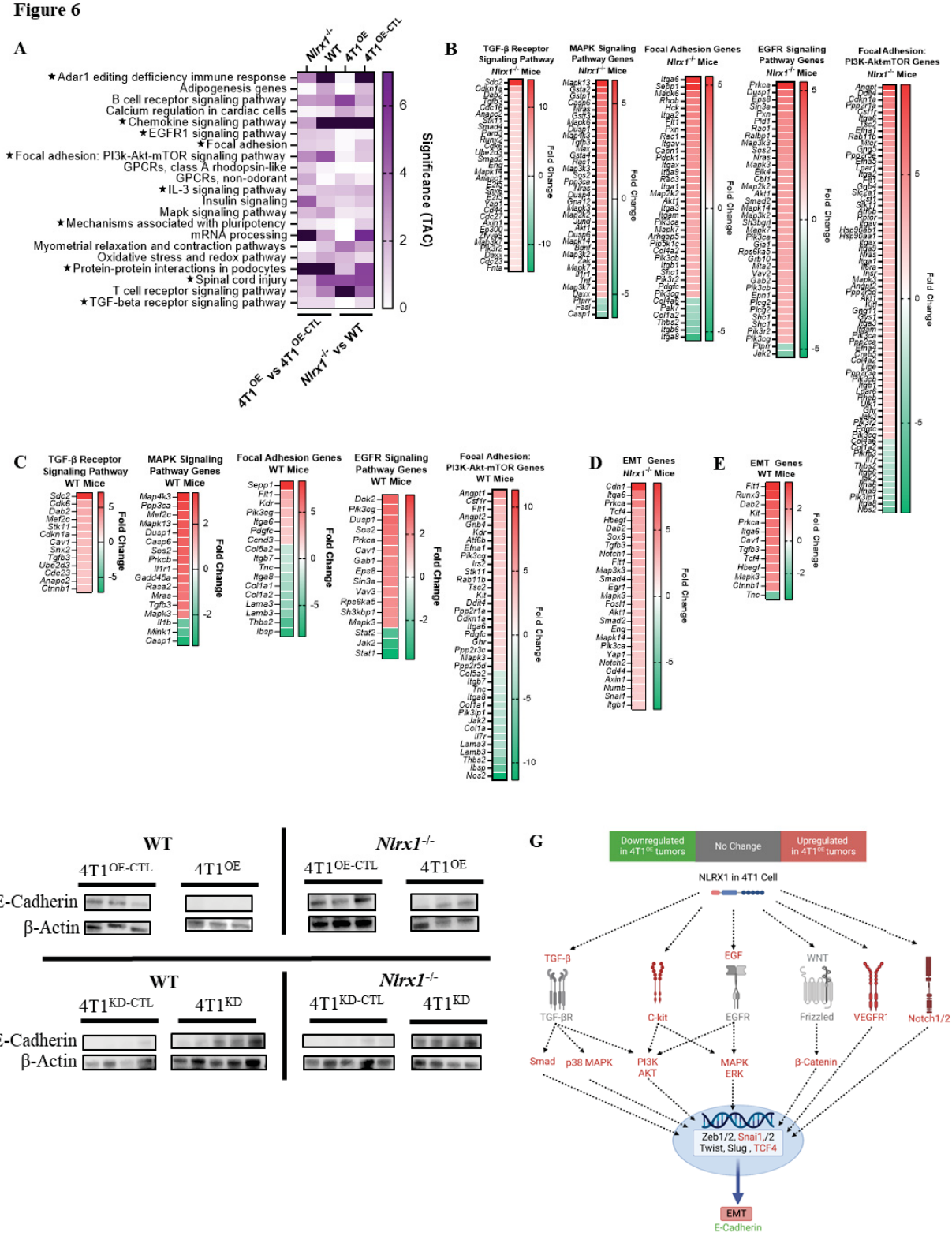
A
Nlrx1-/-
WT
4T1 OE
4T1 OE-CTL
★Adar1 editing defficiency immune response
Adipogenesis genes
B cell receptor signaling pathway
Calcium regulation in cardiac cells
★Chemokine signaling pathway
★EGFR1 signaling pathway
★Focal adhesion
★Focal adhesion: PI3k-Akt-mTOR signaling pathway
GPCRs, class A rhodopsin-like
GPCRs, non-odorant
★IL-3 signaling pathway
Insulin signaling
Mapk signaling pathway
★Mechanisms associated with pluripotency
mRNA processing
Myometrial relaxation and contraction pathways
Oxidative stress and redox pathway
★Protein-protein interactions in podocytes
★Spinal cord injury
T cell receptor signaling pathway
★TGF-beta receptor signaling pathway
Significance (TAC)
4T1 OE vs 4T1 OE-CTL
Nlrx1-/- vs WT
B
TGF-β Receptor Signaling Pathway Nlrx1-/- Mice
MAPK Signaling Pathway Genes Nlrx1-/- Mice
Focal Adhesion Genes Nlrx1-/- Mice
EGFR Signaling Pathway Genes Nlrx1-/- Mice
Focal Adhesion: PI3K-Akt-mTOR Genes Nlrx1-/- Mice
Fold Change
C
TGF-β Receptor Signaling Pathway WT Mice
MAPK Signaling Pathway Genes WT Mice
Focal Adhesion Genes WT Mice
EGFR Signaling Pathway Genes WT Mice
Focal Adhesion: PI3K-Akt-mTOR Genes WT Mice
D
EMT Genes Nlrx1-/- Mice
E
EMT Genes WT Mice

F
WT
Nlrx1-/-
4T1OE-CTL
4T1OE
E-Cadherin
β-Actin
4T1KD-CTL
4T1KD
G
Downregulated in 4T1OE tumors
No Change
Upregulated in 4T1OE tumors
NLRX1 in 4T1 Cell
TGF-β
EGF
WNT
TGF-βR
C-kit
EGFR
Frizzled
VEGFR
Notch1/2
Smad
p38 MAPK
PI3K
AKT
MAPK
ERK
β-Catenin
Zeb1/2, Snai1,/2
Twist, Slug , TCF4
EMT
E-Cadherin

Supplemental Figure S1

Panel 1	Marker	CD45	CD11b	CD11c	Ly6C	Ly6G	F4/80	MHCII
	Antibody #	BioLegend #103128	BioLegend #101216	BioLegend #117328	Thermo Fisher Scientific #48-5932-82	BioLegend #127614	BioLegend #123110	BioLegend #107636
	Macrophages	+	+	+	-	-	+	+
	M-MDSC	+	+	-	+	-	Med	-
	G-MDSC	+	+	-	-	+	-	-
	Classical Dendritic Cell 1	+	-	+	-	-	-	+
	Classical Dendritic Cell 2	+	+	+	-	-	-	+
	Inflammatory Dendritic Cell	+	+	+	+	-	+	+
	Eosinophils	+	+	-	-	-	Med	-

Panel 2	Marker	CD45	CD3	CD8	CD4	FoxP3	NK1.1	CD19
	Antibody #	BioLegend #103128	BioLegend #100228	BioLegend #100751	BioLegend #100434	R&D Systems #IC8214A-100	BioLegend #108708	BioLegend #115520
	CD8 T cell	+	+	+	-	-	-	-
	CD4 T cell	+	+	-	+	-	-	-
	T reg	+	+	-	+	+	-	-
	Double-negative T cell	+	+	-	-	-	-	-
	NK cell	+	-	-	-	-	+	-
	B Cell	+	-	-	-		-	+

Supplemental Figure S2

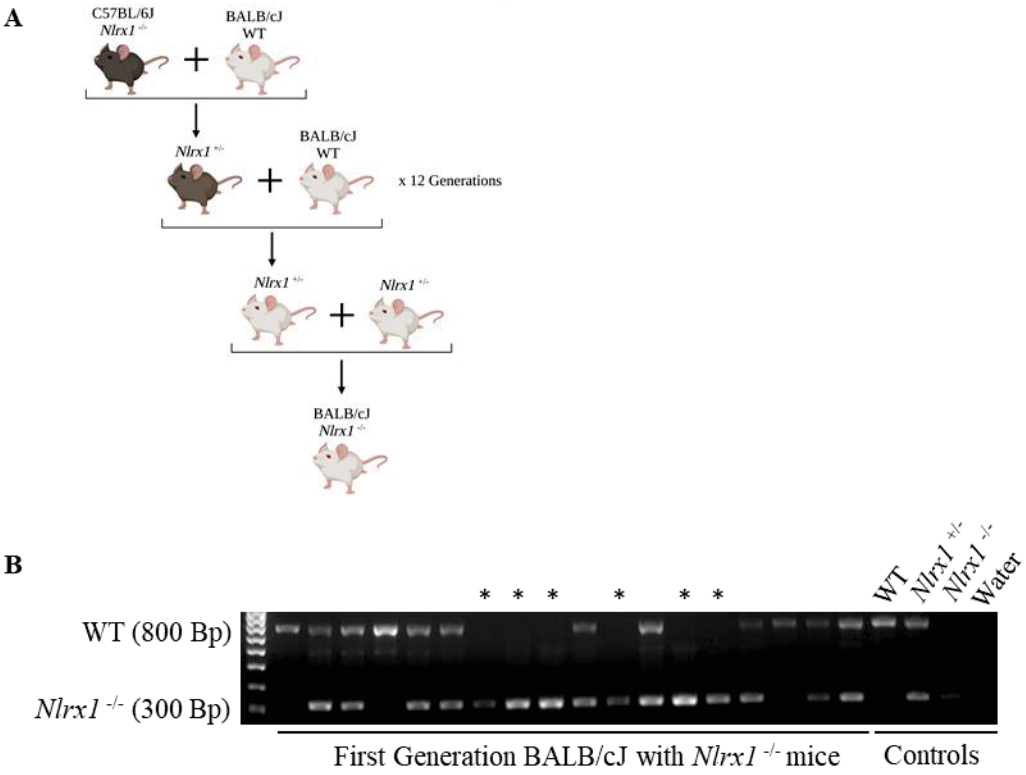

Supplemental Figure S3

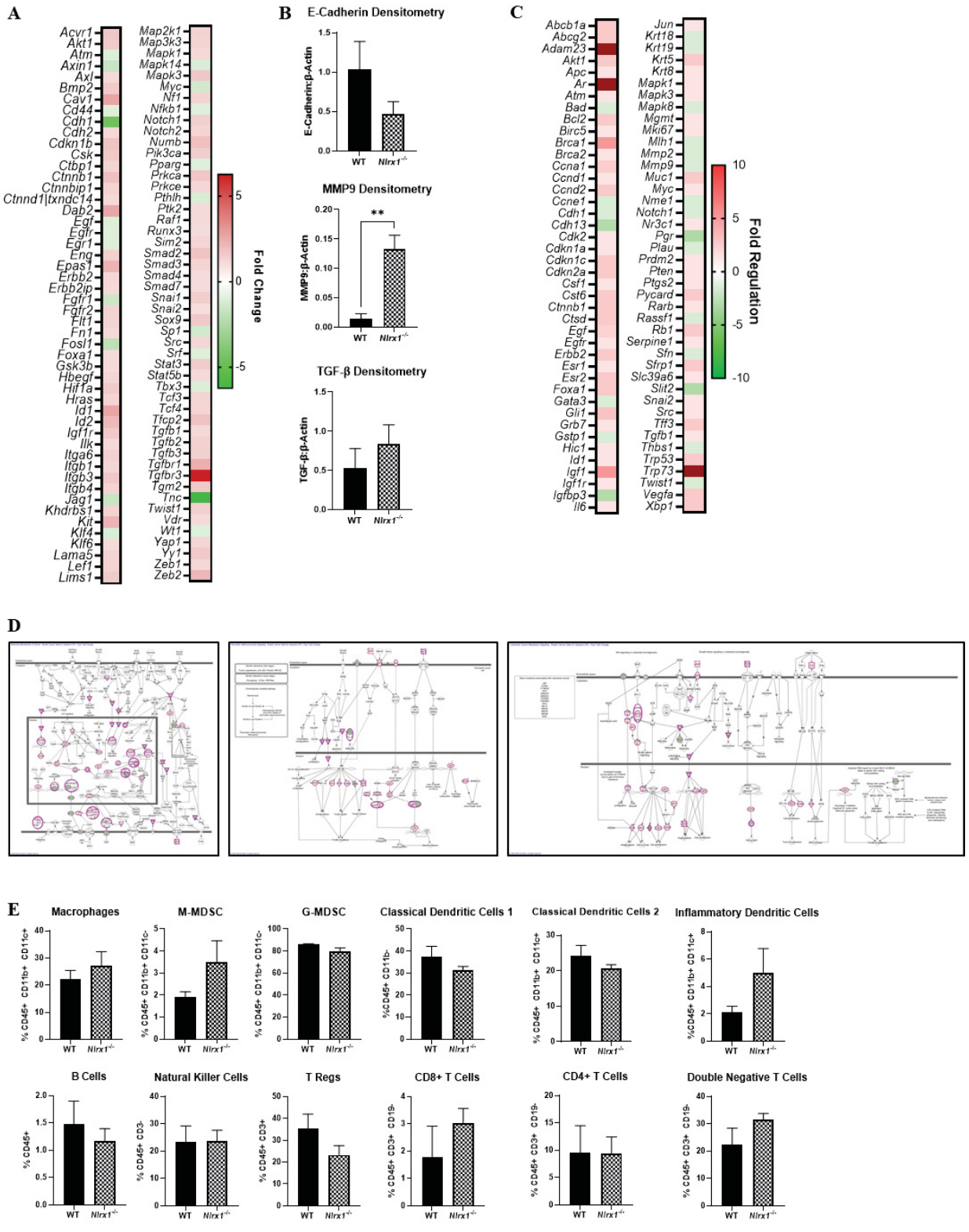

Supplemental Figure S4

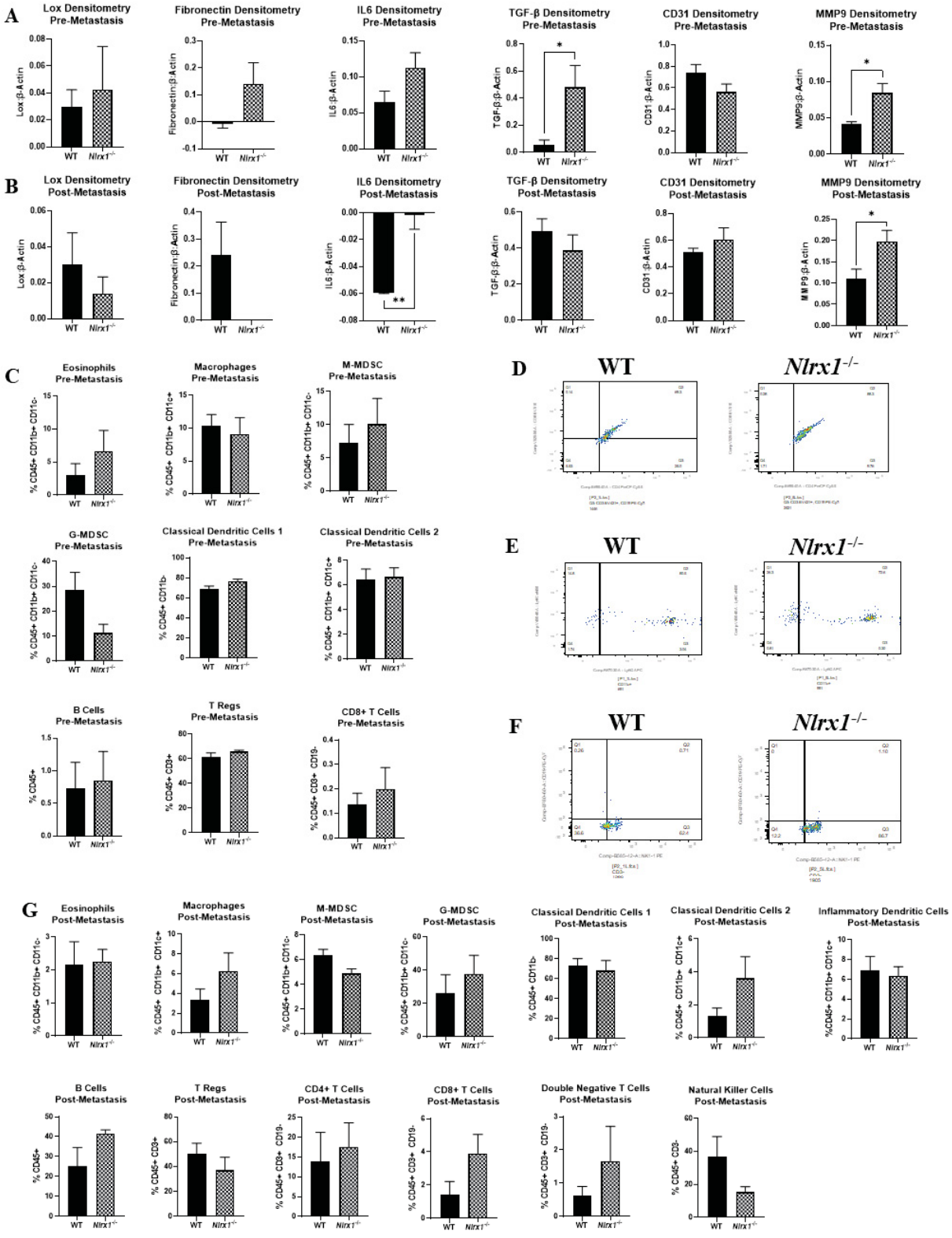

Supplemental Figure S5

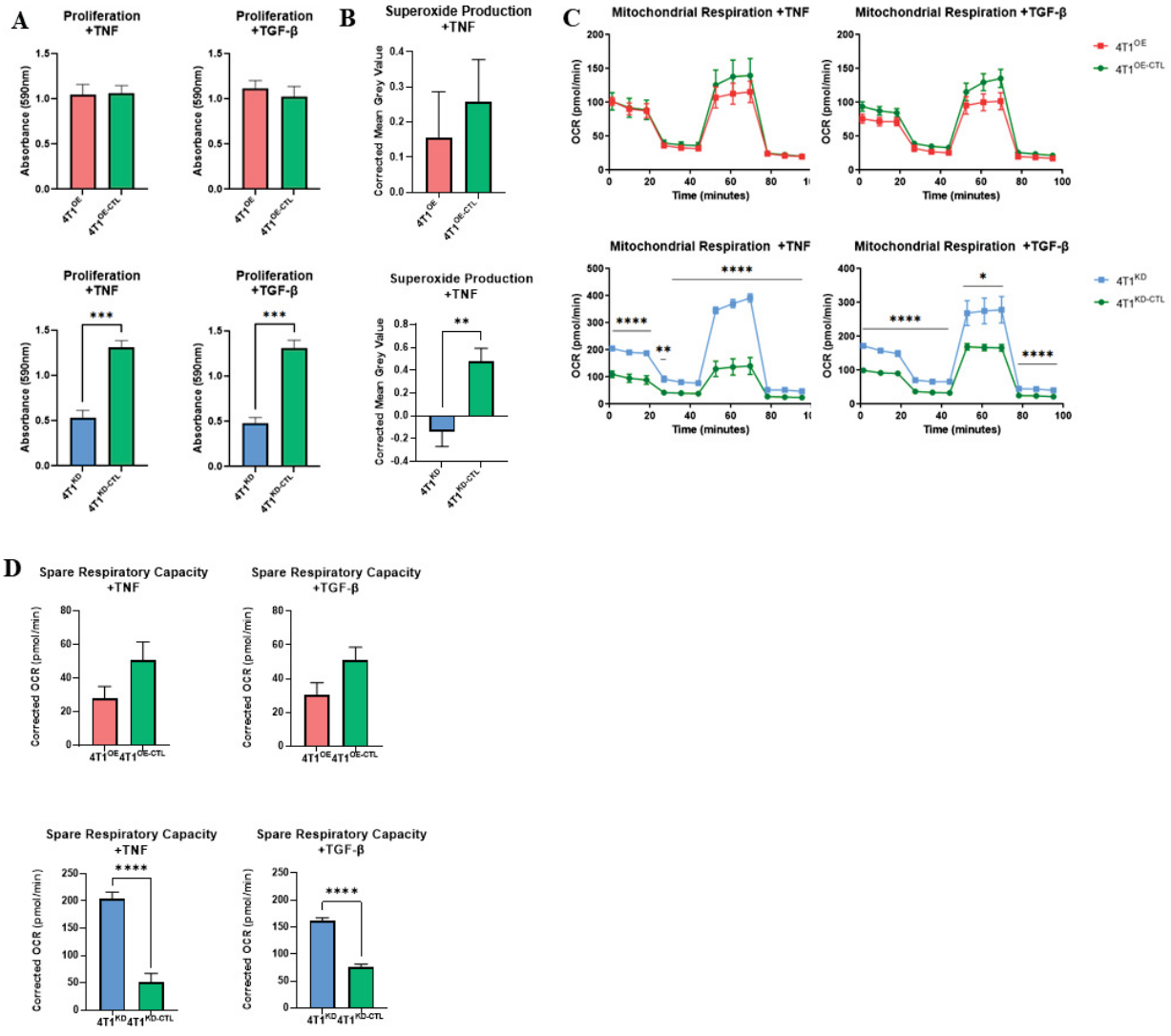

Supplemental Figure S6

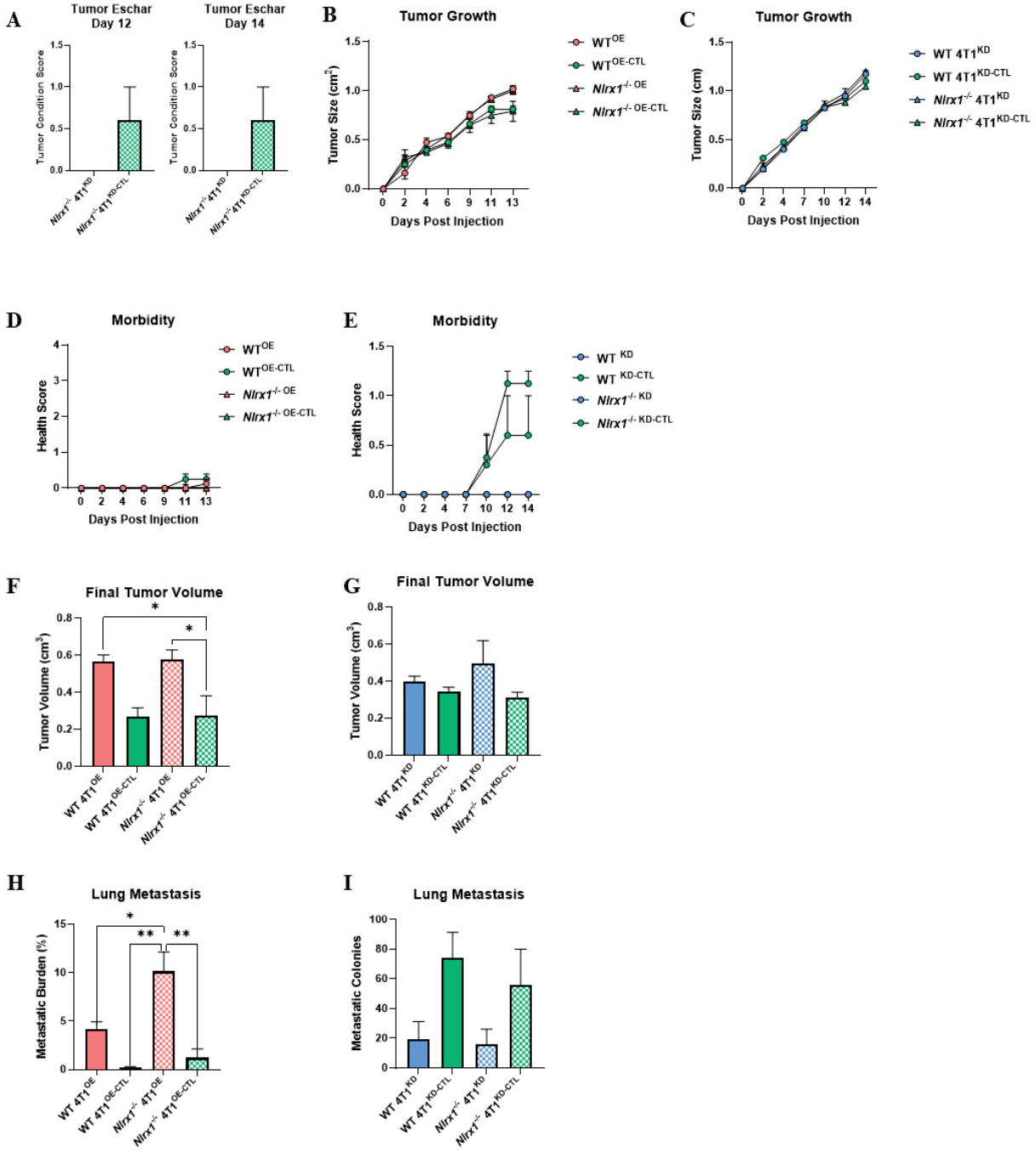

Supplemental Figure S7

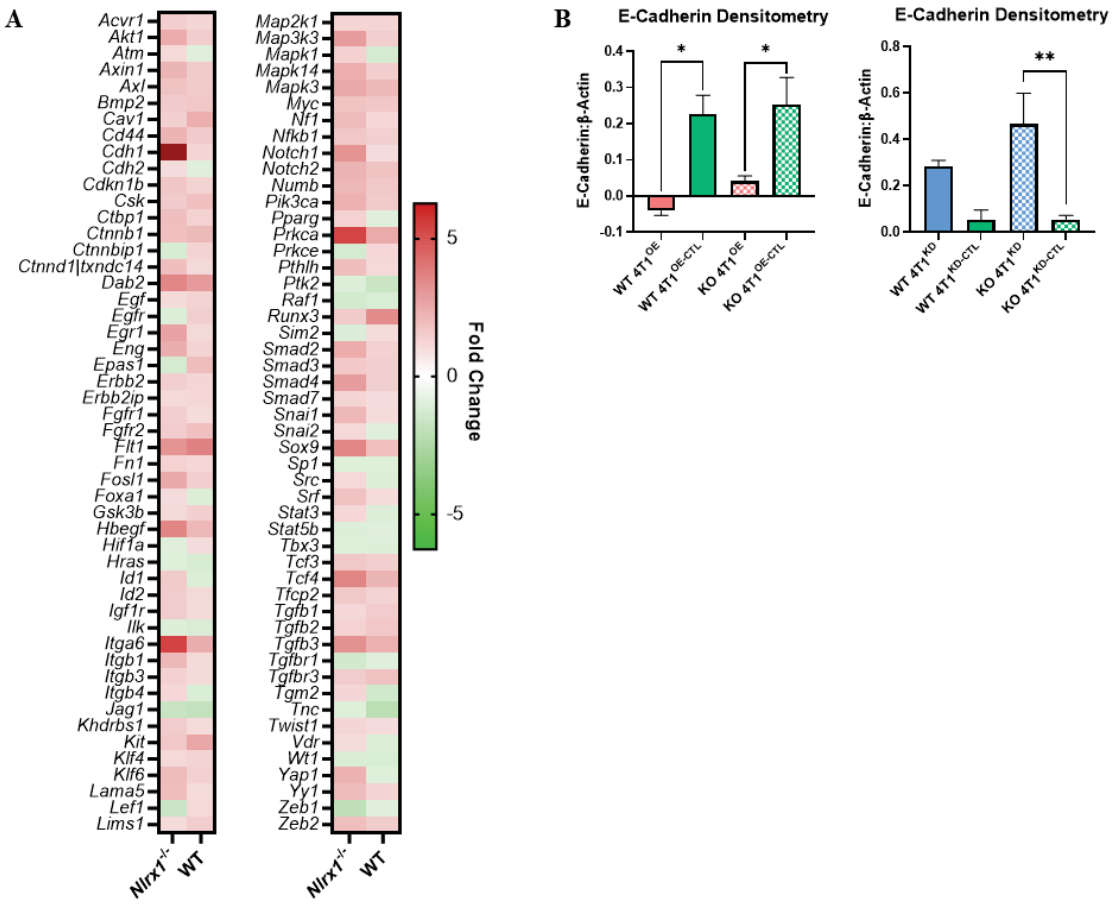

CHAPTER FIVE

NLRX1 Attenuates Cancer-Associated Phenotypes in Murine Pancreatic Tumor Cells

Margaret A. Nagai-Singer[1], Mackenzie K. Woolls[1], Katerina Leedy[1], Holly A. Morrison[1], Irving C. Allen[1]

[1]Department of Biomedical Sciences and Pathobiology, Virginia-Maryland College of Veterinary Medicine, Virginia Tech, Blacksburg, VA, United States.

Running title: NLRX1 protects against aggressive properties in Pan02 cells

Keywords: NOD-like receptor, pattern recognition receptor, pancreatic cancer, transcriptomics

Disclosures: The authors have to conflicting interests to disclose.

Grant Support: This work was funded by the National Institutes of Health, National Cancer Institute R01CA269811 and the National Institute of Biomedical Imaging and Bioengineering R21EB027979. The content is solely the responsibility of the authors and does not necessarily represent the official views of the National Institutes of Health. This work was also supported by the Virginia Maryland College of Veterinary Medicine, the Virginia Tech Center for Engineered Health, the Virginia Tech Institute for Critical Technology and Applied Science, and the Virginia Tech Center for Drug Discovery.

ABSTRACT

NOD-like receptor X1 (NLRX1) is an elusive pattern recognition receptor that generally functions to limit inflammation and many additional biological processes and pathways important to tumor initiation and progression. Indeed, NLRX1 has been implicated in several malignancies, but its role has been found to be either tumor promoting or tumor suppressing depending on several factors, including the type or subtype of cancer and the cell/tissue in which it is expressed. Here, we investigate the role of NLRX1 in pancreatic cancer, which is a highly lethal disease with limited treatment options. Through gain- and loss-of-function studies, we identify tumor suppressing functions of NLRX1 in the Pan02 murine pancreatic tumor cell line. *In vitro* analysis revealed that NLRX1 attenuates several cancer-associated characteristics in Pan02 cells, including suppressing proliferation, migration, ROS levels, and unregulated metabolism while increasing susceptibility to cell death. Through transcriptomics analysis of the Pan02 cell lines we generated to overexpress or knock down NLRX1, we reveal several pathways and processes that likely confer this protective phenotype, including attenuating NF-κB, MAPK, AKT, and inflammasome signaling, and increasing immune recognition and subsequent elimination of tumor cells. Together, we offer insight into the tumor suppressive functions of this understudied NLR in the novel context of one of the most lethal and difficult-to-treat cancers.

INTRODUCTION

While pancreatic cancer is not the most prevalent cancer diagnosis, it is certainly one of the most lethal. In fact, pancreatic cancer is expected to be the third most deadly cancer in the United States in 2022 with an overall 5-year survival rate of 11% that falls to 3% if the tumor has metastasized to distant sites.[1] Despite the decades of research on pancreatic cancer and its potential treatments, there has been an overall increase in death rates since 1930.[2] Therefore, pancreatic cancer patients are in need of improved treatment options that are efficacious and safe. Recent developments in immunotherapies have propelled the immune system into the spotlight where it is recognized for its role in tumorigenesis and disease progression. These developments tend to focus on harnessing the tumor-killing functions of the adaptive immune system. For example, drugs that target the PD-1/PD-L1 interaction between T cells and tumor cells are an promising development and are approved for a small subset of pancreatic cancer patients.[3] Additionally,

pancreatic cancer vaccines using radiation-treated pancreatic cancer cells and GM-CSF to stimulate systemic anti-tumor immunity are currently being tested in clinical trials.[4,5] Beyond the adaptive immune response, the innate immune system provides an often-overlooked route to activate tumor-killing immune cells and alter important signaling pathways that can dictate the outcome of the disease.[6] Specifically, pattern recognition receptors (PRRs) constitute one aspect of innate immunity that regulate the immune response and cancer-associated pathways, and many PRRs are being investigated as drug targets or are in current clinical use.[7,8]

PRRs constitute an arsenal of diverse intracellular and membrane-bound receptors that recognize molecular patterns associated with pathogens (pathogen associated molecular patterns or PAMPs) and damage (damage associated molecular patterns or DAMPs). There are 5 classes of PRRs, including Toll-like receptors (TLRs) and C-type lectin receptors (CLRs) in the cell membrane, and RIG-I-like receptors (RLRs), AIM2-like receptors (ALRs), and NOD-like receptors (NLRs) in the cytosol.[9] Typically functioning as scaffolding proteins, PRRs facilitate the formation of various multiprotein complexes that regulate downstream pathways and often elicit an immune response to address the PAMP or DAMP. TLRs are considered to be the most well-studied and well-understood class of PRR in the context of cancer.[7] As such, the majority of PRR agonists in current clinical use for cancer treatment target TLRs.[7] However, the role of NLRs in cancer remains controversial and requires further exploration.[7]

NLRs generally facilitate the formation of a multiprotein complex known as the "inflammasome" that generates the pro-inflammatory cytokines IL-18 and IL-1β and can initiate an inflammatory type of cell death known as pyroptosis.[10–12] Inflammasomes have been implicated in many types of cancer, including in pancreatic cancer where the NLRP3 inflammasome drives immunosuppression and SNPs in the *NLRP3* gene are common in pancreatic cancer patients.[13,14] However, a subset of NLRs do not subscribe to this inflammasome-forming lifestyle and instead mediate inflammation through other means. These include two NLRs, NOD1 and NOD2, that promote inflammation by recruiting RIP2 to the "NODosome" and subsequently activate the NF-κB and JNK pathways.[15–17] Also included in this unique subset are three NLRs that inhibit inflammation, NLRX1, NLRP12, and NLRC3, which all interfere with NF-κB and interferon signaling and interact with TRAF proteins in the "TRAFasome".[18–23] As one of the non-

inflammasome forming and anti-inflammatory NLRs, NLRX1 deviates from many of the better-understood and well-studied NLRs and therefore its role in different diseases and tissue types remains elusive.

NLRX1 was originally described in host-pathogen interactions where it limits mitochondrial antiviral signaling (MAVS) and inhibits the NF-κB pathway to turn off type 1 interferon (IFN1) production and limit overzealous inflammation.[19,20,24–26] Generally speaking, NLRX1 functions to inhibit inflammation, interferon production, and mitochondrial metabolism, and promotes autophagy, ROS production, and TNF-induced apoptosis, although these findings are not without controversy and appear to be highly dependent on the disease and cellular context.[19,25–37] Because the pathways and processes impacted by NLRX1 are important to tumorigenesis, NLRX1 has recently been studied in the context of different cancers with evidence suggesting it possesses both tumor promoting and tumor suppressing abilities. Indeed, several studies have shown NLRX1 is protective against colon cancer, histiocytic sarcoma, hepatocellular carcinoma, and ER/PR+ breast cancer through signaling pathways including but not limited to NF-κB, MAPK, AKT, and TNF-induced apoptosis.[29,31–33,38,39] Conversely, NLRX1 has been found to be problematic rather than protective in an AOM-only model of colon cancer, HPV-induced head and neck squamous cell carcinoma, and ER/PR- breast cancer where it increases disease burden and promotes aggressive phenotypes.[32,33,40,41] The current literature suggests the role of NLRX1 is highly dependent on cellular context, including the origin, aggressiveness, and disease state of the cell.

To date, the role of NLRX1 in pancreatic cancer is undefined, despite pancreatic cancer being one of the most lethal cancers. Here, we use a murine pancreatic ductal adenocarcinoma cell line (Pan02) to explore how the overexpression or partial loss of NLRX1 impacts the cancer-associated phenotypes of Pan02 cells. Using a stable lentiviral transduction method, we generated Pan02 cells that overexpress NLRX1 ($Pan02^{OE}$) or knock down NLRX1 ($Pan02^{KD}$) and their respective controls ($Pan02^{OE\text{-}CTL}$ and $Pan02^{KD\text{-}CTL}$). We demonstrate that NLRX1 diminishes the cancer-associated phenotypes of Pan02 cells and establish NLRX1 as a protective regulator of tumor-promoting pathways in murine pancreatic tumor cells, including NF-κB, MAPK, AKT, inflammasome, and immune recognition/activation signaling.

MATERIALS AND METHODS

Cell culture and transduction

Pan02 cells were obtained from the National Cancer Institute DCTD Tumor Repository (NCI) and were cultured in RPMI 1640 (ATCC) supplemented with 10% fetal bovine serum (R&D Systems) and 1% penicillin streptomycin (Thermo Fisher Scientific). Cells were incubated at 37°C and 5% CO_2. Pan02 cells were transduced to either overexpress or knockdown murine NLRX1 using lentiviral ORF and shRNA technology (Origene) according to the manufacturer's protocols. Antibiotic selection was used to select for successfully transduced cells using 1 μg/mL puromycin (Santa Cruz Biotechnology) in complete culture media, and successful transduction was confirmed by GFP with a fluorescent microscope and western blot for NLRX1 (Abcam). Cells were authenticated with commercial Mycoplasma testing (Charles River Research Animal Diagnostic Services) and morphology checks. All cells were discarded before 30 passages.

Western blotting

Protein was extracted from transduced Pan02 cells with a protein lysis buffer consisting of 2% SDS, 100mM Tris HCl, 100mM NaCl, 1X protease inhibitor (Thermo Fisher Scientific). Protein concentration was determined by BCA assay (Thermo Fisher Scientific) according to manufacturer's protocols and samples were diluted to 20 μg/mL with reducing sample buffer (Thermo Fisher Scientific) and loaded into pre-cast 4 to 12% Bis-Tris Mini Protein Gels (Thermo Fisher Scientific). Proteins were transferred to a PVDF membrane in 1X TGE + 20% methanol, and blocked for 60 minutes in 5% milk in TBS + 0.1% Tween-20 (TBST). All antibodies were diluted 1:1000 in 5% BSA or 5% milk and incubated overnight at 4°C (CST and Abcam). Wash steps were performed using TBST and images were obtained with iBright imaging (Thermo Fisher Scientific) using an HRP-conjugated secondary antibody (CST) and SuperSignal West Pico or Dura Chemiluminescent Substrate (Thermo Fisher Scientific).

Proliferation assays

Transduced Pan02 cells were seeded at 1 x 10^5 cells per mL in a 12 well plate in complete media +/- 10 ng/mL TNF (PeproTech) and incubated overnight. 24 hours later, cells were stained using NucBlue Live Cell Stain (Thermo Fisher Scientific) according to manufacturer's protocols. Several images per well were acquired on a fluorescent microscope (Invitrogen EVOS M5000)

and automated counting of DAPI+ nuclei was used to determine cell count in each image. Additionally, transduced Pan02 cells were seeded at 1 x 10^4 cells per well in a 96 well plate in complete media and incubated overnight. The following day, media was replaced with experimental media of complete media +/- 10 ng/mL TNF (PeproTech) and allowed to incubate for 24 additional hours. An MTT assay was then performed according to manufacturer's protocols (Abcam).

Cell death assays

Transduced Pan02 cells were seeded at 1 x 10^4 cells per well in a 96 well plate in complete media and allowed to incubate overnight. Media was then replaced with complete media +/- 10 mM H_2O_2 (Fisher Chemical) and allowed to incubate for 24 hours. An LDH assay was performed according to manufacturer's protocols (Thermo Fisher Scientific).

Migration assays

A "scratch" or "wound healing" assay was used to measure migration. Transduced Pan02 cells were seeded at 1 x 10^6 cells per well in a 12 well plate in complete media and incubated overnight. The following day, media was replaced with decreased serum media (1% FBS) and incubated overnight for cells to adjust to the decreased serum content. A 200 µL pipette tip was used to make 3 scratches per well and images of each scratch were taken immediately following the scratch induction (Invitrogen EVOS M5000). At 7 hours post-scratch, images of each scratch were taken at the same location of the initial image. Images were uploaded to Fiji-ImageJ, where the width of the scratch was measured several times per image per timepoint. The rate of migration was calculated as pixels per hour.

Reactive Oxygen Species (ROS) assays

Mitochondrial superoxide levels were determined using analysis of fluorescent microscopy images and fluorometer readings of MitoSOX staining (Thermo Fisher Scientific). For fluorescent images, transduced Pan02 cells were seeded at 1 x 10^5 cells per mL in a 24 well plate and allowed to incubate overnight. The following day, media was replaced with experimental media of complete media +/- 10 ng/mL TNF (PeproTech) and incubated for 24 hours. MitoSOX staining (Thermo Fisher Scientific) was done according to manufacturer's protocol and cells were

counterstained with NucBlue Live Cell Stain (Thermo Fisher Scientific). Fiji-ImageJ was used to split the fluorescent channels, remove background, and measure mean gray value. For the fluorometer readings, transduced Pan02 cells were seeded at 1 x 10^4 cells per well in a 96 well plate and allowed to incubate for 48 hours in complete media. Media was then replaced with experimental media of complete media +/- 100 ng/mL TNF (PeproTech), +/- 45% glucose for one hour. MitoSOX staining (Thermo Fisher Scientific) was done according to manufacturer's protocol and cells were counterstained with NucBlue Live Cell Stain (Thermo Fisher Scientific). Fluorescence was measured using a fluorometer, and RFP (MitoSOX) fluorescence was corrected for DAPI (NucBlue) fluorescence to normalize superoxide levels to the number of cells per well.

Metabolism assays

Transduced Pan02 cells were seeded at 1 x 10^4 cells per well in a 96 well Seahorse XF96 cell culture microplate (Agilent) in complete media and allowed to attach for 3 hours. Media was then replaced with experimental media of complete media +/- 10 ng/mL TNF (PeproTech) and incubated for 24 hours. A Seahorse XF96 Mito Stress test (Agilent) was performed according to manufacturer's protocols at the Virginia Tech Metabolism Core. Spare respiratory capacity, proton leak, and ATP production were calculated according to the Seahorse XF Cell Mito Stress Test calculations.[42]

Transcriptomics and gene expression

Transduced Pan02 cells were seeded at 1 x 10^6 cells per well in a 6 well plate in complete media and incubated overnight. Media was replaced with complete media +/- 100 μM H_2O_2 and incubated another 24 hours. RNA was collected using TRIzol and stored at -80°C until submission to Thermo Fisher (Clariom S, Applied Biosystems) for microarray-based transcriptomics analysis. The Transcriptome Analysis Console (TAC, Thermo Fisher and Applied Biosystems) was used to identify DEGs and top regulated pathways. Gene lists for relevant biological processes were acquired from GeneGlobe's RT^2 Profiler PCR Array list.[43]

Statistical Analysis

Comparisons were analyzed using a two-way unpaired t-test. All figures and analyses were performed in GraphPad Prism. When appropriate, outlier tests were performed to identify and remove any outliers in the data.

RESULTS

NLRX1 alters proliferation, cell death, migration, and ROS levels in Pan02 cells

To elucidate what general functions NLRX1 performs when it is expressed in pancreatic cancer cells, we generated Pan02 cells to either overexpress or knockdown NLRX1 in the pancreatic tumor cells ($Pan02^{OE}$, $Pan02^{OE\text{-}CTL}$, $Pan02^{KD}$, $Pan02^{KD\text{-}CTL}$, **Fig. 1A**). We then performed experiments on these four transduced Pan02 cell lines to assess common characteristics of cancer cells, including proliferation, cell death, migration, and ROS levels. To assess proliferation, which is enhanced in tumor cells, we used automated microscopy counting at 24 hours and an MTT assay at 48 hours. Our Pan02 cell lines were assessed for proliferation under normal conditions or following stimulation with TNF like previously described.[32,33]. At 24 hours, we found that in unstimulated conditions, the knockdown of NLRX1 in $Pan02^{KD}$ cells more than doubled the proliferation compared to their controls, but the overexpression of NLRX1 did not impact proliferation (**Fig. 1B**). Similar trends were observed after stimulation with TNF, although the differences were not significant (**Supplemental Fig. S1A**). At 48 hours, we observed no differences in unstimulated conditions (**Supplemental Fig. S1B**). However, at 48 hours with TNF stimulation, the overexpression of NLRX1 in $Pan02^{OE}$ cells hindered proliferation while the knockdown of NLRX1 promoted proliferation (**Fig. 1C**), suggesting NLRX1 in Pan02 cells attenuates proliferation of the tumor cells.

Next, we challenged cells with H_2O_2 to induce cell death and measured cytotoxicity using an LDH assay. Tumor cells are often able to evade cell death and thus decreased cytotoxicity of the Pan02 cells would indicate an advantage to the tumor cells.[44] $Pan02^{OE}$ cells underwent more cell death as demonstrated by their increased cytotoxicity, indicating the overexpression of NLRX1 increased susceptibility to H_2O_2-induced cell death compared to $Pan02^{OE\text{-}CTL}$ cells (**Fig. 1D**). Conversely, $Pan02^{KD}$ cells demonstrated less cytotoxicity and therefore decreased susceptibility to H_2O_2-induced cell death compared to $Pan02^{KD\text{-}CTL}$ cells (**Fig. 1D**). This indicates that NLRX1 increases death of the tumor cells in response to H_2O_2.

Metastasis is a major driver of cancer-associated mortality and therefore is a crucial element in reducing cancer deaths.[45] As a proxy for potential metastatic ability, we next measured how NLRX1 impacts migratory capacity using a wound healing assay and calculating the rate of migration of the tumor cells. No significant differences were observed between $Pan02^{OE}$ and $Pan02^{OE\text{-}CTL}$ cells, but $Pan02^{KD}$ cells demonstrated a 55% increase in migration compared to $Pan02^{KD\text{-}CTL}$ cells (**Fig. 1E**). This suggests the loss of NLRX1 in Pan02 cells promotes the migratory capabilities of the tumor cell and would indicate a potential for increased metastasis when NLRX1 expression in the tumor is decreased.

Lastly, to measure mitochondrial ROS levels that are typically upregulated in tumor cells, we used MitoSOX to stain mitochondrial superoxide and measured staining intensity with both Fiji-ImageJ and a fluorometer.[46] As a positive control, cells were stimulated with glucose to induce mitochondrial ROS production and indicated no differences in maximal ROS levels (**Supplemental Fig. S1C**). Under normal culture conditions, $Pan02^{OE}$ cells had less superoxide levels than $Pan02^{OE\text{-}CTL}$ cells in both the Fiji-ImageJ and fluorometer measurements (**Fig. 1F-H**). Conversely, $Pan02^{KD}$ cells had more superoxide levels than $Pan02^{KD\text{-}CTL}$ cells in both the Fiji-ImageJ (**Fig. 1G)** and fluorometer measurements (**Fig. 1H**), and is clearly visible in the fluorescent images (**Fig. 1F**). We observed similar trends in cells that were stimulated with TNF (**Supplemental Fig. S1D**). Together, these data suggest that NLRX1 expressed by Pan02 cells is tumor suppressive through limiting proliferation, mitochondrial ROS levels, and migration, while also increasing H_2O_2-induced cell death of the tumor cells.

NLRX1 protects against unregulated energy production in Pan02 cells

To connect the phenotypes observed in the previous section, we next sought to understand how NLRX1 impacts metabolism in Pan02 cells. Using the Seahorse XF Cell Mito Stress test, we revealed a strong role for NLRX1 in mitochondrial respiration and glycolysis. Basal respiration was significantly reduced in $Pan02^{OE}$ cells compared to $Pan02^{OE\text{-}CTL}$ cells, while conversely $Pan02^{KD}$ cells demonstrated an increased basal respiration compared to $Pan02^{KD\text{-}CTL}$ cells (**Fig. 2A**). We then calculated spare respiratory capacity, which is an indicator of a cell's mitochondria to perform adequately under stress conditions.[47] $Pan02^{OE}$ cells demonstrated an improved spare respiratory capacity compared to $Pan02^{OE\text{-}CTL}$ cells, indicating that the overexpression of NLRX1

allows Pan02 cells to respond appropriately to stress conditions (**Fig. 2B**). Conversely, Pan02^{KD} cells demonstrated a decrease in spare respiratory capacity compared to Pan02$^{KD\text{-}CTL}$ cells (**Fig. 2B**). Indeed, a decrease in spare respiratory capacity is a common hallmark of cancer cells caused by their metabolic weakness and having "exhausted" mitochondria.[47] Additionally, proton leak is typically upregulated in cancer cells as a result of their unregulated growth and mitochondrial damage.[46] Consistent with that characteristic and the observed phenotypes thus far, Pan02^{OE} cells had a 33% reduction in proton leak compared to Pan02$^{OE\text{-}CTL}$ cells while Pan02^{KD} cells had a 46% increase in proton leak compared to Pan02$^{KD\text{-}CTL}$ cells (**Fig. 2C**). These data suggest NLRX1 in Pan02 cells improves the overall health and regulation of mitochondria. Conversely, the loss of NLRX1 in Pan02 cells contributes to mitochondrial dysregulation that is consistent with tumor-associated characteristics. Additionally, Pan02^{OE} cells produced 37% less ATP (**Fig. 2D**) and performed less glycolysis (**Fig. 2E**) than Pan02$^{OE\text{-}CTL}$ cells, while Pan02^{KD} cells produced 31% more ATP (**Fig. 2D**) and performed more glycolysis (**Fig. 2E**) than Pan02$^{KD\text{-}CTL}$ cells. This suggests that NLRX1 aids in maintaining regulation of cellular energy production in Pan02 cells. The trends observed in these data were also observed after cells were stimulated with TNF (**Supplemental Fig. S2A-E**). Together, these data indicate a tumor suppressive role for NLRX1 in Pan02 cells where it protects against unregulated energy production.

NLRX1 impacts many pathways associated with cancer and immune system regulation

Considering the impact NLRX1 demonstrated on several cancer-associated phenotypes in our Pan02 cells, we next collected RNA from Pan02^{OE}, Pan02$^{OE\text{-}CTL}$, Pan02^{KD}, and Pan02$^{KD\text{-}CTL}$ cells for transcriptomics analysis (ClariomS). Cells were collected under normal conditions or following a challenge with a low dose of H_2O_2 due to the implication of ROS levels, stress responses, and cell death in the data above. The top 50 up- and down-regulated genes under normal conditions (**Supplemental Fig. S3**) and H_2O_2 conditions (**Supplemental Fig. S4**) are listed in Supplemental Data. Using the Transcriptomics Analysis Console (TAC), we identified the top 20 pathways impacted by NLRX1 expression in the Pan02 cells according to the number of differentially-expressed genes (DEGs) in unstimulated or stimulated conditions (**Fig. 3A-D**). Overall, there is significant overlap in the top 20 pathways between the four comparisons which suggests that many of the pathways identified are impacted by both the loss and gain of NLRX1 expression (**Fig. 3A-D**). Interestingly, many of the pathways identified here are consistent with

pathways identified in previous studies of NLRX1, including PI3K-AKT, MAPK, EGFR, NF-κB, and IL-6 signaling, and these pathways are all important to the initiation and progression of pancreatic cancer.[29,31,38,39,48–52] Additionally, the importance of several cytokines, B cell receptor, T cell receptor, and NF-κB signaling indicates NLRX1 is a regulator of many aspects of immune system function in this model. Because pancreatic cancer is a highly immunosuppressive tumor type, activation of the immune system by NLRX1 is certainly of interest in this model.[53] A Principal Component Analysis (PCA) plot revealed clustering of each Pan02 cell line together, indicating that the differences in NLRX1 expression between each transduced Pan02 cell line is a significant driver of differences in the transcriptome (**Fig. 3E**). Additionally, the presence/absence of the H_2O_2 challenge did not appear to significantly alter the transcriptome within each Pan02 cell line (**Fig. 3E**). Together, here we reveal a strong role for NLRX1 in many pathways associated with pancreatic cancer at the transcript level.

NLRX1 inhibits inflammation, immune evasion, and cancer-associated gene expression signatures

To elaborate on the transcriptomics data, we identified the DEGs between all four comparisons in several biological processes that are important to the *in vitro* phenotypes and top pathways we identified. We identified DEGs related to inflammatory cytokines and receptors (**Fig. 4A**), cancer inflammation and immunity crosstalk (**Fig. 4B**), innate and adaptive immune responses (**Fig. 4C**), mitochondria (**Fig. 4D**), cancer pathways, (**Fig. 4E**), inflammasomes (**Fig. 4F**), oxidative stress (**Fig. 4G**), cellular stress response (**Fig. 4H**), the NF- κB pathway (**Fig. 4I**), and T and B cell activation (**Fig. 4J**). Genes related to these processes were pulled from the gene lists available from GeneGlobe (Qiagen). Within these biological processes, the most upregulated genes in Pan02^{OE} cells include *Csf2*, *Cxcl5*, *Cxcl2*, *Il23a*, *Timm17a*, *Slc25a30*, *Ppp1r15a*, *Foxc2*, *Cxcl3*, *Cxcl1*, *Hmox1*, *Hspa1a*, *Xdh*, *Gsto1*, and *CD74*, and the most downregulated genes in Pan02^{OE} cells include *Il11*, *Ccl2*, *Ackr3*, *Il6*, *Il18*, *Slc25a23*, *Cox10*, *Pgf*, *Sod3*, *Fancc*, *Nod2,* and *Cryab*. As we would expect, many of the most upregulated genes in Pan02^{OE} cells are also downregulated in Pan02^{KD} cells and many of the most downregulated genes in Pan02^{OE} cells are also upregulated in Pan02^{KD} cells (**Fig. 4A-J**). Again, this indicates the partial loss of NLRX1 and the overexpression of NLRX1 have strong and diametric effects on Pan02 cells at the gene expression level and supports the opposing effects of the gain- or loss- of -function studies *in vitro*. The gene expression signatures here suggest a strong role for NLRX1 in limiting inflammation,

including through NF-κB signaling and inflammasomes, inducing an anti-tumor immune microenvironment, and protecting against damaging cellular stress signals.

DISCUSSION

Here, we have established through *in vitro* assays and transcriptomics analysis that NLRX1 in murine pancreatic tumor cells is protective against cancer-associated properties and likewise that the loss of NLRX1 augments cancer-associated properties. Specifically, we demonstrate that the loss of NLRX1 increases proliferation, decreases cell death, promotes migration, sustains higher levels of mitochondrial ROS, contributes to mitochondrial dysregulation, and promotes unregulated energy production. Many of these phenotypes are reversed when NLRX1 is overexpressed, as we would expect. Through transcriptomics analysis, we identified significant pathways regulated by NLRX1 expression and the DEGs in biological processes related to those pathways. Together, these data indicate a significant role for NLRX1 in many pathways and processes important to pancreatic cancer.

Interestingly, our *in vitro* data consistently show similar results between $Pan02^{OE}$ and $Pan02^{KD\text{-}CTL}$ cells and between $Pan02^{KD}$ and $Pan02^{OE\text{-}CTL}$ cells. While we would instead expect similar results between each control cell line, we can reconcile this based on the protein expression of NLRX1 in our transduced cells. For example, $Pan02^{OE}$ and $Pan02^{KD\text{-}CTL}$ cells express similar levels of NLRX1 and therefore they should have similar *in vitro* results, which is what we observed. In other cell lines with altered expression of NLRX1, many of the same *in vitro* phenotypes have been observed, albeit with some conflicting findings. Consistent with our studies in Pan02 cells, in two hepatocellular carcinoma cell lines, NLRX1 increased cell death and decreased migration *in vitro.*[39] Likewise, the overexpression of NLRX1 in HEK293 (human embryonic kidney cells), MCF-7 (human ER/PR+ breast tumor cells), and HeLa (human cervical carcinoma cells) cell lines increased cell death and decreased ATP production.[32,33] In MCF-7 cells, the overexpression of NLRX1 also reduced clonogenicity and migration, both of which are consistent with our findings.[32] However, NLRX1 overexpression in HEK293, MCF-7, and HeLa cells resulted in higher ROS levels, which is not consistent with our data.[32] In another cell line, MDA-MB-231 (human ER/PR- breast tumor cells), the knockdown of NLRX1 was consistent with our results regarding ROS levels.[33] However, the knockdown of NLRX1 in MDA-MB-231 cells

resulted in decreased ATP, decreased proliferation, and decreased migration, all of which are inconsistent with the current study.[33] While differences between cell lines can account for some differences, the current research landscape suggests that the function of NLRX1 is dependent on several factors and likely has complex spatial, temporal, and cell/tissue-specific roles.[36,37] Indeed, the expression of NLRX1 in various human neoplasms compared to healthy tissue can range from almost 3-fold increased to almost 9-fold decreased based on the type of cancer.[31] Even within a specific type of cancer, such as breast cancer and hepatocellular carcinoma, the expression of NLRX1 can vary based on the subtype and aggressiveness of the specific tumor or cell line.[32,33,39] A previous study identified fragment 556–974 of the human NLRX1 protein as being responsible for the protective phenotypes in hepatocellular carcinoma models, but further work is needed to elucidate how NLRX1 is able to function differently in different models and scenarios.

While the phenotypic impacts of NLRX1 expression *in vitro* offer some conflicting data throughout the literature, the biological pathways on which NLRX1 converges between several different models are consistent. Specifically, the protective roles of NLRX1 in various tumor models seem to converge on MAPK, NF-κB, and AKT signaling. NLRX1 has been linked with negative regulation of NF-κB signaling and subsequent protection against tumorigenesis and disease burden in gastric cancer cells challenged with *Helicobacter pylori*, intestinal organoid models of colonic tumorigenesis, AOM/DSS-induced models of colitis-associated cancer and sporadic colon cancer models in *Apc*$^{min/+}$ mice, urethane-induced histiocytic carcinoma, and human gastric cancer samples.[29,31,38,49,50] In several of these same models and a model of hepatocellular carcinoma, NLRX1 also limits AKT signaling to protect against disease.[29,31,39] The studies in colitis-associated cancer and sporadic colon cancer models also revealed that NLRX1 attenuates MAPK, STAT3, and IL-6 signaling pathways.[38] Likewise, our transcriptomics analysis revealed an important role for NLRX1 in pancreatic cancer through NF-κB, AKT, MAPK, and IL-6 signaling and highlights these pathways as likely mechanisms by which NLRX1 asserts its protective qualities in Pan02 cells.

In models where NLRX1 appears to be problematic and/or contributes to more severe disease outcomes, the mechanisms center on mitochondrial function. Specifically in cancers influenced by viral infections, the ability of NLRX1 to inhibit mitochondrial interferon signaling

suggests this function of NLRX1 can be detrimental to the host. Suppressing IFN-β in a model Kaposi's sarcoma-associated herpesvirus (KSHV) suggested that NLRX1 facilitates KSHV replication and reactivation.[54] Additionally, in a model of HPV+ head and neck squamous cell carcinoma (HNSCC), NLRX1 interacts with and degrades STING to decrease IFN-I production and therefore limits tumor control.[40] The ability for NLRX1 to inhibit MAVS and the subsequent IFN-I signaling has also been implicated in persistent Hepatitis C (HCV) infections, which can increase the risk for many types of cancer.[27,55] Our current study did not indicate a significant role of NLRX1 in mitochondrial interferon signaling in Pan02 cells, which is not surprising as pancreatic cancer is not typically driven by viral infections. However, our results do indicate a strong association of NLRX1 with the mitochondria through metabolic and OXPHOS-related pathways and phenotypes which have been previously reported in other models, albeit with the several inconsistent functions as discussed above.[32,33] In ER/PR- human breast cancer, which also is not typically driven by viral infections, NLRX1 enhanced aggressive *in vitro* cancer-associated phenotypes through augmenting mitochondrial respiration and reducing mitophagy and lysosomal formation and function through mitochondria-lysosomal crosstalk.[33]

Our metabolism assays revealed that NLRX1 in Pan02 cells increases spare respiratory capacity, which indicates NLRX1 equips the cells with mitochondria that are able to adapt to stressful conditions. Paired with the decrease in basal respiration and glycolysis caused by NLRX1 overexpression, it appears that NLRX1 shifts the Pan02 cells towards OXPHOS and away from glycolysis under stress conditions, but under normal conditions limits both OXPHOS and glycolysis and thus decreases cellular energy available for proliferation. Likewise, the partial loss of NLRX1 reduced spare respiratory capacity, indicating Pan02^{KD} cells function closer to their maximal respiration under normal conditions and can shift to glycolysis even under stressful conditions. This indicates a flexibility for energy production that Pan02^{KD} cells can use to their advantage and allows for increased proliferation. We also discovered that NLRX1 decreases proton leak. However, because proton leak reduces mitochondrial superoxide production, we would expect to see a subsequent increase in superoxide levels in Pan02^{OE} cells.[56] Conversely, we see a reduction in superoxide levels in Pan02^{OE} cells which indicates the differences in superoxide levels are not due to proton leak but instead are likely due to the decreased basal respiration in Pan02^{OE} cells. Interestingly, superoxide dismutase 3 (*Sod3)* was one of the most downregulated

genes in Pan02^{OE} cells and also substantially upregulated in Pan02^{KD} cells. Because SOD3 reduces superoxide, this gene expression pattern might appear counterintuitive to our superoxide data. However, we believe the role of *Sod3* in Pan02 cells is primarily responsible for promoting pro-growth AKT and MAPK signaling in Pan02^{KD} cells and similarly limiting these pathways in Pan02^{OE} cells.[57]

Additionally, many aspects of immune regulation were implicated in our analysis, including inflammation, chemokines, B cell and T cell signaling, NF-κB pathway, and TGF-β signaling. As we would expect with the historical ability of NLRX1 to suppress inflammation, the pro-inflammatory cytokines *Il6* and *Il18* were significantly downregulated in the presence of excess NLRX1 and upregulated following the partial loss of NLRX1. Aberrant IL-6 and IL-18 levels both create a tumor microenvironment that is favorable for the tumor cells by promoting survival and establishing an immunosuppressive environment, suggesting that NLRX1 could protect against pancreatic tumors through regulating inflammation and inflammatory cytokines.[52,58,59] The regulation of IL-18 and many other inflammasome-related genes also indicates that NLRX1 suppresses inflammasome function in Pan02 cells. The NLRP3 inflammasome has been shown to promote immune evasion in pancreatic cancer, specifically by differentiating T cells into pro-tumor populations (Th2, Th17, and T regs) and preventing the activation of tumor-killing CD8+ T cells.[13] Our data suggest that NLRX1 can limit these immune evasion effects of the inflammasome by attenuating inflammasome signaling. Likewise, GM-CSF (*Csf2*) was significantly upregulated in Pan02^{OE} cells and downregulated in Pan02^{KD} cells. GM-CSF stimulates an anti-tumor immune response through priming CD4+ and CD8+ T cells, in part through recruiting and activating dendritic cells, and is currently being investigated for use in pancreatic cancer vaccines.[4,5,60–62] Through upregulating *Csf2*, NLRX1 is potentially helpful in promoting immune recognition of pancreatic tumors.

In conclusion, we have unearthed several phenotypes in murine pancreatic tumor cells that are impacted by NLRX1. Our data suggest NLRX1 serves in a protective capacity against several cancer-associated phenotypes, including proliferation, evading cell death, migration, ROS, and unregulated mitochondrial respiration and glycolysis. These phenotypes are likely driven by a combination of suppressed NF-κB, MAPK, and AKT signaling and inflammasome function. Our

data also suggest NLRX1 could aid in reversing the immunosuppressive environment in pancreatic tumors to aid in immune-mediated tumor killing. However, while we offer promising insight into how NLRX1 impacts pancreatic cancer and potentially could be developed as a drug target, the enigmatic and inconsistent functions of NLRX1 between different cells, tumors, and tissues warrants further mechanistic exploration.

ACKNOWLEDGEMENTS

The authors would like to thank Dr. Rebecca M. Brock, Hannah M. Ivester, Juselyn D. Tupik, Imran Khan, Dr. Brie Trusiano, and Bettina Heid for their logistical support that made this work possible. We would also like to thank the Metabolism Core at Virginia Tech and Dr. Tom Cecere for their expertise.

REFERENCES

1. Survival Rates for Pancreatic Cancer. https://www.cancer.org/cancer/pancreatic-cancer/detection-diagnosis-staging/survival-rates.html.
2. American Cancer Society. Cancer Statistics Center. *American Cancer Society | Cancer Facts & Statistics* http://cancerstatisticscenter.cancer.org/.
3. Cancer Research Institute. Immunotherapy for Pancreatic Cancer. *Cancer Research Institute* https://www.cancerresearch.org/en-us/immunotherapy/cancer-types/pancreatic-cancer.
4. Johns Hopkins Medicine. Pancreatic Cancer Vaccine. https://www.hopkinsmedicine.org/health/conditions-and-diseases/pancreatic-cancer/pancreatic-cancer-vaccine (2022).
5. Sidney Kimmel Comprehensive Cancer Center at Johns Hopkins. *A Safety and Feasibility Trial of Boost Vaccinations of a Lethally Irradiated, Allogeneic Pancreatic Tumor Cell Vaccine Transfected With the GM-CSF Gene*. https://clinicaltrials.gov/ct2/show/study/NCT01088789 (2022).
6. Demaria, O. *et al.* Harnessing innate immunity in cancer therapy. *Nature* **574**, 45–56 (2019).
7. Bai, L. *et al.* Promising targets based on pattern recognition receptors for cancer immunotherapy. *Pharmacological Research* **159**, 105017 (2020).
8. Man, S. M. & Jenkins, B. J. Context-dependent functions of pattern recognition receptors in cancer. *Nat Rev Cancer* **22**, 397–413 (2022).
9. Rothschild, D. E., McDaniel, D. K., Ringel-Scaia, V. M. & Allen, I. C. Modulating inflammation through the negative regulation of NF-κB signaling. *Journal of Leukocyte Biology* **103**, 1131–1150 (2018).
10. Kayagaki, N. *et al.* Non-canonical inflammasome activation targets caspase-11. *Nature* **479**, 117–121 (2011).
11. Martinon, F., Burns, K. & Tschopp, J. The inflammasome: a molecular platform triggering activation of inflammatory caspases and processing of proIL-beta. *Mol Cell* **10**, 417–426 (2002).
12. Shi, J. *et al.* Cleavage of GSDMD by inflammatory caspases determines pyroptotic cell death. *Nature* **526**, 660–665 (2015).
13. Daley, D. *et al.* NLRP3 signaling drives macrophage-induced adaptive immune suppression in pancreatic carcinoma. *J Exp Med* **214**, 1711–1724 (2017).
14. Miskiewicz, A. *et al.* The Q705K and F359L Single-Nucleotide Polymorphisms of NOD-Like Receptor Signaling Pathway: Association with Chronic Pancreatitis, Pancreatic Cancer, and Periodontitis. *Arch Immunol Ther Exp (Warsz)* **63**, 485–494 (2015).
15. da Silva Correia, J., Miranda, Y., Leonard, N., Hsu, J. & Ulevitch, R. J. Regulation of Nod1-mediated signaling pathways. *Cell Death Differ* **14**, 830–839 (2007).
16. Kobayashi, K. S. *et al.* Nod2-dependent regulation of innate and adaptive immunity in the intestinal tract. *Science* **307**, 731–734 (2005).
17. Tattoli, I., Travassos, L. H., Carneiro, L. A., Magalhaes, J. G. & Girardin, S. E. The Nodosome: Nod1 and Nod2 control bacterial infections and inflammation. *Semin Immunopathol* **29**, 289–301 (2007).
18. Schneider, M. *et al.* The innate immune sensor NLRC3 attenuates Toll-like receptor signaling via modification of the signaling adaptor TRAF6 and transcription factor NF-κB. *Nat Immunol* **13**, 823–831 (2012).

19. Allen, I. C. *et al.* NLRX1 Protein Attenuates Inflammatory Responses to Infection by Interfering with the RIG-I-MAVS and TRAF6-NF-κB Signaling Pathways. *Immunity* **34**, 854–865 (2011).
20. Moore, C. B. *et al.* NLRX1 is a regulator of mitochondrial antiviral immunity. *Nature* **451**, 573–577 (2008).
21. Allen, I. C. *et al.* NLRP12 suppresses colon inflammation and tumorigenesis through the negative regulation of noncanonical NF-κB signaling. *Immunity* **36**, 742–754 (2012).
22. Zhang, L. *et al.* NLRC3, a member of the NLR family of proteins, is a negative regulator of innate immune signaling induced by the DNA sensor STING. *Immunity* **40**, 329–341 (2014).
23. Chen, S.-T. *et al.* NLRP12 Regulates Anti-viral RIG-I Activation via Interaction with TRIM25. *Cell Host Microbe* **25**, 602-616.e7 (2019).
24. Xia, X. *et al.* NLRX1 Negatively Regulates TLR-Induced NF-κB Signaling by Targeting TRAF6 and IKK. *Immunity* **34**, 843–853 (2011).
25. Lei, Y., Wen, H. & Ting, J. P. Y. The NLR protein, NLRX1, and its partner, TUFM, reduce type I interferon, and enhance autophagy. *Autophagy* **9**, 432–433 (2013).
26. Lei, Y. *et al.* The mitochondrial proteins NLRX1 and TUFM form a complex that regulates type I interferon and autophagy. *Immunity* **36**, 933–946 (2012).
27. Qin, Y. *et al.* NLRX1 Mediates MAVS Degradation To Attenuate the Hepatitis C Virus-Induced Innate Immune Response through PCBP2. *J Virol* **91**, e01264-17 (2017).
28. Soares, F. *et al.* NLRX1 does not inhibit MAVS-dependent antiviral signalling. *Innate Immun* **19**, 438–448 (2013).
29. Tattoli, I. *et al.* NLRX1 Acts as an Epithelial-Intrinsic Tumor Suppressor through the Modulation of TNF-Mediated Proliferation. *Cell Reports* **14**, 2576–2586 (2016).
30. Tattoli, I. *et al.* NLRX1 is a mitochondrial NOD-like receptor that amplifies NF-κB and JNK pathways by inducing reactive oxygen species production. *EMBO Rep* **9**, 293–300 (2008).
31. Coutermarsh-Ott, S. *et al.* NLRX1 suppresses tumorigenesis and attenuates histiocytic sarcoma through the negative regulation of NF-λB signaling. *Oncotarget* **7**, 33096–33110 (2016).
32. Singh, K. *et al.* NLRX1 acts as tumor suppressor by regulating TNF-α induced apoptosis and metabolism in cancer cells. *Biochimica et Biophysica Acta (BBA) - Molecular Cell Research* **1853**, 1073–1086 (2015).
33. Singh, K. *et al.* NLRX1 regulates TNF-α-induced mitochondria-lysosomal crosstalk to maintain the invasive and metastatic potential of breast cancer cells. *Biochimica et Biophysica Acta (BBA) - Molecular Basis of Disease* **1865**, 1460–1476 (2019).
34. Zhang, H. *et al.* NLRX1 Deletion Increases Ischemia-Reperfusion Damage and Activates Glucose Metabolism in Mouse Heart. *Front Immunol* **11**, 591815 (2020).
35. Leber, A. *et al.* NLRX1 regulates effector and metabolic functions of CD4+ T cells. *J Immunol* **198**, 2260–2268 (2017).
36. Pickering, R. J. & Booty, L. M. NLR in eXile: Emerging roles of NLRX1 in immunity and human disease. *Immunology* **162**, 268–280 (2021).
37. Fekete, T., Bencze, D., Bíró, E., Benkő, S. & Pázmándi, K. Focusing on the Cell Type Specific Regulatory Actions of NLRX1. *Int J Mol Sci* **22**, 1316 (2021).

38. Koblansky, A. A. *et al.* The Innate Immune Receptor NLRX1 Functions as a Tumor Suppressor by Reducing Colon Tumorigenesis and Key Tumor-Promoting Signals. *Cell Rep* **14**, 2562–2575 (2016).
39. Hu, B. *et al.* NOD-like receptor X1 functions as a tumor suppressor by inhibiting epithelial-mesenchymal transition and inducing aging in hepatocellular carcinoma cells. *J Hematol Oncol* **11**, 28 (2018).
40. Luo, X. *et al.* HPV16 drives cancer immune escape via NLRX1-mediated degradation of STING. *J Clin Invest* **130**, 1635–1652 (2020).
41. Soares, F. *et al.* The Mitochondrial Protein NLRX1 Controls the Balance between Extrinsic and Intrinsic Apoptosis. *J Biol Chem* **289**, 19317–19330 (2014).
42. Agilent Technologies, Inc. Seahorse XF Cell Mito Stress Test Kit User Guide. 20 (2019).
43. QIAGEN. rt2 profiler pcr arrays - GeneGlobe. https://geneglobe.qiagen.com/us/product-groups/rt2-profiler-pcr-arrays.
44. Hanahan, D. & Weinberg, R. A. Hallmarks of Cancer: The Next Generation. *Cell* **144**, 646–674 (2011).
45. Ayres Pereira, M. & Chio, I. I. C. Metastasis in Pancreatic Ductal Adenocarcinoma: Current Standing and Methodologies. *Genes (Basel)* **11**, 6 (2019).
46. Baffy, G. Mitochondrial uncoupling in cancer cells: Liabilities and opportunities. *Biochimica et Biophysica Acta (BBA) - Bioenergetics* **1858**, 655–664 (2017).
47. Marchetti, P., Fovez, Q., Germain, N., Khamari, R. & Kluza, J. Mitochondrial spare respiratory capacity: Mechanisms, regulation, and significance in non-transformed and cancer cells. *The FASEB Journal* **34**, 13106–13124 (2020).
48. Lei, Y. *et al.* EGFR-targeted mAb therapy modulates autophagy in head and neck squamous cell carcinoma through NLRX1-TUFM protein complex. *Oncogene* **35**, 4698–4707 (2016).
49. Fan, Z., Pan, J., Wang, H. & Zhang, Y. NOD-like receptor X1, tumor necrosis factor receptor-associated factor 6 and NF-κB are associated with clinicopathological characteristics in gastric cancer. *Exp Ther Med* **21**, 208 (2021).
50. Castaño-Rodríguez, N., Kaakoush, N. O., Goh, K.-L., Fock, K. M. & Mitchell, H. M. The NOD-like receptor signalling pathway in Helicobacter pylori infection and related gastric cancer: a case-control study and gene expression analyses. *PLoS One* **9**, e98899 (2014).
51. Polireddy, K. & Chen, Q. Cancer of the Pancreas: Molecular Pathways and Current Advancement in Treatment. *J Cancer* **7**, 1497–1514 (2016).
52. Holmer, R., Goumas, F. A., Waetzig, G. H., Rose-John, S. & Kalthoff, H. Interleukin-6: a villain in the drama of pancreatic cancer development and progression. *Hepatobiliary Pancreat Dis Int* **13**, 371–380 (2014).
53. Martinez-Bosch, N., Vinaixa, J. & Navarro, P. Immune Evasion in Pancreatic Cancer: From Mechanisms to Therapy. *Cancers (Basel)* **10**, 6 (2018).
54. Ma, Z. *et al.* NLRX1 negatively modulates type I IFN to facilitate KSHV reactivation from latency. *PLoS Pathog* **13**, e1006350 (2017).
55. Hwang, J. P. *et al.* Oncologic Implications of Chronic Hepatitis C Virus Infection. *JOP* **15**, 629–637 (2019).
56. Cheng, J. *et al.* Mitochondrial Proton Leak Plays a Critical Role in Pathogenesis of Cardiovascular Diseases. *Adv Exp Med Biol* **982**, 359–370 (2017).
57. Laukkanen, M. O. Extracellular Superoxide Dismutase: Growth Promoter or Tumor Suppressor? *Oxid Med Cell Longev* **2016**, 3612589 (2016).

58. Nakamura, K. *et al.* Dysregulated IL-18 Is a Key Driver of Immunosuppression and a Possible Therapeutic Target in the Multiple Myeloma Microenvironment. *Cancer Cell* **33**, 634-648.e5 (2018).
59. van Duijneveldt, G., Griffin, M. D. W. & Putoczki, T. L. Emerging roles for the IL-6 family of cytokines in pancreatic cancer. *Clin Sci (Lond)* **134**, 2091–2115 (2020).
60. Chu, Y. *et al.* Efficacy of GM-CSF-producing tumor vaccine after docetaxel chemotherapy in mice bearing established Lewis lung carcinoma. *J Immunother* **29**, 367–380 (2006).
61. Mach, N. *et al.* Differences in dendritic cells stimulated in vivo by tumors engineered to secrete granulocyte-macrophage colony-stimulating factor or Flt3-ligand. *Cancer Res* **60**, 3239–3246 (2000).
62. Hong, I.-S. Stimulatory versus suppressive effects of GM-CSF on tumor progression in multiple cancer types. *Exp Mol Med* **48**, e242 (2016).

FIGURE LEGENDS

Figure 1. NLRX1 attenuates cancer-associated properties in Pan02 cells.

A. Western blot analysis of NLRX1 expression in transduced Pan02 cell lines and schematic of generated reagents and their color scheme. **B-C.** Differences in proliferation as assessed by (**B**) automated counting and (**C**) MTT assay. n = 6-8 per cell line. **D**. Differences in H_2O_2-induced cell death quantified by LDH assay. n = 3 per cell line. **E**. Differences in migration as calculated by pixels per hour via scratch assay. n = 8-14 per cell line. **F**. Representative fluorescent images of MitoSOX, an indicator for mitochondrial superoxide. DAPI shows NucBlue nuclear staining, GFP shows the GFP tag from the lentiviral (LV) construct, and RFP shows MitoSOX staining. **G-H.** Fluorescent intensity was measured by (**G**) Fiji-ImageJ and (**H**) a fluorometer. n = 3-4 per cell line. Representative of at least 2 independent experiments for all assays. All quantification data were analyzed using a two-way unpaired T test and shown as mean ± SE. *$p \leq 0.05$, **$p \leq 0.01$, ***$p \leq 0.001$, **** $p \leq 0.0001$.

Figure 2. NLRX1 limits mitochondrial dysfunction and cellular energy production.

A-D. From the Seahorse XF Cell Mito Stress kit, we observed differences in (**A**) basal respiration, (**B**) spare respiratory capacity, (**C**) proton leak, (**D**) ATP production, and (**E**) glycolysis. n = 7 per cell line. Representative of 1 independent experiment. All data were analyzed using a two-way unpaired T test and shown as mean ± SE. *$p \leq 0.05$, **$p \leq 0.01$, ***$p \leq 0.001$, **** $p \leq 0.0001$.

Figure 3. Top 20 pathways impacted by NLRX1 in Pan02 cells.

A-D. Transcriptomics analysis of our transduced Pan02 cell lines revealed the top 20 pathways between (**A**) $Pan02^{OE}$ and $Pan02^{OE\text{-}CTL}$ cells in normal conditions, (**B**) $Pan02^{KD}$ and $Pan02^{KD\text{-}CTL}$ cells in normal conditions, (**C**) $Pan02^{OE}$ and $Pan02^{OE\text{-}CTL}$ cells in H_2O_2 conditions, and (**D**) $Pan02^{KD}$ and $Pan02^{KD\text{-}CTL}$ cells in H_2O_2 conditions. Top pathways were determined by the number of DEGs and are listed alphabetically with their significance determined in TAC. **E**. Principal Component Analysis (PCA) mapping shows the clustering patterns for each of the 8 samples.

Figure 4. Gene expression signatures of relevant biological processes.

A-J. Fold change of DEGs between $Pan02^{OE}$ and $Pan02^{OE\text{-}CTL}$ cells in normal conditions, $Pan02^{KD}$ and $Pan02^{KD\text{-}CTL}$ cells in normal conditions, $Pan02^{OE}$ and $Pan02^{OE\text{-}CTL}$ cells in H_2O_2 conditions, and

Pan02^{KD} and Pan02$^{KD\text{-}CTL}$ cells in H_2O_2 conditions in biological processes relevant to observed *in vitro* phenotypes and top pathways. Gene lists were pulled from Qiagen/GeneGlobe.

SUPPLEMENTAL FIGURE LEGENDS

Supplemental Figure S1. Expansion on NLRX1 attenuates cancer-associated properties in Pan02 cells.

A-B. Differences in proliferation as assessed by (**A**) automated counting and (**B**) MTT assay under TNF stimulation. n = 3-8 per cell line. **C-D**. Fluorometer measurements of MitoSOX staining for mitochondrial superoxide stimulated with (**C**) glucose as a positive control or (**D**) TNF. Representative of 1-2 independent experiments for all assays. All data were analyzed using a two-way unpaired T test and shown as mean ± SE. *p ≤ 0.05, **p ≤ 0.01, ***p ≤ 0.001, **** p ≤ 0.0001.

Supplemental Figure S2. Expansion on NLRX1 limits mitochondrial dysfunction and cellular energy production.

A-D. From the Seahorse XF Cell Mito Stress kit, we observed differences under TNF conditions in (**A**) basal respiration, (**B**) spare respiratory capacity, (**C**) proton leak, (**D**) ATP production, and (**E**) glycolysis. n = 5-7 per cell line. Representative of 1 independent experiment. All data were analyzed using a two-way unpaired T test and shown as mean ± SE. *p ≤ 0.05, **p ≤ 0.01, ***p ≤ 0.001, **** p ≤ 0.0001.

Supplemental Figure S3. Top 50 up- and down-regulated genes in unstimulated conditions.

A-B. Based on the microarray transcriptomics assay, we list the top 50 up- and down-regulated DEGs between (**A**) Pan02^{OE} and Pan02$^{OE\text{-}CTL}$ cells, and (**B**) between Pan02^{KD} and Pan02$^{KD\text{-}CTL}$ cells in normal conditions. Listed in order of fold change.

Supplemental Figure S4. Top 50 up- and down-regulated genes following H_2O_2 stimulation.

A-B. Based on the microarray transcriptomics assay, we list the top 50 up- and down-regulated DEGs between (**A**) Pan02^{OE} and Pan02$^{OE\text{-}CTL}$ cells, and (**B**) between Pan02^{KD} and Pan02$^{KD\text{-}CTL}$ cells after low-dose H_2O_2 challenge. Listed in order of fold change.

FIGURES

Figure 1

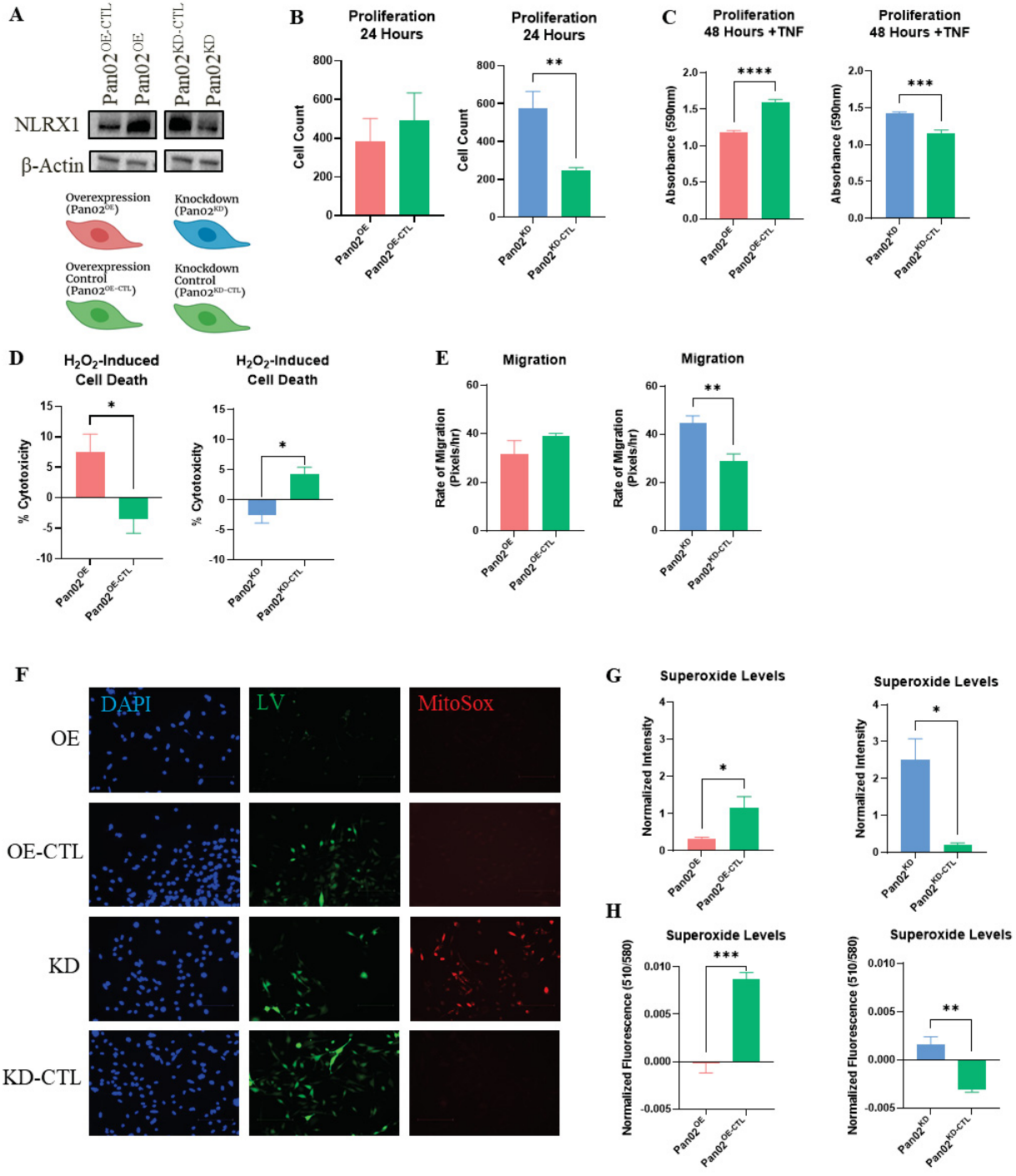

Figure 2

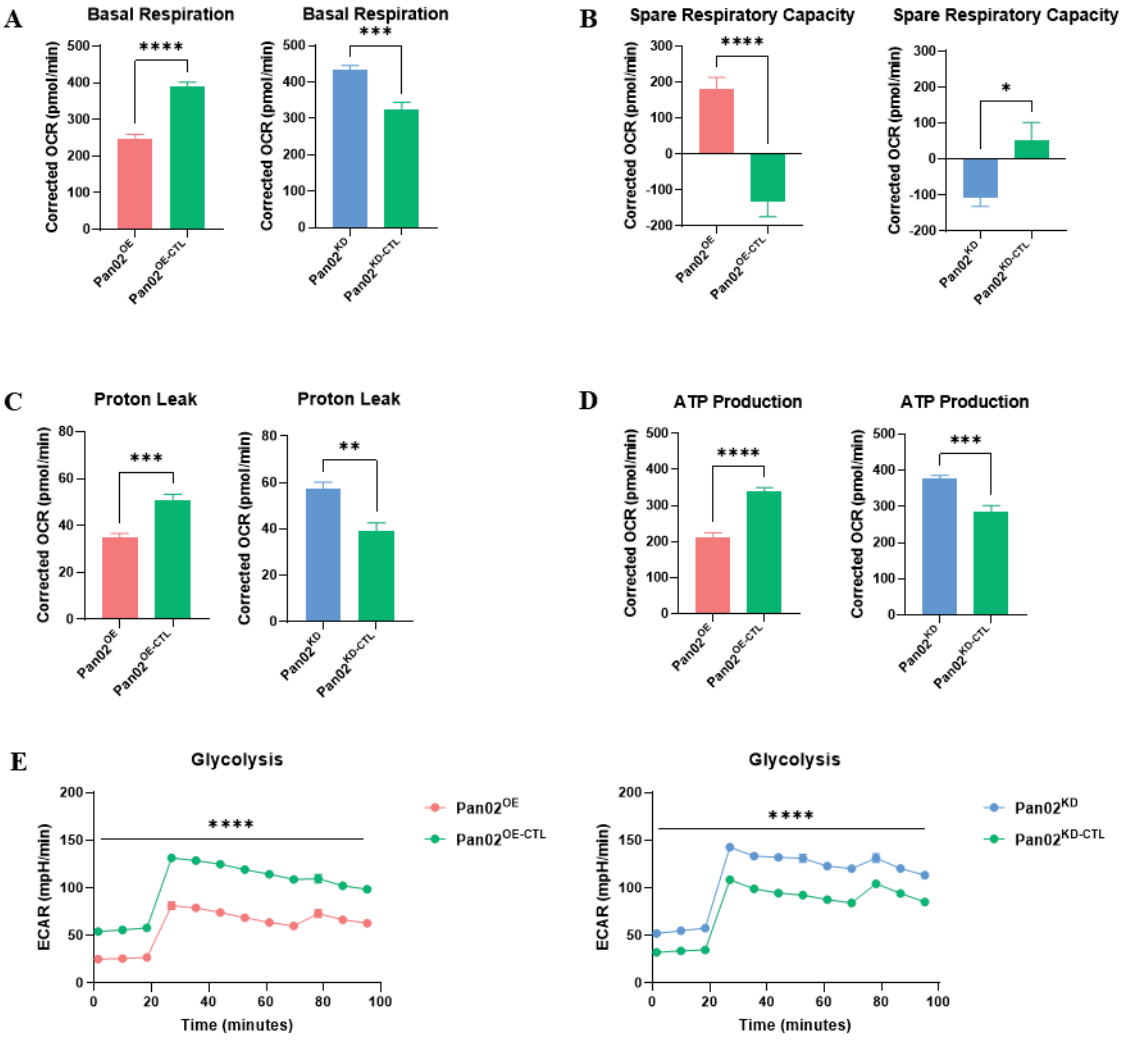
A
Basal Respiration
Corrected OCR (pmol/min)
****
Pan02OE
Pan02OE-CTL
Basal Respiration
***
Pan02KD
Pan02KD-CTL
B
Spare Respiratory Capacity
****
Spare Respiratory Capacity
*
C
Proton Leak
***
Proton Leak
**
D
ATP Production
****
ATP Production
***
E
Glycolysis
ECAR (mpH/min)
Time (minutes)
Pan02OE
Pan02OE-CTL
Glycolysis
Pan02KD
Pan02KD-CTL

Figure 3

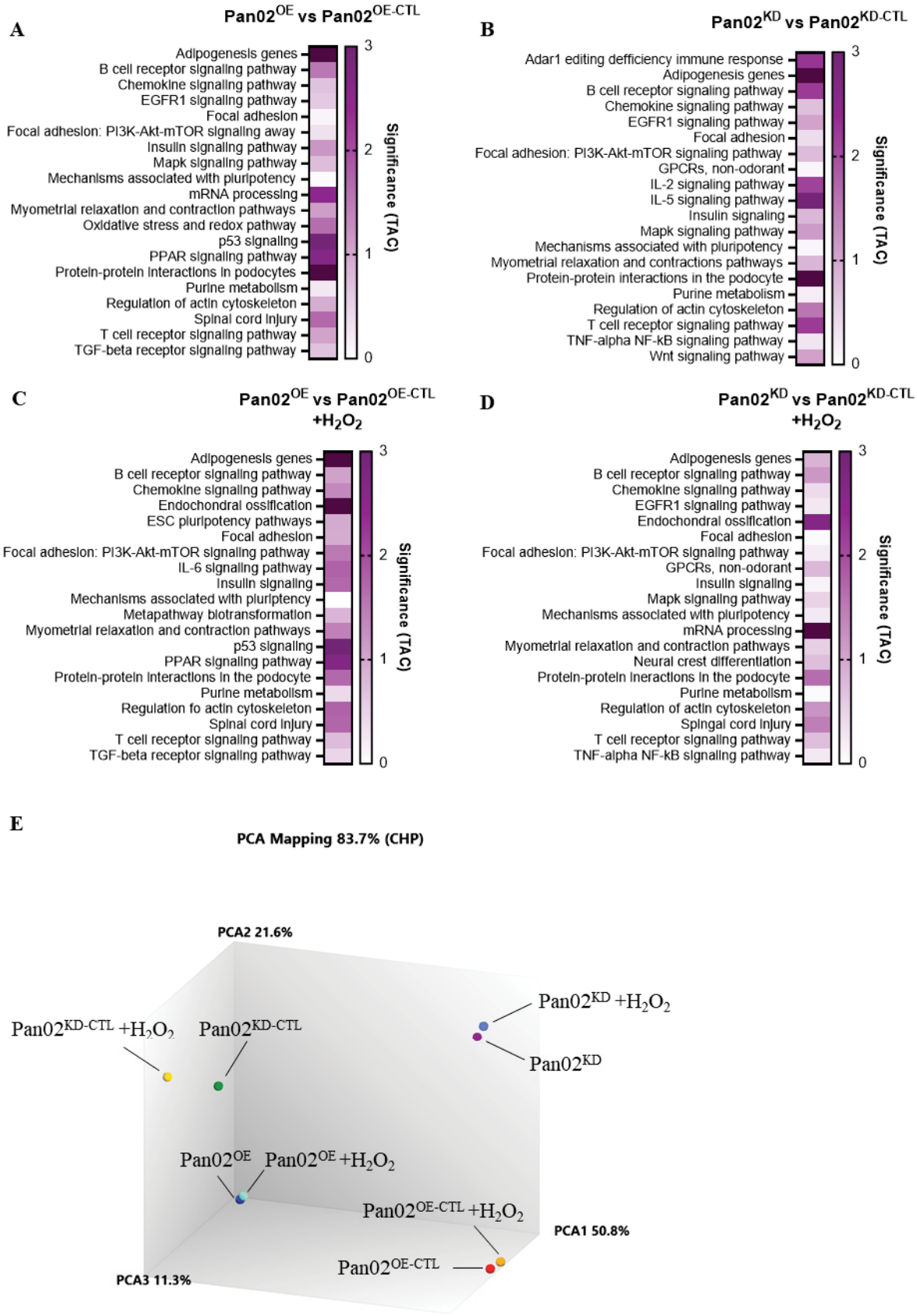
A
Pan02OE vs Pan02OE-CTL
Adipogenesis genes
B cell receptor signaling pathway
Chemokine signaling pathway
EGFR1 signaling pathway
Focal adhesion
Focal adhesion: PI3K-Akt-mTOR signaling away
Insulin signaling pathway
Mapk signaling pathway
Mechanisms associated with pluripotency
mRNA processing
Myometrial relaxation and contraction pathways
Oxidative stress and redox pathway
p53 signaling
PPAR signaling pathway
Protein-protein interactions in podocytes
Purine metabolism
Regulation of actin cytoskeleton
Spinal cord injury
T cell receptor signaling pathway
TGF-beta receptor signaling pathway
Significance (TAC)
B
Pan02KD vs Pan02KD-CTL
Adar1 editing defficiency immune response
Adipogenesis genes
B cell receptor signaling pathway
Chemokine signaling pathway
EGFR1 signaling pathway
Focal adhesion
Focal adhesion: PI3K-Akt-mTOR signaling pathway
GPCRs, non-odorant
IL-2 signaling pathway
IL-5 signaling pathway
Insulin signaling
Mapk signaling pathway
Mechanisms associated with pluripotency
Myometrial relaxation and contractions pathways
Protein-protein interactions in the podocyte
Purine metabolism
Regulation of actin cytoskeleton
T cell receptor signaling pathway
TNF-alpha NF-kB signaling pathway
Wnt signaling pathway
Significance (TAC)
C
Pan02OE vs Pan02OE-CTL +H2O2
Adipogenesis genes
B cell receptor signaling pathway
Chemokine signaling pathway
Endochondral ossification
ESC pluripotency pathways
Focal adhesion
Focal adhesion: PI3K-Akt-mTOR signaling pathway
IL-6 signaling pathway
Insulin signaling
Mechanisms associated with pluriptency
Metapathway biotransformation
Myometrial relaxation and contraction pathways
p53 signaling
PPAR signaling pathway
Protein-protein interactions in the podocyte
Purine metabolism
Regulation fo actin cytoskeleton
Spinal cord injury
T cell receptor signaling pathway
TGF-beta receptor signaling pathway
Significance (TAC)
D
Pan02KD vs Pan02KD-CTL +H2O2
Adipogenesis genes
B cell receptor signaling pathway
Chemokine signaling pathway
EGFR1 signaling pathway
Endochondral ossification
Focal adhesion
Focal adhesion: PI3K-Akt-mTOR signaling pathway
GPCRs, non-odorant
Insulin signaling
Mapk signaling pathway
Mechanisms associated with pluripotency
mRNA processing
Myometrial relaxation and contraction pathways
Neural crest differentiation
Protein-protein interactions in the podocyte
Purine metabolism
Regulation of actin cytoskeleton
Spingal cord injury
T cell receptor signaling pathway
TNF-alpha NF-kB signaling pathway
Significance (TAC)
E
PCA Mapping 83.7% (CHP)
PCA2 21.6%
Pan02KD-CTL +H2O2
Pan02KD-CTL
Pan02KD +H2O2
Pan02KD
Pan02OE
Pan02OE +H2O2
Pan02OE-CTL +H2O2
PCA1 50.8%
Pan02OE-CTL
PCA3 11.3%

Figure 4

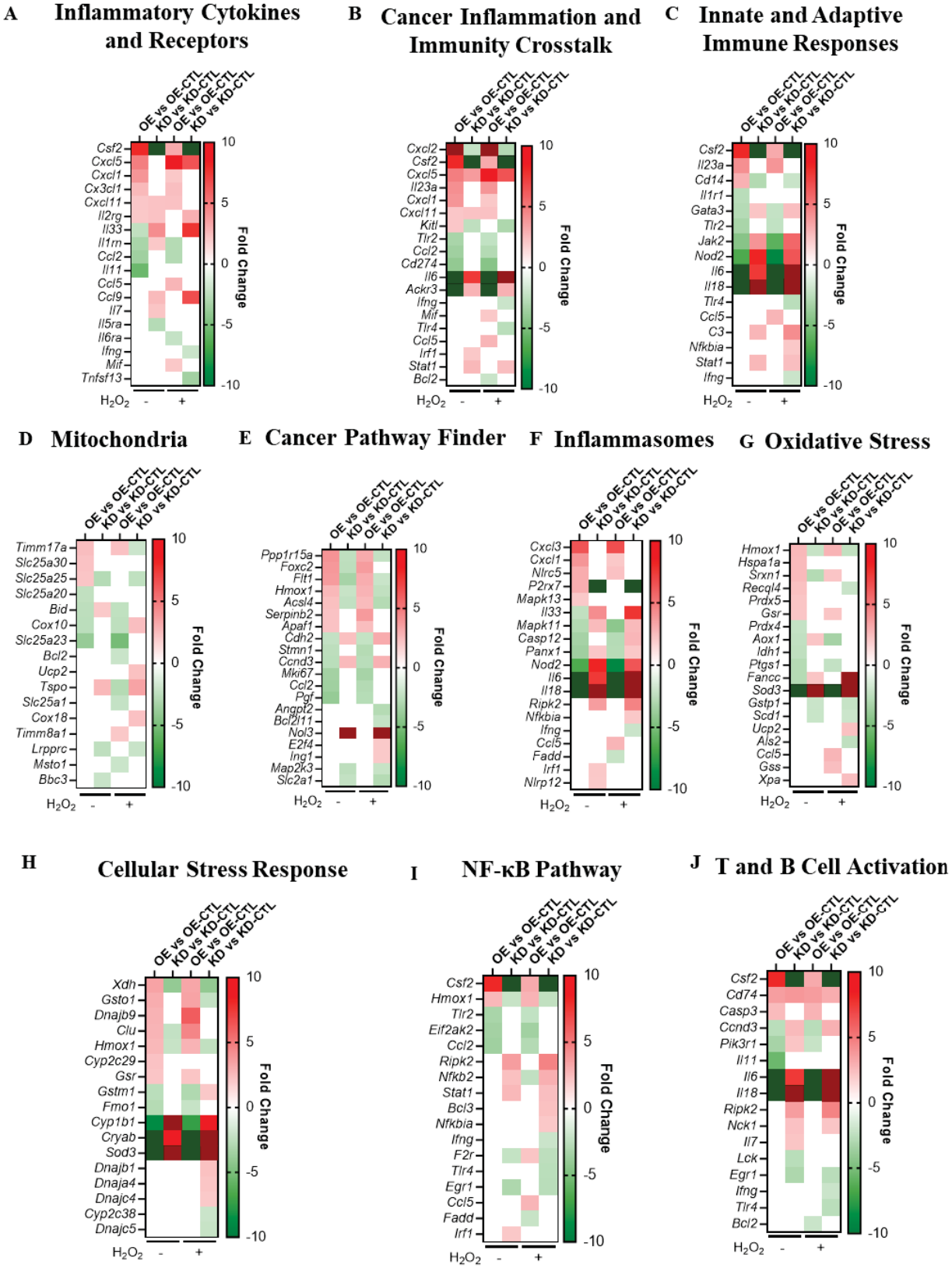
A Inflammatory Cytokines and Receptors
B Cancer Inflammation and Immunity Crosstalk
C Innate and Adaptive Immune Responses
D Mitochondria
E Cancer Pathway Finder
F Inflammasomes
G Oxidative Stress
H Cellular Stress Response
I NF-κB Pathway
J T and B Cell Activation
OE vs OE-CTL
KD vs KD-CTL
OE vs OE-CTL
KD vs KD-CTL
Fold Change
10
5
0
-5
-10
H2O2 - +

SUPPLEMENTAL FIGURES

Supplemental Figure S1

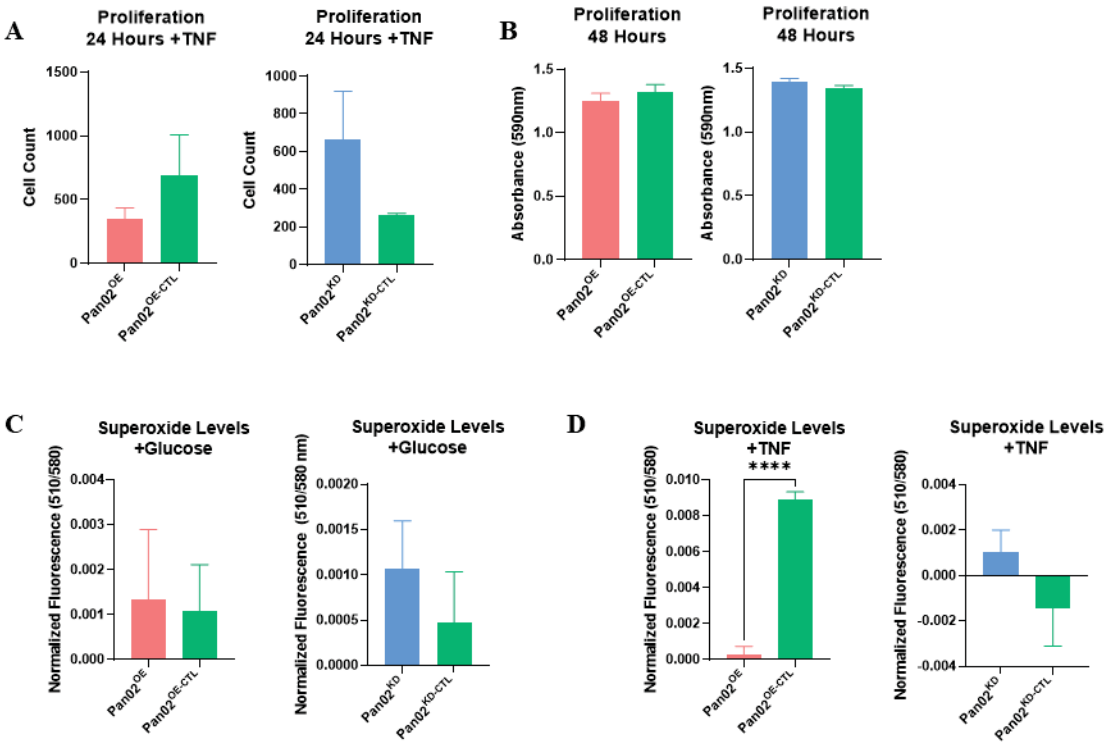

Supplemental Figure S2

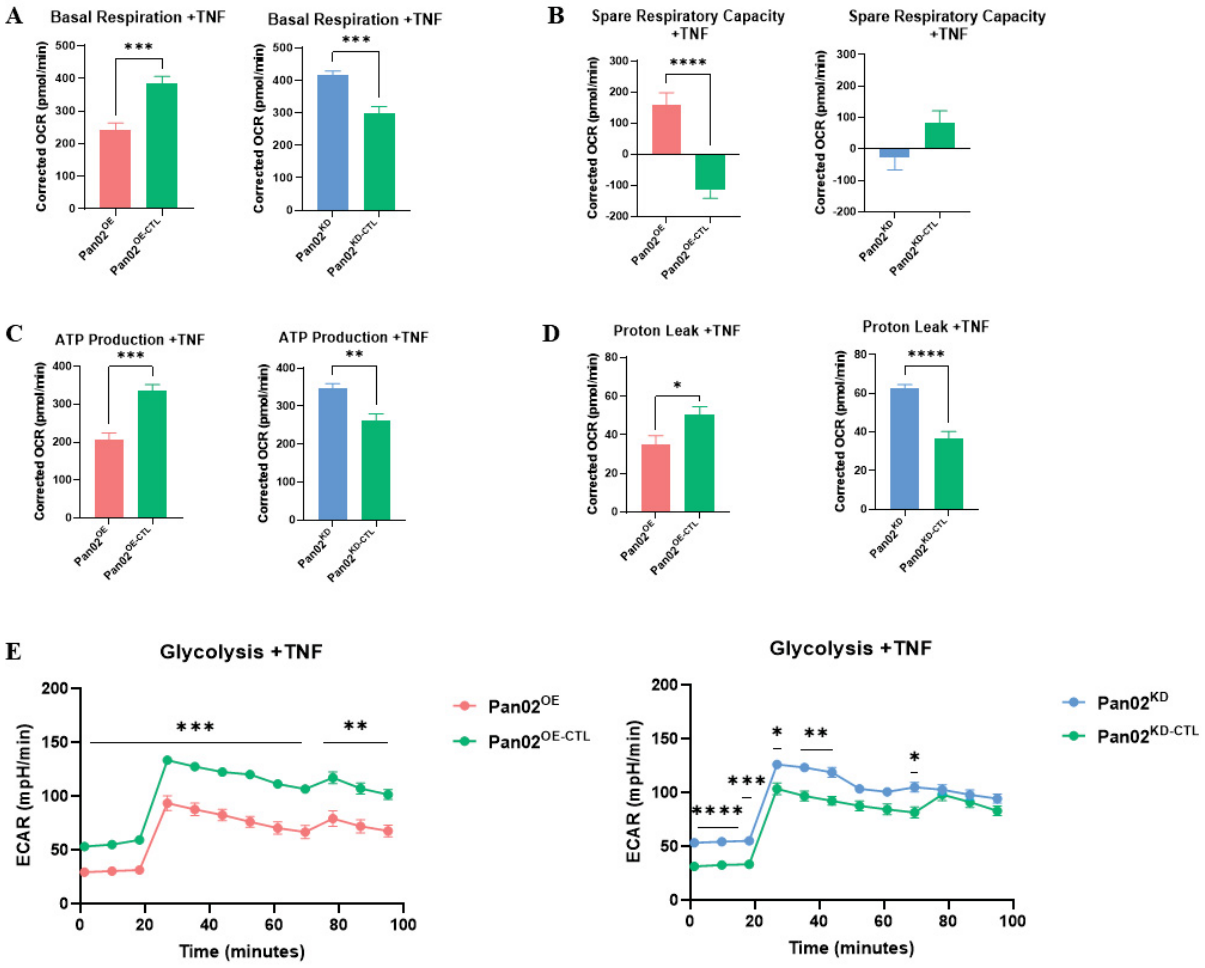

Supplemental Figure S3

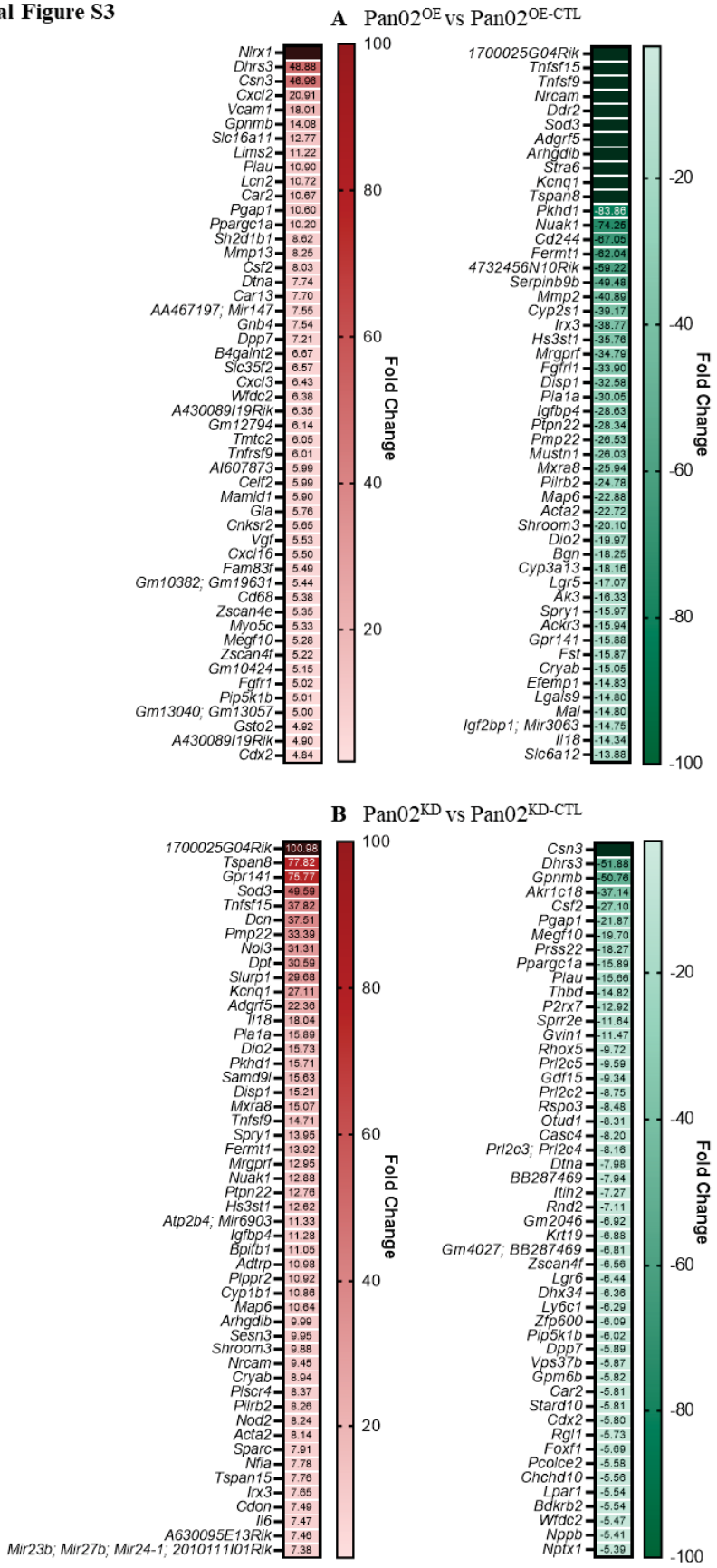

Supplemental Figure S4

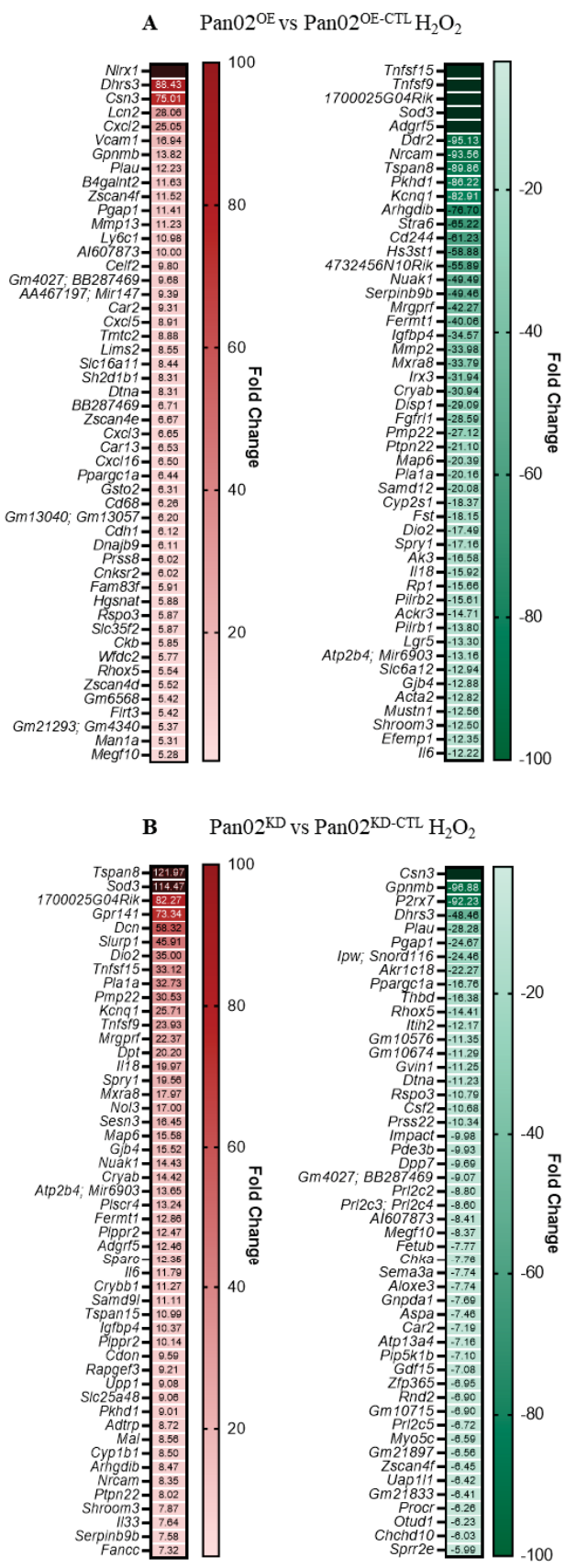

CHAPTER SIX

Conclusions and Future Directions

Margaret A. Nagai-Singer

Pattern recognition receptors (PRRs) offer critical regulation of many biological pathways, processes, and immune system functions. Because of this, PRRs are of interest in many diseases, including cancer.[1–3] As we discuss throughout the chapters above, the loss or gain of NLRX1 has been shown to produce robust phenotypes in many different cancer and infectious disease models, demonstrating that NLRX1 is a promising candidate for drug development in various diseases, including cancer. An NLRX1 agonist called NX-13 is currently being developed for inflammatory bowel disease and is in clinical trials for ulcerative colitis.[4,5] However, the work presented here indicates that NLRX1 function is highly variable based on cellular context. We demonstrate diametric roles for NLRX1 between healthy host cells and murine mammary tumor cells, and between murine mammary tumor cells and murine pancreatic cancer cells. There is certainly a need to uncover the driving mechanisms influencing the multifaceted roles of NLRX1 to clearly understand the potential risks and benefits of developing and using an NLRX1 agonist for treatment of any disease. Additionally, based on the dependency on cellular context that we identify, our data indicate that any NLRX1 agonist or antagonist would likely need to be targeted to a specific cell type to be most effective. For example, our studies in a murine model of triple-negative breast cancer (TNBC) indicate NLRX1 is protective when expressed in healthy host cells but problematic when expressed in murine mammary tumor cells. This would suggest the need for an NLRX1 agonist that targets non-tumor cells, or an NLRX1 antagonist that targets mammary tumor cells.

Many PRRs have well-defined PAMPs or DAMPs that they are responsible for recognizing. For example, TLR4 is most well-known for recognizing lipopolysaccharide (LPS) but can also recognize other PAMPs.[6,7] It is possible that, because NLRX1 is a PRR with no currently-identified DAMP or PAMP, that the specific binding of certain DAMPs or PAMPs can regulate the function of NLRX1 in different cellular circumstances. NLRX1 is known to function downstream of TLR signaling, so it is possible that variations in upstream signaling can also dictate the role of NLRX1.[8,9] Identifying exactly what DAMPs and PAMPs NLRX1 interacts with would

be helpful in elucidating the role of NLRX1 in different cellular contexts. Additionally, heightened reactive oxygen species (ROS) levels can drive proliferation and migration of cancer cells and can drive AKT and MAPK signaling pathways.[10–12] The ability for ROS to act as signaling molecules, combined with the ability of NLRX1 to mediate ROS levels, suggests that this interaction is worthy of further mechanistic evaluation. It is particularly interesting that previous literature suggests the ER/PR status of a mammary tumor can influence the role of NLRX1 in breast cancer, and identifying the DAMPs/PAMPs, signaling molecules, or biochemical pathways responsible for this would be crucial to understanding NLRX1 in different types of breast cancer.[13,14]

Furthermore, because PRRs are experts at forming multiprotein complexes, it is possible that the various players in NLRX1-mediated multiprotein complexes dictate NLRX1 function in various diseases through cleavage or post-translational modifications. Each domain in the NLRX1 structure has its own function, and therefore isoforms, cleavage, and/or truncated versions of NLRX1 might influence its function. Indeed, this is the case for another enigmatic protein called PTHrP (*PTHLH*), which functions as a tumor promoter or tumor suppressor in different contexts. This is very similar to the observed roles of NLRX1. Current literature suggests that the role of PTHrP is dependent on the stage of the disease and the presence/absence of certain functional domains in the protein structure.[15] Therefore, studies investigating the individual functions of each of the different domains (LRR, NACHT, and N-terminal "X" domain) of NLRX1 might reveal a functional tumor promoting or tumor suppressing domain(s). Likewise, interactions between NLRX1 and proteins like PTHrP in a multiprotein complex could also be of interest in defining additional key players in NLRX1 function.

Despite the diametric phenotypes caused by the presence/overexpression and absence/knock-down of NLRX1 in our cell lines and animals, there is consistency regarding the biological pathways and processes that are impacted. As we discuss in both Chapters Four and Five, NLRX1 seems to converge on epithelial-mesenchymal transition (EMT), MAPK, and AKT signaling in the mammary tumor model and NF-κB, MAPK, and AKT signaling in the pancreatic tumor model. Additional processes implicated between both models include limiting the formation of the metastatic niche, limiting inflammation through regulating the inflammasome, and the recruitment of immune cells. Many of these processes are also implicated elsewhere in the

literature as we discuss throughout the previous chapters. Together, this suggests that the pathways NLRX1 regulates are consistent, but that the actual regulation of these consistent pathways varies between models.

Beyond educated speculation of what is driving the diametric roles of NLRX1 in the work presented here, there are limitations to the current studies that should be noted. In Chapter Four, the TNBC study could have been aided by incorporating data from human tumors. However, previous studies have shown that NLRX1 expression in human breast tumors varies depending on the ER/PR status and the stage of the disease.[13,14] It would be interesting to engraft human TNBC cells with altered NLRX1 levels into immunocompromised mice to see if the *in vivo* problematic role of NLRX1 expressed in TNBC cells is consistent across mouse and human TNBC cell lines. It would also be beneficial to perform transcriptomics analysis on $4T1^{KD}$ and $4T1^{KD\text{-}CTL}$ tumors from WT and *Nlrx1*$^{-/-}$ mice to compare with the transcriptomics analysis of $4T1^{OE}$ and $4T1^{OE\text{-}CTL}$ tumors that we did perform. It is also worth exploring other phenotypes present in our 4T1 *in vivo* model that we simply did not assess in the current studies. We did collect brain tissue for metastatic analysis in one study, but no metastatic colonies formed and therefore we decided to exclude brain metastasis from our future evaluations. Future studies could include the collection of lymph nodes to analyze any changes to metastasis, flow, and immune cells present, or the collection of bone which would be highly relevant if any interactions with PTHrP are discovered.

In the pancreatic tumor model, the lack of an *in vivo* phenotype was certainly a limitation. None of the mice developed any metastasis in the lung or liver. Additionally, no differences in tumor size, survival, or morbidity were observed. This model was performed using a subcutaneous injection of Pan02 cells in the flank, meaning it is not an orthotopic model like the mammary tumor model is. This could be a reason we did not observe a phenotype *in vivo* and suggests that exploring orthotopic models for the transduced Pan02 cells might offer better results. Additionally, for the *in vitro* studies, we were highly interested in exploring the subcellular localization of NLRX1 through electron microscopy. Due to logistical circumstances, we were not able to perform these experiments. However, should the logistical circumstances be resolved, it would beneficial to perform these studies to understand if and how NLRX1 shuttles between different subcellular locations and what impact that has on NLRX1 function.

Together, this work explores NLRX1 as a complex and enigmatic regulator of immune system function and cancer-associated pathways. We also develop an updated method to quantify lung metastasis in the mammary tumor model, which will help standardize data acquired from the widely-used 4T1 model. The data presented in Chapter Four and Chapter Five identify the role of NLRX1 in two of the deadliest cancers in the United States. We identify phenotypes driven by NLRX1 and mechanisms responsible for those phenotypes. This work aims to help elucidate the controversial role of NLRX1, and ultimately, we show that the role of NLRX1 is highly variable based on the type of cell and the type of cancer. This indicates that the driving factors behind the diametric roles of NLRX1 require further research before broadly developing and testing NLRX1 agonists/antagonists. However, the robust phenotypes induced by altering NLRX1 levels suggest this proposed future work is worth exploring.

In the larger context of things, exploring the function of one signaling protein is a tiny piece of the puzzle of using science to improve the health of our planet and its inhabitants. That is of course not to minimize any of the work performed here and its significance, but for any of the research presented here today to become fruitful in that endeavor, we must all protect our environment, our democracy, and our most vulnerable populations. Curing cancer is great, but it really only means something if we have a habitable planet to cure it on where everyone can access the healthcare they need regardless of sociocultural status.

REFERENCES

1. Bai, L.; Li, W.; Zheng, W.; Xu, D.; Chen, N.; Cui, J. Promising Targets Based on Pattern Recognition Receptors for Cancer Immunotherapy. *Pharmacological Research* **2020**, *159*, 105017. https://doi.org/10.1016/j.phrs.2020.105017.
2. Li, D.; Wu, M. Pattern Recognition Receptors in Health and Diseases. *Sig Transduct Target Ther* **2021**, *6* (1), 1–24. https://doi.org/10.1038/s41392-021-00687-0.
3. Man, S. M.; Jenkins, B. J. Context-Dependent Functions of Pattern Recognition Receptors in Cancer. *Nat Rev Cancer* **2022**, *22* (7), 397–413. https://doi.org/10.1038/s41568-022-00462-5.
4. Landos Biopharma Inc. *A Randomized, Double-Blind Study to Evaluate the Safety, Tolerability, and Pharmacokinetics of Oral NX-13 in Active Ulcerative Colitis*; Clinical trial registration NCT04862741; clinicaltrials.gov, 2022.
5. Leber, A.; Hontecillas, R.; Zoccoli-Rodriguez, V.; Ehrich, M.; Chauhan, J.; Bassaganya-Riera, J. Exploratory Studies with NX-13: Oral Toxicity and Pharmacokinetics in Rodents of an Orally Active, Gut-Restricted First-in-Class Therapeutic for IBD That Targets NLRX1. *Drug Chem Toxicol* **2022**, *45* (1), 209–214. https://doi.org/10.1080/01480545.2019.1679828.
6. Poltorak, A.; He, X.; Smirnova, I.; Liu, M. Y.; Van Huffel, C.; Du, X.; Birdwell, D.; Alejos, E.; Silva, M.; Galanos, C.; Freudenberg, M.; Ricciardi-Castagnoli, P.; Layton, B.; Beutler, B. Defective LPS Signaling in C3H/HeJ and C57BL/10ScCr Mice: Mutations in Tlr4 Gene. *Science* **1998**, *282* (5396), 2085–2088. https://doi.org/10.1126/science.282.5396.2085.
7. Lu, Y.-C.; Yeh, W.-C.; Ohashi, P. S. LPS/TLR4 Signal Transduction Pathway. *Cytokine* **2008**, *42* (2), 145–151. https://doi.org/10.1016/j.cyto.2008.01.006.
8. Xia, X.; Cui, J.; Wang, H. Y.; Zhu, L.; Matsueda, S.; Wang, Q.; Yang, X.; Hong, J.; Songyang, Z.; Chen, Z. J.; Wang, R.-F. NLRX1 Negatively Regulates TLR-Induced NF-KB Signaling by Targeting TRAF6 and IKK. *Immunity* **2011**, *34* (6), 843–853. https://doi.org/10.1016/j.immuni.2011.02.022.
9. Allen, I. C.; Moore, C. B.; Schneider, M.; Lei, Y.; Davis, B. K.; Scull, M. A.; Gris, D.; Roney, K. E.; Zimmermann, A. G.; Bowzard, J. B.; Ranjan, P.; Monroe, K. M.; Pickles, R. J.; Sambhara, S.; Ting, J. P. Y. NLRX1 Protein Attenuates Inflammatory

Responses to Infection by Interfering with the RIG-I-MAVS and TRAF6-NF-KB Signaling Pathways. *Immunity* **2011**, *34* (6), 854–865. https://doi.org/10.1016/j.immuni.2011.03.026.

10. Aggarwal, V.; Tuli, H. S.; Varol, A.; Thakral, F.; Yerer, M. B.; Sak, K.; Varol, M.; Jain, A.; Khan, Md. A.; Sethi, G. Role of Reactive Oxygen Species in Cancer Progression: Molecular Mechanisms and Recent Advancements. *Biomolecules* **2019**, *9* (11), 735. https://doi.org/10.3390/biom9110735.
11. Sarmiento-Salinas, F. L.; Delgado-Magallón, A.; Montes-Alvarado, J. B.; Ramírez-Ramírez, D.; Flores-Alonso, J. C.; Cortés-Hernández, P.; Reyes-Leyva, J.; Herrera-Camacho, I.; Anaya-Ruiz, M.; Pelayo, R.; Millán-Pérez-Peña, L.; Maycotte, P. Breast Cancer Subtypes Present a Differential Production of Reactive Oxygen Species (ROS) and Susceptibility to Antioxidant Treatment. *Frontiers in Oncology* **2019**, *9*.
12. Nogueira, V.; Hay, N. Molecular Pathways: Reactive Oxygen Species Homeostasis in Cancer Cells and Implications for Cancer Therapy. *Clin Cancer Res* **2013**, *19* (16), 4309–4314. https://doi.org/10.1158/1078-0432.CCR-12-1424.
13. Singh, K.; Roy, M.; Prajapati, P.; Lipatova, A.; Sripada, L.; Gohel, D.; Singh, A.; Mane, M.; Godbole, M. M.; Chumakov, P. M.; Singh, R. NLRX1 Regulates TNF-α-Induced Mitochondria-Lysosomal Crosstalk to Maintain the Invasive and Metastatic Potential of Breast Cancer Cells. *Biochimica et Biophysica Acta (BBA) - Molecular Basis of Disease* **2019**, *1865* (6), 1460–1476. https://doi.org/10.1016/j.bbadis.2019.02.018.
14. Singh, K.; Poteryakhina, A.; Zheltukhin, A.; Bhatelia, K.; Prajapati, P.; Sripada, L.; Tomar, D.; Singh, R.; Singh, A. K.; Chumakov, P. M.; Singh, R. NLRX1 Acts as Tumor Suppressor by Regulating TNF-α Induced Apoptosis and Metabolism in Cancer Cells. *Biochimica et Biophysica Acta (BBA) - Molecular Cell Research* **2015**, *1853* (5), 1073–1086. https://doi.org/10.1016/j.bbamcr.2015.01.016.
15. Edwards, C. M.; Johnson, R. W. From Good to Bad: The Opposing Effects of PTHrP on Tumor Growth, Dormancy, and Metastasis Throughout Cancer Progression. *Front Oncol* **2021**, *11*, 644303. https://doi.org/10.3389/fonc.2021.644303.